



Dedicated to innovation in aerospace



Provincie Noord-Brabant

PUBLIC



Europese Unie

Europees Fonds voor Regionale Ontwikkeling

NLR-CR-2019-100-RevEd-1 | July 2023

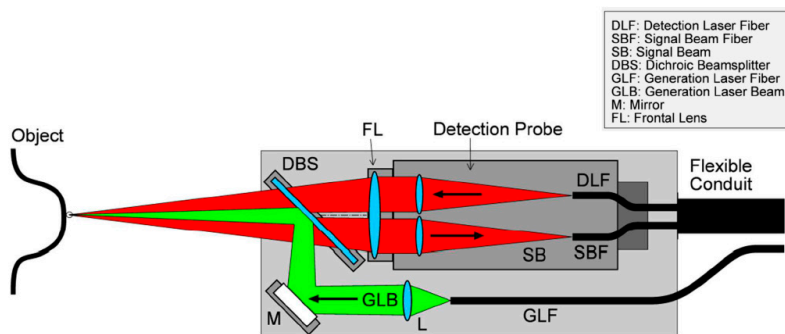
Round Robin Test Results of Laser Ultrasonic Systems on Composite Panels

CUSTOMER: OPZuid (Operationeel Programma Zuid-Nederland)



Royal NLR - Netherlands Aerospace Centre

Round Robin Test Results of Laser Ultrasonic Systems on Composite Panels



Head of a co-linear laser generation and detection probe (Ref. 26)

Problem area

In the DCMC project, several in-service inspection techniques are evaluated on composite reference specimens. Previous investigations regarding Lock-in Thermography and Laser Shearography are documented in ref.1 and ref.2. One of these techniques is Laser Ultrasonics (LU).

The in-service components to be inspected provides usually only one-sided access if the component is not removed from the aircraft. This eliminates various forms of ultrasonic inspection techniques, such as immersive C-scan and through-transmission modes. LU does not require physical contact with the structure under inspection nor a couplant medium, which are advantageous properties for the inspection. Two co-linear laser beams are used instead of standard ultrasonic piezo transducers. A generation laser beam (pulsed) produces non-destructively, by thermo-elastic effect, a stress-field at the surface of the part, which in turn produces ultrasonic waves. Ultrasonic waves reflected or scattered by the back-wall or flaws are detected by the detection laser beam and an optical interferometer based on the Doppler shift. Received signals are further processed as in conventional ultrasonic inspection to display A-, B- and C-scans.

REPORT NUMBER

NLR-CR-2019-100-RevEd-1

AUTHOR(S)

E.R. Rademaker
 J. Platenkamp
 J.S. Hwang

REPORT CLASSIFICATION

ONGERUBRICEERD

DATE

July 2023

KNOWLEDGE AREA(S)

Health Monitoring and Maintenance of Aircraft
 Aerospace Structures Testing

DESCRIPTOR(S)

Non-destructive Evaluation
 Ultrasonic testing
 Laser Ultrasonics

In WP 2 of the DCMC project, a round robin program with three composite panels with artificial defects is carried out by testing these panels with laser ultrasonic equipment of various suppliers. Main goal of the round robin is to understand the quality of the current LU techniques.

Description of work

A round robin program is carried out by testing three composite panels with artificial defects inspected by laser-ultrasonic equipment of various providers (X-NDT, Technatom, Xarion, Tecnar and Optech Ventures). Most tests except for X-NDT were witnessed by NLR staff, which gave also the opportunity to discuss the procedures and test results with the manufacturers of LU-equipment. The tests reference standard is obtained from the NLR C-scan immersion ultrasonics facility. Round robin results are mutually compared and compared to the NLR reference results. Final results and conclusions are reported in the current document.

Results and conclusions

Laser ultrasonics is a relatively new (and rather expensive) NDI technique with a number of advantages for in-service inspection of composite aerospace structures. It is essentially non-contact, requires only one-sided access and has a high tolerance to the incidence angle of the laser beam with the part ($\pm 20-35^\circ$) and to the distance between the scanning laser head and the part (typical distance $\frac{1}{4}$ m). It is suitable for automated inspection of complex shaped composite parts. The quality of the test results is somewhat less, though sufficient, in comparison with the quality obtained from the ultrasonic C-scan facility. Special care has to be taken to prevent surface ablation by both the generation and detection lasers (characteristic spot sizes of about 10 and 1 mm respectively). Use of LU-equipment requires safety measures and optimal laser setup for each part under inspection. The latter causes that laser ultrasonics currently is more applied to quality inspection during the manufacturing phase. More investigation in ablation aspects for a range of material types will give more insight in the in-service applications.

Applicability

Robotized laser ultrasonic inspection equipment in a MRO environment can be introduced for the inspection of relatively thin composite parts (thickness up to about 10 to 15 mm).



Dedicated to innovation in aerospace

PUBLIC



Provincie Noord-Brabant



Europese Unie

Europees Fonds voor Regionale Ontwikkeling

NLR-CR-2019-100-RevEd-1 | July 2023

Round Robin Test Results of Laser Ultrasonic Systems on Composite Panels

CUSTOMER: OPZuid (Operationeel Programma Zuid-Nederland)

AUTHOR(S):

E.R. Rademaker

NLR

J. Platenkamp

NLR

J.S. Hwang

NLR

*The owner and/or contractor have granted permission to publish this report.
 Content of this report may be cited on the condition that full credit is given to the owner and/or contractor.
 Commercial use of this report is prohibited without the prior written permission of the owner and/or contractor.*

CUSTOMER	OPZuid (Operationeel Programma Zuid-Nederland)
CONTRACT NUMBER	31B1.0730 (PROJ-007230)
OWNER	NLR
DIVISION NLR	Aerospace Vehicles
DISTRIBUTION	Unlimited
CLASSIFICATION OF TITLE	UNCLASSIFIED

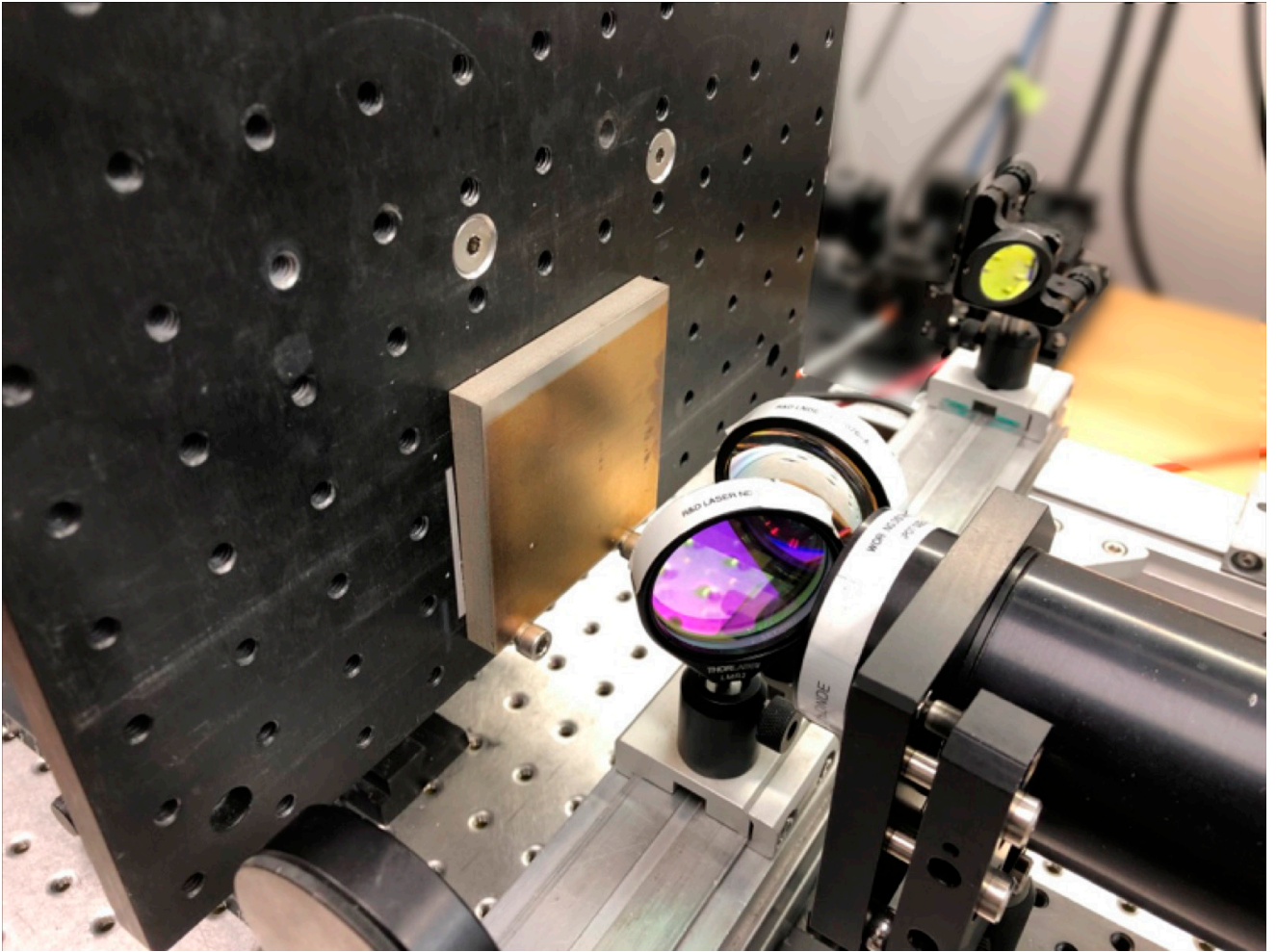
APPROVED BY:	Date	
AUTHOR	D.J. Platenkamp J.S. Hwang	03-08-2023 03-08-2023
REVIEWER	H.P. Jansen	03-08-2023
MANAGING DEPARTMENT	P. Arendsen	03-08-2023

Summary

In the DCMC project Work Package (WP) 2, several non-destructive in-service inspection techniques are evaluated on composite reference specimens. Laser Ultrasonics (LU) is one of three methods being evaluated, next to thermography and shearography. This report describes results from the round robin program with three composite panels including artificial defects. The round robin is carried out by testing these panels with LU equipments from various suppliers. Main goal of the round robin is to understand the quality of the current LU techniques.

For detecting defects in the composite aircraft structure, ultrasonic inspection is a well-established method to perform non-destructive Inspection (NDI). The in-service components to be inspected provides usually only one-sided access if the component is not removed from the aircraft. This eliminates the single through-transmission or reflector plate inspection techniques (immersion C-scan) and only leaves the pulse-echo technique as a viable method. In comparison to the conventional ultrasonic inspection method, LU does not require physical contact with the structure under inspection nor a couplant medium. LU method uses two co-linear laser beams for generating and detecting ultrasonic waves in the material. A generation laser beam (pulsed) produces non-destructively, by thermo-elastic effect, a stress at the surface of the part, which in turn produces ultrasonic waves. Ultrasonic waves reflected or scattered by the back-wall or flaws are detected by the detection laser beam and an optical interferometer based on the Doppler shift. Received signals are further processed as in conventional ultrasonic inspection to display A-, B- and C-scans.

From this study, it is concluded that LU is a relatively new (and rather expensive) NDI technique with a number of advantages for in-service inspection of composite aerospace structures. It is essentially non-contact, requires only one-sided access and has a high tolerance to the incidence angle of the laser beam with the part ($\pm 20-35^\circ$). Further the distance between the scanning laser head and the part is typically between ¼ m to 2 m, which is a safe distance for automation concepts with no risk for collisions. Therefore, it is concluded that LU is suitable for automated inspection of complex shaped composite parts. The quality of the test results is somewhat less, though sufficient, in comparison with the quality obtained from the ultrasonic C-scan facility. Special care has to be taken to prevent surface ablation by both the generation and detection lasers (characteristic spot sizes of about 10 and 1 mm respectively). Use of LU-equipment requires safety measures and optimal laser setup for each part under inspection. The latter causes that laser ultrasonics currently is more applied to quality inspection during the manufacturing phase.



Tecnar laser ultrasonic equipment

Contents

Abbreviations	7
1 Introduction	8
1.1 Ultrasonic Inspection	8
1.2 Conventional ultrasonic inspection	10
1.3 In-service ultrasonic inspection	11
2 Laser ultrasonic inspection	13
2.1 LUT Hardware	15
2.2 LUT processing software	18
2.3 Selection of LUT hardware for DCMC round robin	19
3 Round robin composite specimens	20
3.1 CFRP specimens	20
3.1.1 Specimen NLR-B	20
3.1.2 Specimen NLR-D	21
3.2 RTM calibration specimen #2118	21
4 Test equipment description and test results of the round robin	23
4.1 NLR C-scan conventional ultrasonic inspection as baseline reference	23
4.1.1 NLR C-scan facility	23
4.1.2 Experimental results	24
4.2 X-NDT UPIs PE	26
4.2.1 X-NDT equipment	26
4.2.2 Experimental results	28
4.3 Tecnatom	35
4.3.1 TecnaLUS	35
4.3.2 Experimental results	36
4.4 Xarion	42
4.4.1 Xarion optical microphone	42
4.4.2 Experimental results	44
4.5 Tecnar equipment	50
4.5.1 Tecnar equipment at CSL	50
4.5.2 Experimental results	51
4.6 Optech Ventures	54
4.6.1 Optech Ventures equipment	54
4.6.2 Experimental results	56
4.7 Discolouration	60
5 Discussion/recommendation	61
6 Conclusions	64

7	References	65	
	Appendix A	Composite specimens	67
	Appendix B	Base-line UT inspection	70
	Appendix B.1	Specimen NLR-B	70
	Appendix C	Laser ultrasonic PE-UPI inspection	80
	Appendix C.1	Specimen NLR-B	80
	Appendix C.2	Specimen NLR-D	82
	Appendix C.3	RTM specimen #2118	85

Abbreviations

ACRONYM	DESCRIPTION
ABB	Asea Brown Boverly
ACUT	Air Coupled Ultrasonic Testing
AWPI	Anomalous Wave Propagation Imaging
BAM	Bundesanstalt für Materialforschung und -prüfung
DTT	Double Through-Transmission
FBH	Flat-Bottomed Holes
LU	Laser Ultrasonics
LUCIE	Laser Ultrasonic Composite Inspection
LUT	Laser Ultrasonic Testing
MIR	Mid-InfraRed
Nd	Neodymium doped
Nd:YAG	Neodymium doped Yttrium Aluminium Garnet (Y ₃ Al ₅ O ₁₂)
NDI/NDT	Non-Destructive Inspection/Testing
OESL	Opto-Electro-Structural Laboratory
OPO	Optical Parametric Oscillator
PA	Phased Array
PE	Pulse Echo
PEBR	Pulse-Echo Backwall Reflection
PEFR	Pulse-Echo Flaw Reflection
PRR	Pulse Repetition Rate
PZT	Lead Zirconate Titanate
SHM	Structural Health Monitoring
TA	ThermoAcoustic
TecnaLUS	Tecnatom Laser Ultrasonic System
TOF	Time-Of-Flight
UL	Ultimate Load
UPI	Ultrasonic Propagation Imaging
USI	Ultrasonic Spectral Imaging
UT	Ultrasonic Testing
UWPI	Ultrasonic Wave Propagation Imaging
VTWAM	Variable Time Window Amplitude Mapping
WUPI	Wavelet-transformed Ultrasonic Propagation Imaging

1 Introduction

1.1 Ultrasonic Inspection

Ultrasonic inspection (UT) makes use of high-frequency ultrasonic waves, in fact propagating mechanical vibrations with a frequency in the range of about 0.5 - 50 MHz. Different vibration modes are possible, depending on how the particles in the material oscillate, of which longitudinal and transverse waves are the most widely used wave types in ultrasonic testing. With longitudinal waves (also called compression or pressure waves) the particles oscillate in the direction of wave propagation and with transverse waves (also called shear waves) the particles oscillate perpendicularly to the direction of wave propagation. Besides these two modes other vibration modes exist, such as surface (Rayleigh) waves and guided (Lamb) waves. References 2 and 3 present a good overview of the different modes of vibration and, more general, of the basic principles and applications of UT. A main advantage of using ultrasonic inspection is that besides the location and size of the defects and flaws, also the depth beneath the surface can be determined.

A primary conclusion of reference 1, see also the results summarised in table 1.1, is that ultrasonic inspection (UT) is the primary method for in-service inspection of composite structures, especially regarding its capability for the detection, sizing and depth estimation of defects.

Table 1.1: Summary of the capabilities of the NDI methods (Ref. 1)

Inspection Characteristic		NDE technique							
		Visual	Tap Test Woodpecker	Bondmaster PC Swept/RF	Ultrasonic Inspection			Shearography Heat/Vacuum	Thermography Lockin/Transient
				Acoustocam	UT-PA	RapidScan			
Detection	Impact	+	+	0/+	+ /++	++	++	++	+
	Delamin.	-	0	0	++	++	++	-/0	-/0
	Disbond	-	0	0	+	+ /++	++	0	0/+
Defect sizing		-	0	0	+	++	++	+	+
Depth estimation		-	-	-	+	++	++	-	-
Portability		++	++	++	+	+	+	+	0
Field of view		~1 m2	Spot	Spot	25 mm2	68 mm	50-100 mm	220x160 mm	~1 m2
Couplant required		No	No	No	Yes	Yes	Minimal	No	No
Inspection speed		++	0	0	+	+	+	+	++
Level of training		Low	Low	High	Medium	High	High	High	High
Equipm. costs [k€]		0	< 10	12-15	40-60	40-60	95-110	100-120	130-150

The major limitation of standard UT inspection, however, is the need to use a couplant between the UT transducer and the test part. This requirement limits the UT technique for automated inspection applications. The RapidScan™ technique does not require, or only minimal, couplant but its transducer system (roller probe) requires to be in contact with the test part and is therefore not very suited for in-service applications where large surface areas have to be scanned in a fast way (the RapidScan™ can be considered more as a local inspection technique). Evidently, there is a need for a UT technique that does not need a couplant and is well suited for automated inspection applications. Two candidate UT techniques for this have emerged in recent years, namely air coupled UT (ACUT) and laser ultrasonics (LU).

The ACUT technique has the inherent limitation of the large mismatch of the acoustic impedance between UT transducer and air. As a result, ACUT generally works with special low-frequency transducers (50 – 300 kHz) that consequently have a negative influence on the sensitivity of inspection (being related to the UT frequency). ACUT is

therefore currently mainly used in the single through-transmission mode using two transducers (transmitter, receiver) and hence less suited for in-service applications (Ref. 2). It is remarked that there are developments in ACUT for in-service applications using guided waves in the pitch-catch mode, as discussed in reference 3 and illustrated in figure 1.1. There are even developments that use ACUT in a pure pulse-echo mode with perpendicular excitation and reception of the UT waves with a single thermo-acoustic (TA) transducer (Ref. 4). But, these developments have a relatively low TRL value and the TA transducer is currently still in the prototype phase (development by the institute BAM in Berlin).

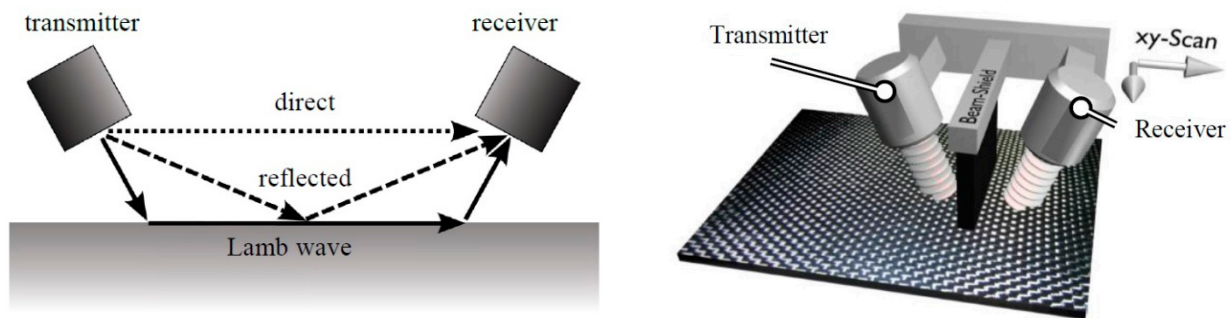


Figure 1.1: Air coupled UT inspection in pitch-catch mode by making use of guided waves (Figures 1 and 2 from Ref. 3)

Laser ultrasonics (LU) is also a candidate UT technique that does not require physical contact with the structure under inspection. Current LU systems, however, operate at higher TRL level than the prototype ACUT systems in pulse-echo mode. LU in principle employs laser scanning systems for both the excitation and the reception of ultrasonic waves with one-sided access of the structure to be inspected. It is therefore very suitable for fully automated application during production and in-service inspections. An additional advantage of LU is the high tolerance relative to the incidence angle of the laser beam with the part ($\pm 20-35^\circ$) and to the distance between the scanning laser head and the part (Ref. 5). As a result, the inspection time can be significantly reduced, especially for the inspection of large, complex shaped parts.

A distinction between available and suitable (laser) ultrasonic inspection techniques for composites can be also made on basis of application type:

1. Ultrasonic inspection at/after manufacturing, where currently the C-scan is the basic technique.
2. Current in-service inspection techniques mainly based on small, transportable and manually operated equipment for relatively small scan areas using a coupling medium.

There are already some known applications of LU at/after manufacturing. Therefore, it is interesting to investigate and evaluate how a relatively new and evolving LU technique can be used for in-service inspection. This report describes the results of a round robin exercise with three composite panels with artificial damages and flaws tested by laser ultrasonic equipment of various suppliers. Prior to the description of the round robin tests, a general introduction of current and main inspection technique on composite specimens is given in the sequel. Furthermore it is noted that the description and format of the round robin results for the X-NDT UPI is somewhat more extended than those of other LUT-suppliers. Main reason is that used X-NDT UPI round robin results are obtained from previously (and also recently) carried out tests. This besides time and budget saving has also the advantage to zoom in on more details making the reader more familiar with the laser ultrasonic inspection technique.

1.2 Conventional ultrasonic inspection

Ultrasonic C-scan inspection is currently the primary method for the quality control of composite specimens. It provides a 2-dimensional plan view (called C-scan) of internal defects in the material, whilst automatically scanning the specimen in a raster pattern (scan plus index movement). Because air is not an adequate transmitting medium for ultrasonic waves, a coupling medium is used between the transducer and material. This can be realised in different ways. For manufacture inspection, UT is often carried out with the part totally immersed in water, or with the water-jet (squitter) method where the ultrasonic beam is collimated in a narrow water beam. For the present investigation, the immersion technique is used to provide a base-line UT inspection because it enables the application of focused transducers yielding a more sensitive inspection capability.

When the UT transducer is directed perpendicularly to the material surface, longitudinal waves will be transmitted into the specimen. When these waves hit a material interface (e.g. the specimen backwall), both reflection and transmission of the waves will occur with their ratio depending on the difference in acoustic impedance (product of material density and wave velocity). Material defects constitute extra interfaces and these will result in extra reflection signals and in a decrease of the transmitted signal. These signals can be observed in the time domain (called A-scan) and an electronic gate can be placed at different positions in the time-domain to allow different inspection techniques. For the base-line inspection discussed in this report, the so-called 'reflector-plate' set-up was used with the following inspection techniques (all techniques with one transducer acting both as transmitter and receiver, see figure 1.2):

a) Amplitude measurements

The amplitude of UT reflection signals falling in the electronic gate of the UT unit is measured.

- Double Through-Transmission method (DTT), with the gate of the UT unit placed over the reflector-plate reflection (signal 'd' in Fig. 1.2).
- Pulse-Echo Backwall Reflection method (PEBR), with the gate of the UT unit placed over the backwall reflection of the specimen (signal 'c' in Fig. 1.2).
- Pulse-Echo Flaw Reflection method (PEFR), with the gate of the UT unit placed between the front and backwall reflections of the specimen (signals 'b' and 'c' in Fig. 1.2).

b) Time-of-Flight measurement (TOF)

A wide gate of the UT unit is placed over all relevant reflections behind the reflection of the front surface of the specimen (signal 'b' in Fig. 1.2). Instead of measuring the amplitude of the UT signal now the wave travel time of the reflected UT signal is measured. The relative position of a defect reflection signal on the time base gives information about the depth of the defect. The resulting C-scan is, therefore, often also called 'thickness scan'.

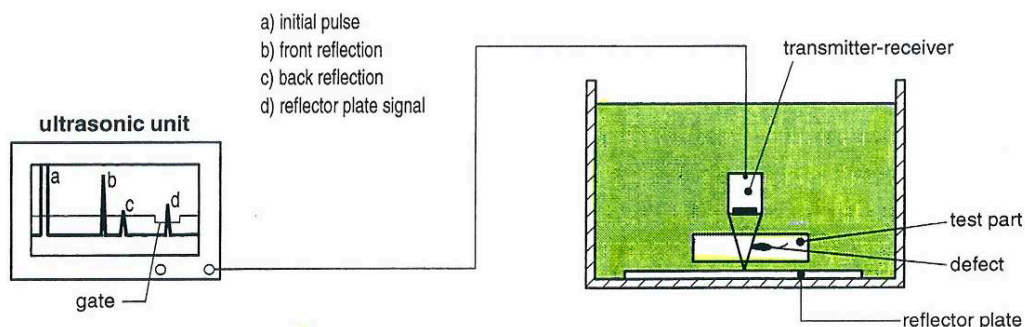


Figure 1.2: Ultrasonic C-scan inspection using the reflector-plate technique in immersion (test part immersed in a water tank)

1.3 In-service ultrasonic inspection

Inspection of parts in service with ultrasonic technique differs from the general automated C-scan inspection procedures after manufacturing. In the first place, the components to be inspected will be in installed position, therefore, the inspection surface will be accessible from one side only. This eliminates the single through-transmission or reflector plate inspection techniques and only leaves the pulse-echo technique as viable option. Secondly, the immersion and water-jet inspection modes are not practical and, hence, the material surface has to be covered locally by a couplant. The resulting basic set-up for in-service UT inspection is depicted in figure 1.3. Different gating positions of the UT unit can again be used to retrieve different defect information modes such as PEBR, PEFR and TOF, as mentioned in section 1.2.

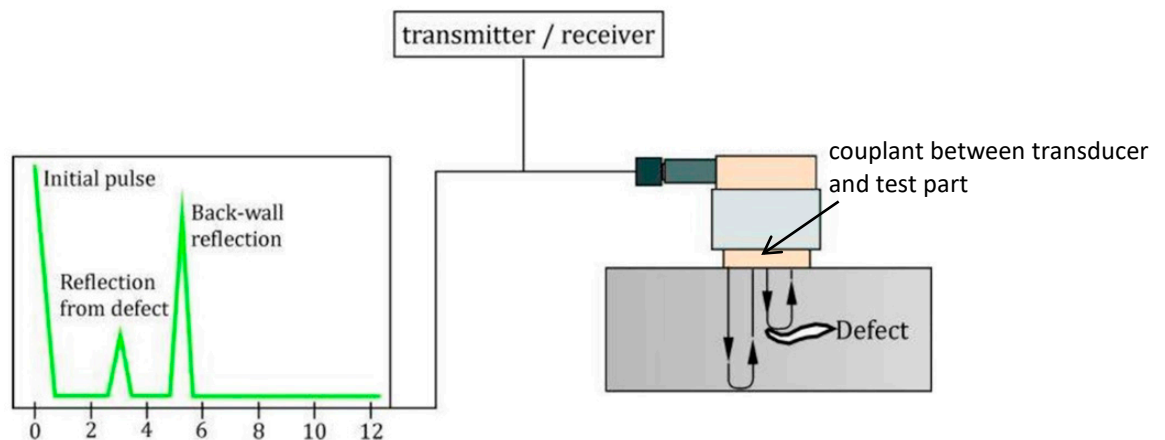


Figure 1.3: Basic set-up for pulse-echo UT used for in-service inspections (left: time-domain UT signals in relative units)

Manual UT inspection with a single UT transducer is a widely accepted method to perform inspection. However, since the probe has only limited size, inspecting a large part can be cumbersome. Small and portable C-scan systems producing a two-dimensional plan view do exist (e.g. Andscan of NDT Solutions Inc., Thetascan of Silverwing UK Ltd, etc.) but a more attractive UT inspection technique has emerged, the so-called phased array ultrasonic technique (PAUT). This is a special UT technique that makes use of transducers consisting of multiple ultrasonic elements (currently up to 256 elements) that each can be driven independently. The PA transducers can have a different geometry (e.g. linear, matrix and annular) and the PA beams can be steered, scanned, swept and focused electronically by applying different electronic time delays to the elements. There is also a special PAUT technique that uses no or only little couplant. An example is the RapidScan™ of Sonatest Ltd. that employs a UT phased array probe housed within a rubber coupled and water-filled wheel probe (Ref. 6), see figure 1.4 (left). The conformable, rubber tyre is acoustically matched to water, providing low loss coupling into the test part. The probe can be used without couplant but, generally, a fine water spray on the test part is used for optimum coupling.

Finally, the Norwegian company DolphiTech AS has developed a handheld, UT imaging camera for fast and real-time UT inspection of CFRP products (Ref. 7), see figure 1.4 (middle and right). The camera, DolphiCam™, presents a high-resolution C-scan image over an area of 31 x 31 mm of the specimen utilising an array of 124 x 124 piezoelectric sensing elements. The array is responsive over a wide array range of ultrasound frequencies (2 – 6 MHz, centre frequency about 3.8 MHz). Different ways of presentation of the inspection result are possible, see for example figure 1.4 for the detection of impact damage in a CFRP specimen. There are two models of the camera: DolphiCam™ model CF08 for the inspection of CFRP material with thickness up to 8 mm and model CF16 for the inspection of CFRP material with thickness up to 16 mm. The difference between the models is the different thickness of the silicone

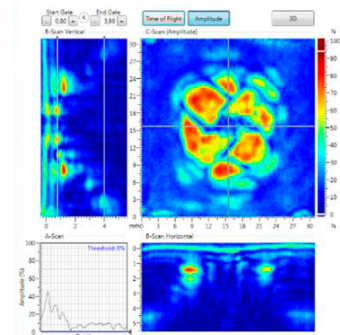
based membrane (functioning as delay line) in front of the transducer (2.8 mm for the CF08 model, 4-5 mm for the CF16 model). The membrane enables dry coupling inspection on painted or shiny surfaces but application of a couplant (e.g. a fine water spray) will always provide a better inspection result.



PAUT RapidScan™



DolphiCam™



A-, B- and C-scans

Figure 1.4: PAUT RapidScan™ (left, Ref. 6) and DolphiCam™ with different ways of presentation of impact damage (middle and right, Ref. 7)

2 Laser ultrasonic inspection

Laser Ultrasonics (LU) is a special UT technique that does *not* require physical contact with the structure under inspection. This is realised by employing laser scanning systems for both the excitation (generation) and the reception (detection) of ultrasonic waves with one-sided access of the structure to be inspected, see figure 2.1. As shown in this figure, two co-linear laser beams scan the part to be inspected. The generation laser beam (pulsed laser) produces non-destructively, by thermo-elastic effect, a stress at the surface of the part. This in turn produces an ultrasonic wave launched perpendicular to the surface (longitudinal wave), independent of its shape and of the laser beam orientation. For completeness, it is noted that also additional (spurious) waves may be generated (shear, Rayleigh and Lamb waves), which may complicate the analysis of target longitudinal waves (in pulse-echo or transmission modes). Ultrasonic waves reflected or scattered by the back-wall or flaws are finally detected by the detection laser beam and an optical interferometer (e.g. confocal Fabry-Perot or photorefractive interferometer), which senses the Doppler shift of the scattered light produced by the ultrasonic surface motion. Received signals are further processed as in conventional ultrasonic inspection to display A-scans, B-scans and C-scans (Ref.8).

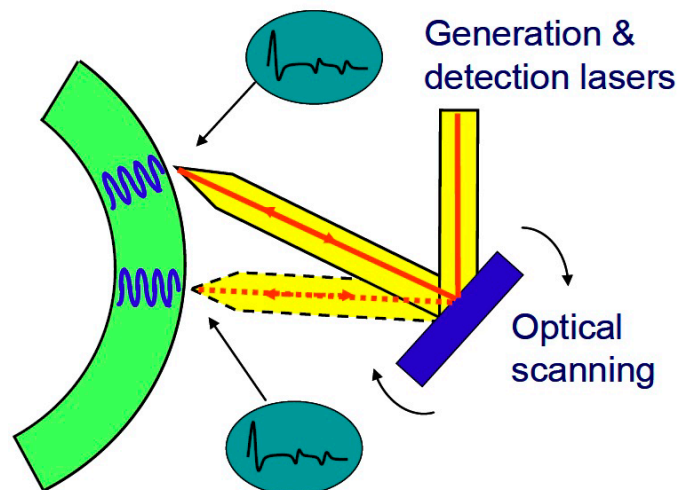


Figure 2.1: Principle of laser-ultrasonics for contoured part inspection. Depiction of the inspection of two locations, determined by the optical scanner (Fig. 1 from Ref. 8)

Being non-contact and the necessity of only one-sided access to the structure under inspection makes LU very suitable for fully automated application during production and in-service inspections. An example of LU for in-service application is given in figure 2.2, showing the inspection of the fuselage of a CF18 in a maintenance hangar and the resulting C-scan of the horizontal stabilizer made of composite material. A folding mirror was herewith used for steering the beams upwards for underneath inspection. An additional advantage of LU is the high tolerance relative to the incidence angle of the laser beam with the part ($\pm 20\text{-}35^\circ$) and to the distance between the scanning laser head and the part (typically between $\frac{1}{4}$ m and 2 m, Ref. 5). Other advantages of LU are that it can be used on both composite and metallic structures, that surface preparation and paint removal are not necessary, and that it can be used in ambient or high temperatures (Refs 9 and 10). As a result, the inspection time can be significantly reduced, especially for the inspection of large, complex shaped parts.

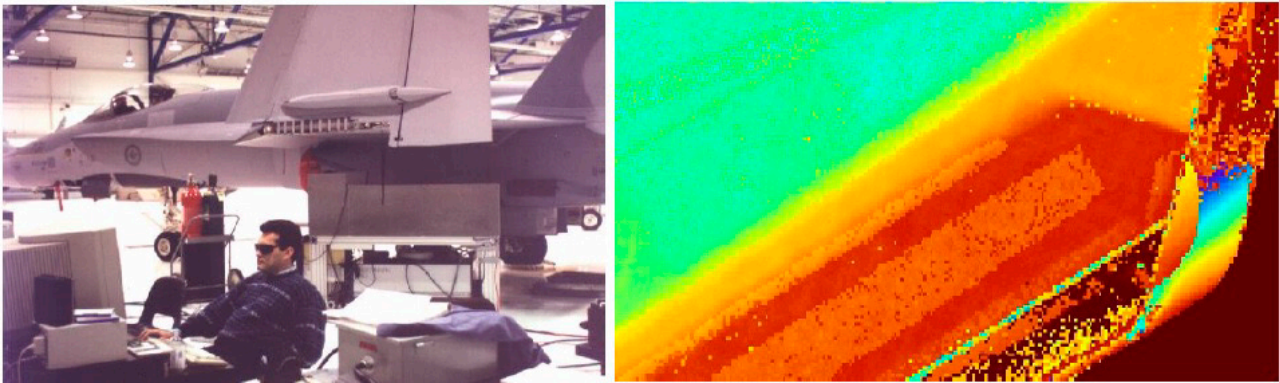


Figure 2.2: LU in-service inspection of a CF18 and resulting C-scan of the horizontal stabilizer (Fig. 4 from Ref. 8)

The generation of the UT waves in the material under inspection is a critical issue. Ideally, the generation process is non-destructively and governed by the thermo-elastic effect. The process, however, is different for composite and metallic structures and is dependent on the type of laser and its wavelength, pulse width and energy. In any case, ablation of the surface caused by too high pulse energy should be avoided. In this respect, the inspection of composite materials is easier than metals because the presence of a thin epoxy layer at the outer surface (without fibres, thickness about 10 to 100 μm) allows better penetration of the laser pulse in the material. Absorption of the laser energy then produces a local temperature elevation which, in turn, creates a local thermal expansion. This sudden thermal expansion generates mainly longitudinal UT waves in a direction normal to the surface, independent of the angle of incidence (Ref. 11). For metals, on the other hand, ablation of the surface occurs more easily and the laser excitation generally results in a more complex combination of wave types (e.g. longitudinal, transverse and surface waves). In this report, however, only the LU inspection of composite materials will be considered. Further, an important difference between LU and conventional UT signals is their bandwidth: LU signals are typically significantly more broadband yielding higher ultrasonic frequencies in the signal that can result in some difficulties in the analysis of the reflection signal responses (Ref. 11).

LU systems often use a pulsed CO_2 laser for the generation of UT waves because its infrared wavelength (10.6 μm) is strongly absorbed in most organic materials (Ref. 11). A disadvantage of this wavelength, however, is that the laser beam cannot be coupled into flexible, optical fibres and that rigid, mirror reflection systems have to be used to steer and manipulate the laser beam towards the inspection surface. This limits the use for in-service inspections. This is also the reason why present LU systems more frequently use generation lasers working at shorter wavelengths such as Nd:YAG lasers with wavelength of 532 (green) or 1064 nm. At these wavelengths, the laser light can be coupled into optical fibres yielding much more flexible UT systems. A disadvantage of the shorter wavelength, however, is that ablation of the surface occurs more easily. Reference 12 and 13 present a good overview of the differences between the various generation laser types. As discussed in these references, the recent use of optical parametric oscillator (OPO) lasers working at a mid-range wavelength of about 3 to 4 μm . The objective of the use of mid-infrared (MIR) generation lasers is to combine both advantages of visible/near infrared and far-infrared generation lasers. Reference 13 also describes the development of a fully-fibre coupled LU head with MIR OPO generation to put on a robot arm for the NDI of CFRP components.

Besides the obvious advantages of LU inspection (e.g. non-contact, one-sided access and high tolerance relative to the incidence angle of the laser beam) there are also some limitations. References 9 and 10 mention for example the following limitations: high cost of equipment, limited portability of current systems, laser safety issues, sensitivity to environmental vibrations, risk of ablation/discolouration of the material surface, and broadband signal with limited strength at particular frequencies (possibility of lower depth coverage). As already mentioned in the Introduction, however, there are recent developments in LU systems that claim having overcome important limitations.

2.1 LUT Hardware

There are a number of companies that develop and produce LU systems, even fully robotised. The drawback of these systems, however, is their cost price. For example, the Spanish company Tecnatom S.A. and the American company PaR Systems Inc. produce LU systems that have a cost price far exceeding 1 M€. Figure 2.3 illustrates the LUCIE system of Tecnatom S.A. while inspecting a composite fuselage part. With the LUCIE system, the twofold scanning laser head (one laser for the interrogation and generation of ultrasound in the part and another, almost co-linear laser interferometric system for the detection of UT reflection signals) is mounted on a robot that can scan a complex shaped part following a predetermined scan profile.



Figure 2.3: LUCIE system of the company Tecnatom S.A. inspecting an Airbus composite fuselage part (Ref. 14)

However, there are recent developments in LU systems at lower cost price. For example, the American company Optech Ventures LLC produces a small LU system for less than 200 k€ that employs a fixed laser measurement head while the part is translated/scanned in front of this measurement head, see figure 2.4 (left). The company can also deliver, at higher cost, a system with a robot-mounted laser measurement head, see figure 2.4 (right).

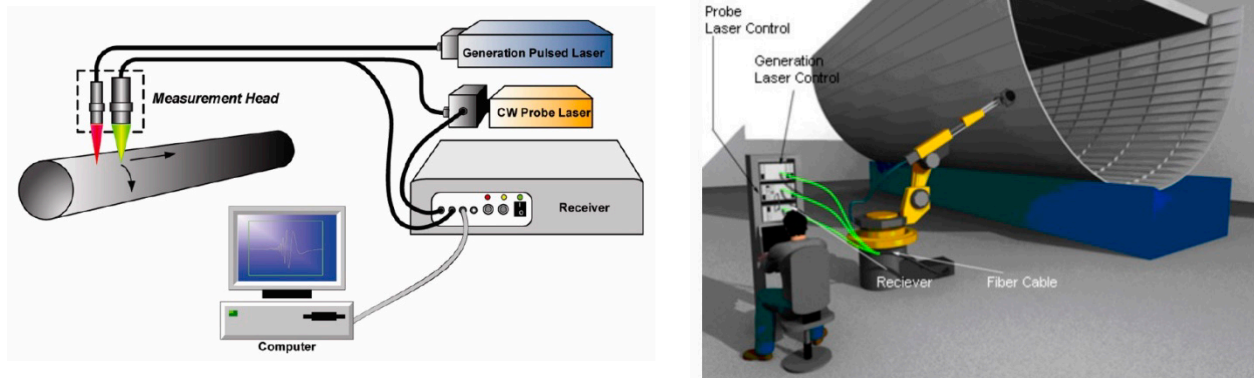


Figure 2.4: LU systems of Optech Ventures LLC, basic system (left) and robotised system (right) (Figs. from Ref. 15)

The Canadian Company Tecnar has recently delivered to Boeing a turn-key laser ultrasonics robotic system for the inspection of large aerospace structures, see figure 2.5. Tecnar laser-ultrasonic equipment is modular and can also be sequentially acquired. A basic turn-key system amounts to 350 k€.



Figure 2.5: Tecnar Ultimate laser ultrasonic system (Ref. 16)

The robotised Tecnar Ultimate system combines:

1. Pulse detection laser (Nd:YAG): Proprietary long-pulse, high-power frequency stabilized laser.
2. Control unit: Adapted, computer-controlled data acquisition, processing and storage.
3. Detection interferometer: Robust laser-ultrasonic detection unit based on a fast-response photorefractive crystal.
4. Generation laser (Nd:YAG): Short-pulsed laser for non-contact ultrasound generation and
5. Optical probe.

In recent years the NLR has had contact with the South Korean company Space NDT (X-NDT) Inc. This company has developed a special and low-cost (about 160 k€, price level 2015) LU technique called Ultrasonic Propagation Imaging (UPI). The technique employs one scanning laser system and one piezoelectric transducer (e.g. PZT) that is mounted at a fixed location on the test part, see figure 2.6. The scanning laser generates different wave types at each grid point of the scan area after which the piezoelectric sensor records the response of a guided wave having travelled the distance between grid point and sensor. The responses of each grid point are collected and further processed with different

algorithms. Present defects change the responses of the guided waves and can therefore be identified in the resulting C-scan presentations. There is also a UPI version where the guided wave responses are not collected with a surface mounted piezoelectric sensor but with a fully noncontact laser Doppler vibrometer system directed at a fixed location of the test part.

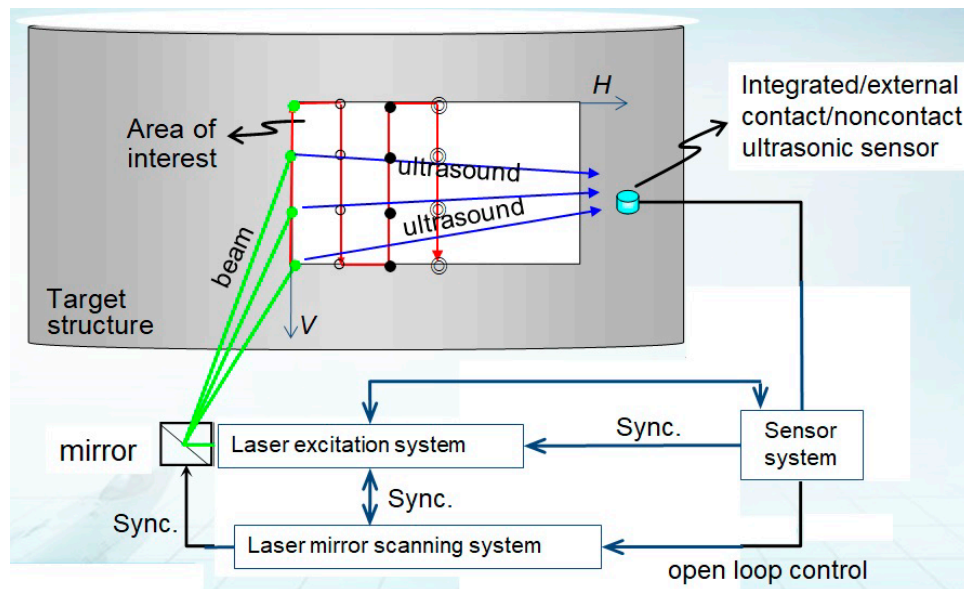


Figure 2.6: LU inspection using the Ultrasonic Propagation Imaging (UPI) technique (Ref. 17)

A drawback of the UPI technique employing guided waves is the complexity of wave transmission through composite materials with their high anisotropy. X-NDT Inc. has developed a number of visualization algorithms such as UWPI (space-time domain representation of the wave field), USI (ultrasonic spectral imaging to visualize defects in the frequency domain), WUPI (wavelet-transformed ultrasonic propagation imaging), AWPI (anomalous wave propagation imaging) and VTWAM (variable time window amplitude mapping), see reference 18, but the sensitivity, accuracy and reliability of defect detection remains limited when compared to standard UT inspection with perpendicular interrogation and employing longitudinal waves. However, X-NDT Inc. has recently developed a relatively low-cost LU system (about 240 k€) that does work in a pure pulse-echo mode (PE-UPI) while using longitudinal waves (Refs 19 and 20, Fig. 2.7). This system is of interest for the DCMC round robin test program.



Figure 2.7: PE-UPI laser ultrasonic system of the South Korean company X-NDT. Field inspection of a T-50 horizontal stabilizer (Ref. 21)

An in-service laser ultrasonic inspection system can be bought as turn-key system or as a modular system, where the user develops a part of the hardware and/or software. Turn-key systems are rather expensive, but hardware (robot, LUT-equipment) and software are included. Normally, extension of the applicability of the in-service inspection features requires modifications by the supplier. Another route is to purchase a modular laser ultrasonics system and further develop the hardware and/or own acquisition and processing software. The purchase costs are lower, but much research effort has to be invested in further developments.

2.2 LUT processing software

Software related to turn-key LUT equipment consists of:

1. Robotic software for scanning and damage avoidance.
2. Synchronisation of generation and detection lasers.
3. Data-acquisition software for the detection laser.
4. Various post-processing software (at different scientific levels) for calculating A, B and C scans and defect analysis and
5. Presentation software plotting the found defect parameters on a drawing/picture of the investigated object.

One should be aware when the choice is made to partly develop own software, a considerable effort is required. It is expected that the LUT data-bases are very substantial based on the consideration that the ultrasonic test frequencies are rather high.

2.3 Selection of LUT hardware for DCMC round robin

A DCMC Round robin program has started on laser ultrasonic testing (LUT). The following equipment has been selected on basis of the equipment described in section 2.1 to participate in the program:

1. X-NDT PE-UPI
2. Tecnatom TechnaLUS
3. Xarion optical microphone
4. Tecnar
5. Optech Ventures

3 Round robin composite specimens

The capability of the laser ultrasonic PE-UPI for the detection of relevant in-service defects was investigated using three composite specimens: two CFRP specimens with artificial delaminations/disbonds and impact damages, and one thick RTM specimen with flat-bottomed holes (FBH).

3.1 CFRP specimens

At NLR, a composite benchmark of five CFRP specimens being relevant for aircraft and helicopter primary structures is available and served as reference for the evaluation of selected NDI methods. The specimens comprised the following structural details: a solid laminate (two thicknesses, 2.7 and 5.4 mm), a solid laminate with T-shaped stiffeners, a plain sandwich structure, and a chamfered sandwich structure with L-shaped ribs/frames. Two specimens from this benchmark were selected for the present investigation: the solid laminate with T-shaped stiffeners (NLR-B) and the chamfered sandwich structure (NLR-D).

The material of the CFRP specimens is based on carbon fabric (HTA Aerospace grade carbon fibres and HexPly M18-1 resin). For the sandwich specimens a Hexcel HRH-10 Nomex[®] honeycomb core with thickness 19 mm and cell size 5 mm was used. The specimens include a number of the following real and artificial defects: low-velocity impact damages, interply delaminations in the (outer) skin and disbonds. The low-velocity impact damages in the specimens were created by means of a guided drop weight device with an impactor with hemispherical steel tup of diameter 0.5 or 1.0 inch. The interply delaminations and disbonds were simulated by Tygavac TFG 075/1 foils of different diameter (Fothergill Tygaflor Ltd.). Tygavac is a non-porous PTFE (Teflon) coated glass fabric with a nominal thickness of 0.075 mm. All specimens were provided, before impact, with a standard paint system used on military weapon systems (Aerodur 37047 CF primer and PUR-Declack topcoat).

3.1.1 Specimen NLR-B

Specimen NLR-B is a solid laminate with three T-shaped stiffeners, see figure 3.1 for a structural detail. The laminate has dimensions of 485 x 294 mm, with thickness 6.0 mm. The laminate is 24 layers with quasi-isotropic lay-up. The stiffener pitch is 100 mm. The specimen contains the following defects (21 in total):

- Impact damages with impact energy in the range of 20 to 70 Joule. The impacts are inflicted both mid-bay and on the edge of the stiffeners.
- Interply delaminations in the skin simulated by Teflon foils of diameter 0.25, 0.5 and 1 inch, and placed at three different through-the-thickness positions (depths of 0.75, 2.25 and 5.25 mm).
- Skin-to-stiffener disbonds simulated by Teflon foils of diameter 0.25, 0.5, 1 and 2 inch.

Figure A1 in Appendix A gives an overview of the specimen with all defect locations.

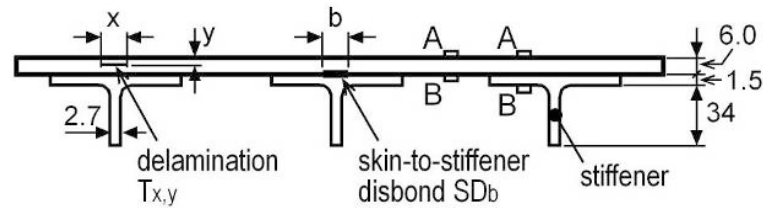


Figure 3.1: Structural detail of specimen NLR-B, a solid laminate with three T-shaped stiffeners

3.1.2 Specimen NLR-D

Specimen NLR-D is a chamfered sandwich structure with three L-shaped ribs/frames, see figure 3.2 for a structural detail. The panel has dimensions of 905 x 800 mm, with outer/inner skin thickness 3.0/1.5 mm. The Nomex honeycomb has a height of 19 mm. The outer skin laminate is 12 layers with quasi-isotropic lay-up; the inner skin laminate is 6 layers with quasi-isotropic lay-up. The specimen contains the following defects (22 in total):

- Impact damages with impact energy in the range of 20 to 70 Joule. The impacts are inflicted both mid-bay and on the stiffeners.
- Interply delaminations in the outer skin simulated by Teflon foils of diameter 0.25, 0.5 and 1 inch. The foils are placed at the rib/frame locations and at three different through-the-thickness positions (depths of 0.75, 1.50 and 2.25 mm).
- Skin-to-rib/frame disbonds simulated by Teflon foils of diameter 0.25, 0.5, 1 and 2 inch.

Figure A2 in Appendix A gives an overview of the specimen with all defect locations.

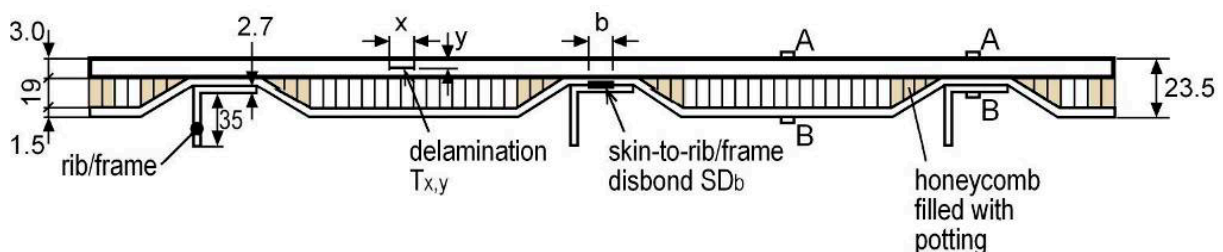


Figure 3.2: Structural detail of specimen NLR-D, a chamfered sandwich structure with three L-shaped ribs/frames

3.2 RTM calibration specimen #2118

Specimen #2118 is an RTM specimen with flat-bottomed holes (FBH), see figure 3.3. The specimen was made for calibration purpose of UT inspection of thick-walled composite parts. The dimensions of this specimen are 200 x 100 x 27.4 mm. The material of the specimen is based on carbon fabric (Tenax HTA 5131 carbon fibres and Cytec Cycom 823 resin). The laminate is 92 layers with quasi-isotropic lay-up. The specimen has 17 FBH's of which 15 FBH's comprise all combinations of 3 diameters (6, 8 and 12 mm) and 5 hole depths (4.4, 8.9, 13.1, 18.0 and 22.5 mm). Furthermore, 2 FBH's both of diameter 6 mm are included for evaluation of the near-surface resolution; the depth of these holes is 1 mm below the surface (one hole relative to the front surface and the other hole relative to the back surface). Table 2 specifies the diameter and the distance to the front surface (inspection surface) for the different FBH's.

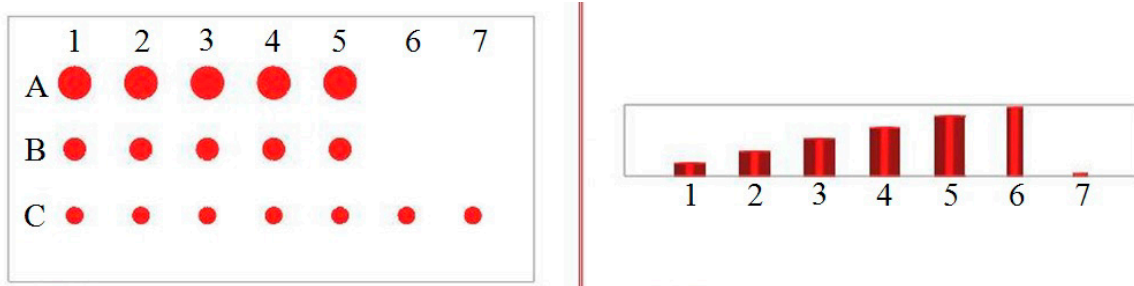


Figure 3.3: RTM calibration specimen #2118 with flat-bottomed holes

Table 3.1: Diameter and distance to front surface for the FBH's in RTM specimen #2118

FBH No.	1	2	3	4	5	6	7
A \varnothing 12 mm	22.5	18.0	13.1	8.9	4.4	-	-
B \varnothing 8 mm	22.5	18.0	13.1	8.9	4.4	-	-
C \varnothing 6 mm	22.5	18.0	13.1	8.9	4.4	1	26.4

4 Test equipment description and test results of the round robin

4.1 NLR C-scan conventional ultrasonic inspection as baseline reference

4.1.1 NLR C-scan facility

Ultrasonic C-scan inspections can be carried out with dedicated multi-axis scan systems. Figure 4.1 shows the C-scan equipment at NLR. It is a 12-axis scanner of Ultrasonic Sciences Ltd. with a scan window of 4.0 x 2.5 x 2.5 m. It can be used both in the immersion and water-jet inspection mode. Complex geometry components (double curved) can be scanned with both the pulse-echo and through-transmission technique.



Figure 4.1: Ultrasonic C-scan equipment at NLR

4.1.2 Experimental results

Base-line ultrasonic inspection of the three specimens was carried out using the C-scan equipment shown in figure 4.1 and the UT techniques depicted in figure 1.2 and described in Chapter 1.2 (UT gate techniques DTT, PEBR, PEFR and TOF). Most measurements were done in immersion using focused UT transducers, yielding the highest sensitivity of inspection. Only for the chamfered sandwich structure NLR-D, an additional inspection in single through-transmission mode (TT) with two UT transducers (focused transmitter and straight-beam receiver) was done using water-jets to enable the determination of the quality of the honeycomb material (due to its high attenuation for ultrasound).

The results of the base-line UT C-scan inspections were taken from earlier investigations, viz. reference 1 for specimens NLR-B and NLR-D and reference 7 for specimen #2118.

4.1.2.1 CFRP specimen NLR-B

All base-line C-scan measurements for specimen NLR-B were done in immersion using a 5 MHz focused transducer (IM-5-19-R80, S/N 2753 B101). The instrument settings for these measurements are given in reference 1. The inspection results are given in Appendix B.1, figures B1 – B4. An overview of the results is given in figure 4.2.

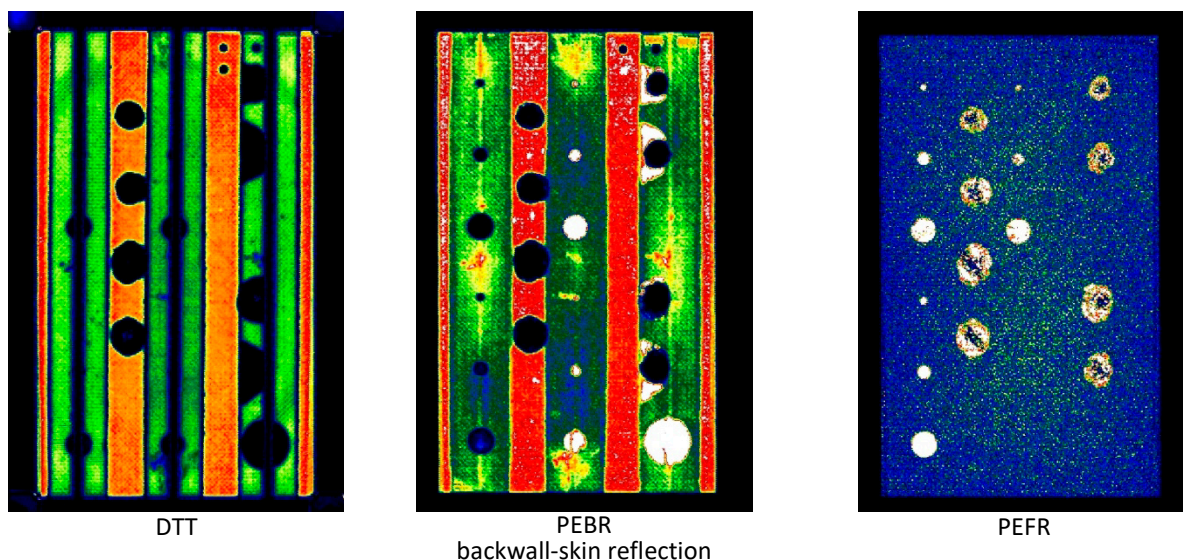


Figure 4.2: Overview of baseline UT C-scan inspection results for specimen NLR-B

The base-line UT C-scan results for specimen NLR-B have been discussed in detail in reference 1. In summary, we can say that the combination of different inspection techniques (DTT, PEBR and PEFR) resulted in the reliable detection of almost all defects in the panel. Only one small defect with size of 6 mm (skin-to-stiffener disbond SD1) was qualified as detectable with limitation. The sizing of defects is fairly accurate but deviations in the range of 1 to 2 mm can easily occur. The depth estimation of defects has a varying accuracy but, generally, it is very accurate with deviations in the range of only 0.1 to 0.2 mm.

4.1.2.2 CFRP specimen NLR-D

Most base-line C-scan measurements for specimen NLR-D were done in immersion using a 5 MHz focused transducer (IM-5-19-R80, S/N 2753 B101). An additional single through-transmission inspection (TT) was done with water jets with a 2.25 MHz focused transmitter (IM-2.25-19-F76, S/N 2913 0101) and a 2.25 straight-beam receiver (IM-2.25-19R118, S/N 2913 B101). The instrument settings for these measurements are given in reference 1. The inspection results are given in Appendix B.2, figures B5 – B8. An overview of the results is given in figure 4.3.

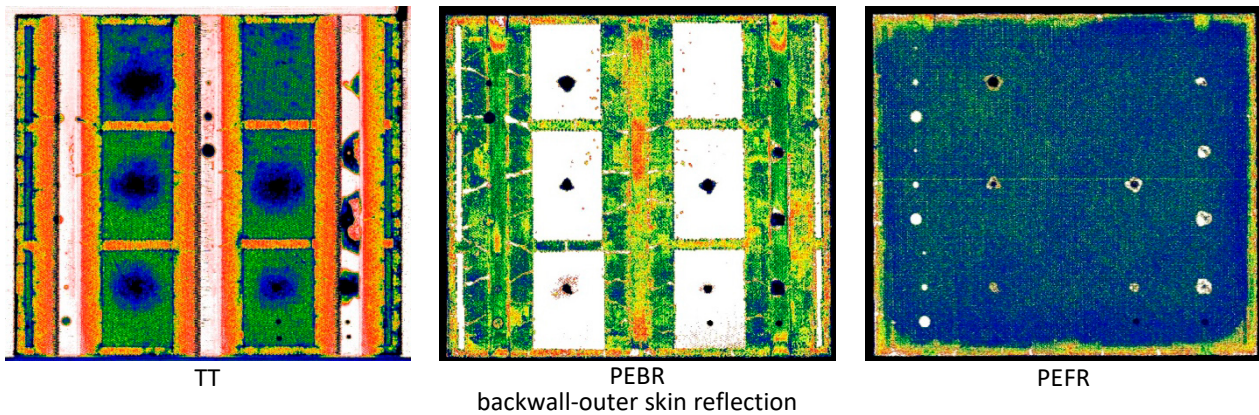


Figure 4.3: Overview of baseline UT C-scan inspection results for specimen NLR-D

The base-line UT C-scan results for specimen NLR-D have again been discussed in detail in reference 1. In line with NLR-B specimen, the conclusions are similar to those for specimen NLR-B. Only the small skin-to-stiffener disbond SD1 (diameter 6 mm) was qualified as detectable with limitation, similar to the results from NLR-B. Moreover, the conclusions for defect sizing and depth estimation are similar, with one remark that the largest disbond SD4 in panel D was largely undersized (37 instead of 51 mm).

4.1.2.3 RTM specimen #2118

All base-line C-scan measurements for RTM specimen #2118 were done in immersion using a 2.25 MHz focused transducer (IM-2.25-19-F76, S/N 2913 0101). The instrument settings for these measurements are given in reference 7. The inspection results are given in Appendix B.3, figures B9 – B10. An overview of the results is given in figure 4.4.

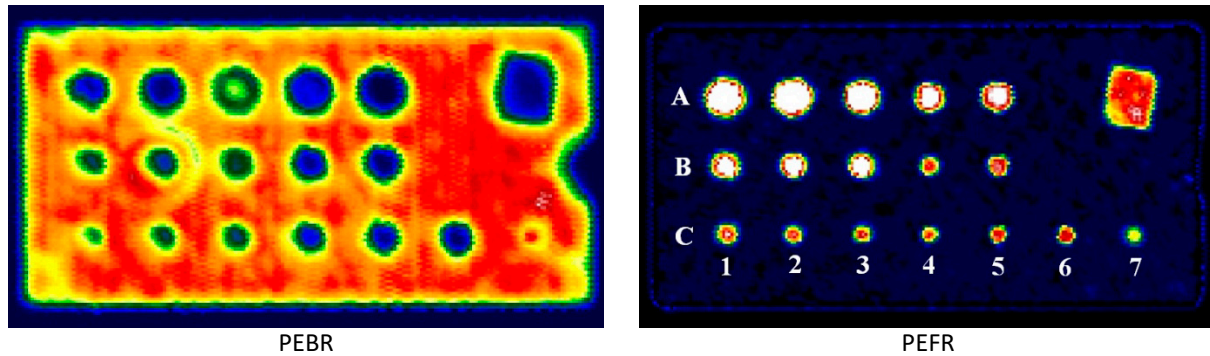


Figure 4.4: Overview of baseline UT C-scan inspection results for RTM specimen #2118

The base-line UT C-scan results for RTM specimen #2118 generated DAC/TCG application (Distance Amplitude Curve & Time Corrected Gain) have been discussed in detail in reference 7. The figures show that the combination of the different gating techniques (PEBR, PEFR and TOF) provides a reliable detection of all FBH's, both in location and depth. Also the FBH's located near the front and back wall surface are well detectable which confirms a good near- and far surface resolution. The PEFR inspection clearly shows the best detection performance. The defect indication in the upper right corner is the detection of a foil which was erroneously left during manufacturing of the specimen. The analysis in reference 7 showed that the PEFR inspection also yielded the most accurate sizing of the FBH's, with a maximum error of 3 mm for the larger holes (diameter 12 mm) at larger depths. The last is most probably due to the increasing beam width caused by beam spread at larger depth. And finally, the analysis showed that the TOF scan (Fig. B10) could not detect FBH C7 (located 1 mm from the back wall) due to the dynamic range of the selected colour palette. On the other hand, the TOF scan could accurately determine the depth of the other FBH's with a maximum deviation of less than 1 mm.

4.2 X-NDT UPIs PE

4.2.1 X-NDT equipment

Laser ultrasonic inspection of the three specimens was carried by the South Korean company X-NDT using the PE-UPI system shown in figure 2.7 and figure 4.5. The test report of the measurements is given in ref. 23 and test results are analysed and reported by Heida in ref. 24. A summary of this report is included in Appendices B, detailed baseline NLR C-scan results on the three test panels. The X-NDT UPI PE test results are summarized in Appendices C.

Figure 4.5 gives a schematic view of the PE-UPI system. The scanning laser head contains both the generation laser (for the interrogation and generation of ultrasound in the part) and the sensing laser (laser Doppler vibrometer for the detection of UT reflection signals). The two laser beams are directed towards the specimen in a co-linear way using an internal mirror system inside the scanner laser head. This laser head is coupled to a 2-axis translation mechanism in order to make a 2-dimensional C-scan of the specimen (scan in vertical direction, index in horizontal direction, maximum scan area about 500 x 500 mm²). The generation laser is a Q-switched Nd:YAG laser working at a wavelength of 1064 nm. Q-switching is a technique by which a laser can be made to produce a pulsed output beam (Ref. 25). The energy of the Q-switched laser pulse was set at 4 mJ for the present investigation.

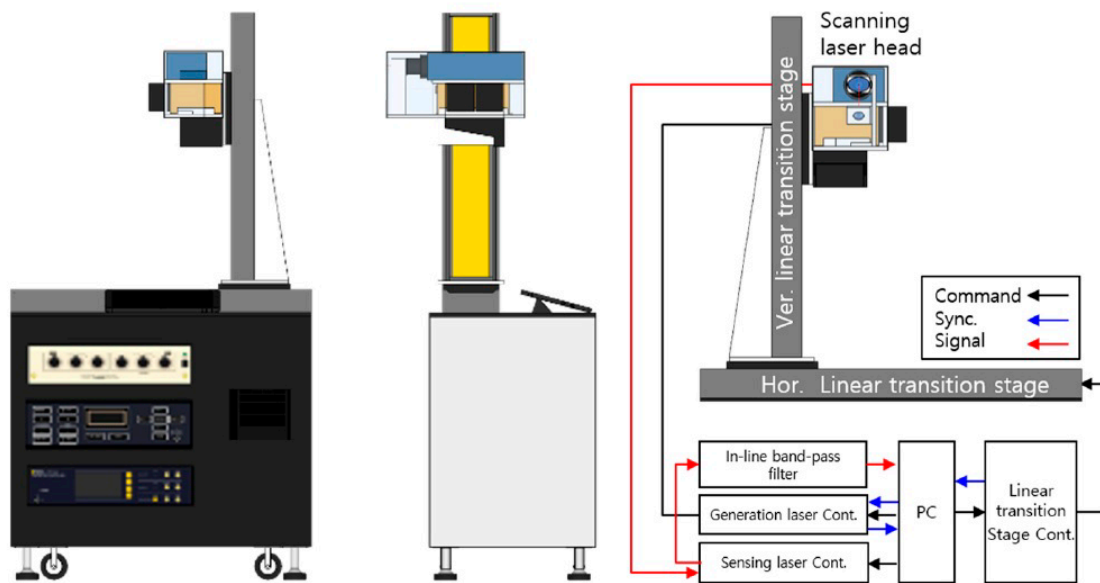


Figure 4.5: Schematic view of the PE-UPI system of the South Korean company X-NDT, Inc. (Ref. 21)

The reflected UT wave signals are acquired by a 633 nm laser Doppler vibrometer with a sensitivity of 10 (mm/s)/V. The acquired signals are generally band-pass frequency filtered. The complete waveforms for each laser impingement point on the specimen are stored and used to make a full-field ultrasonic wave propagation imaging (UWPI) movie, in fact a 3-dimensional video of the 2-dimensional sequential display of the reflected UT wave amplitudes in time. After that, a number of post image processing algorithms can be applied of which the variable time window amplitude map (VTWAM) algorithm is most important. With the VTWAM algorithm it is possible to visualize the damages by mapping the average signal values in a chosen specific time range from the UWPI data, see figure 4.6. It is also possible to add the image amplitudes of multiple time ranges to produce one image that includes all defects at different depths (mVTWAM image).

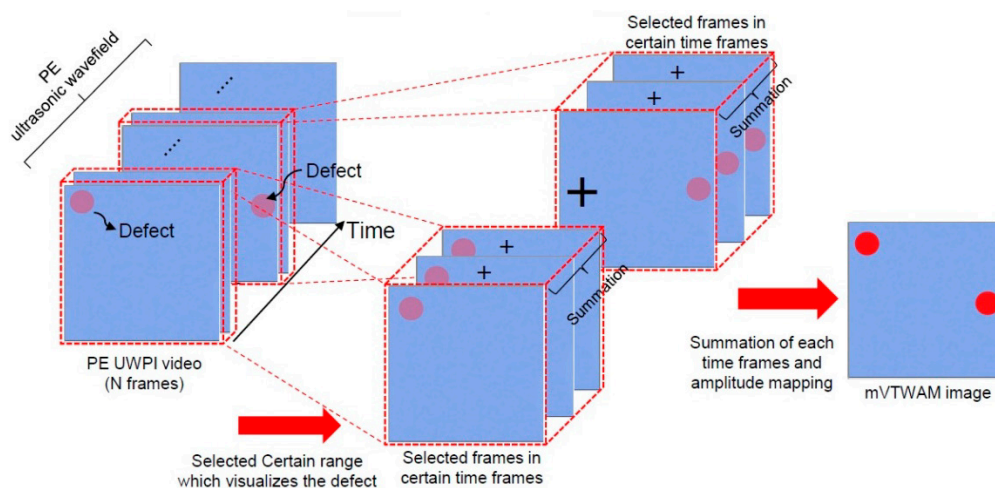


Figure 4.6: Data visualization with the variable time window amplitude map (VTWAM) algorithm (Ref. 24)

Figure 4.7 shows the PE-UPI system in more detail and in action for measurement on specimen NLR-D. The system is portable with a weight of about 130 kg. For all measurements a stand-off distance (specimen to laser head) of 0.6 m was used. Scanning at farther distances is possible but as the laser ultrasonic sensor has local sensitivity maxima at every 0.2 m. Shorter distances are also possible and can be chosen in the same way. The scan speed was 1 kHz pulse repetition rate (PRR) with a 0.25 mm spatial interval for all measurements.



Figure 4.7: PE-UPI system in different views (left) and inspecting specimen NLR-D (right)

4.2.2 Experimental results

Contrary to the other tests, the experiments on the three test panels were not witnessed by NLR-staff.

4.2.2.1 CFRP specimen NLR-B

The PE-UPI inspection results for specimen NLR-B are given in Appendix C, figures C1 and C2. A scan area of 480 x 290 mm² was used for this specimen. The UWPI movie in figure C1 contains the sequential display of all individual C-scan images of the reflected UT wave amplitudes in time over a total time period of 51.1 μ s. It is a whole propagation video in which the defects are visualized in different time, providing depth information. Figure C2 shows two examples (freeze frames) of the UWPI results at the specific times of 11.7 and 13.4 μ s. These times have been selected by the PE-UPI system operator as being relevant and providing information about the presence of defects in this panel. The choice for these freeze frames, however, is a user's choice based on experience with the PE-UPI system. Obviously, other freeze frames can also be selected, and figure 4.8 gives three more examples at different propagation times. The different images in this figure clearly show the different views of present defects and structural details such as the presence of three stiffeners.

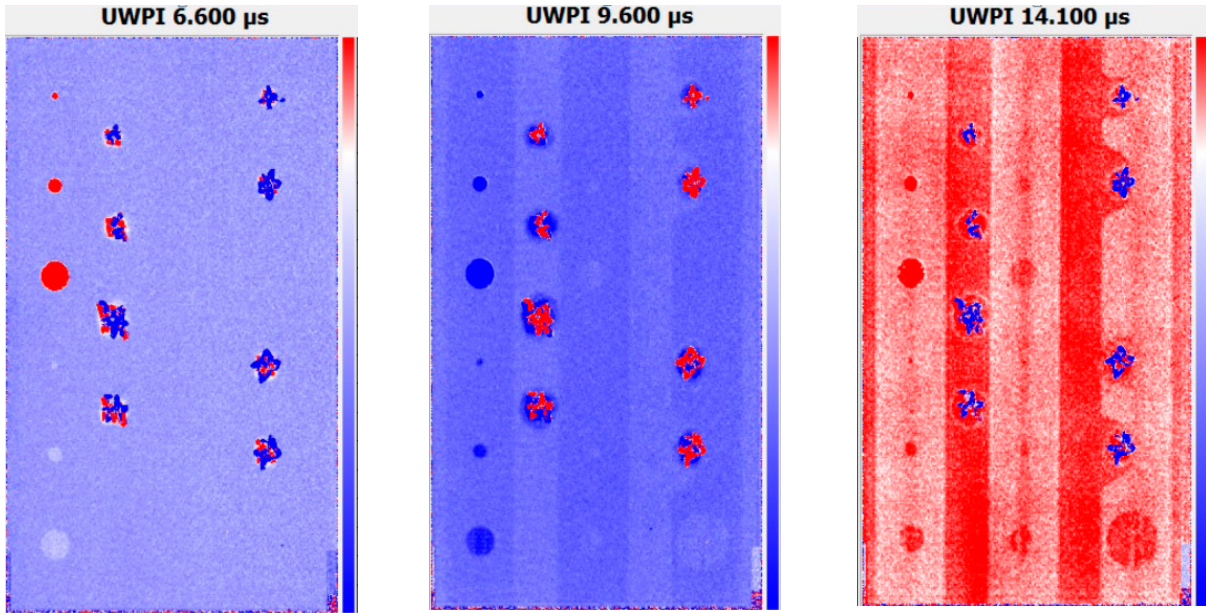


Figure 4.8: Selection of three PE-UPI freeze frames at different times from the UWPI wave propagation movie of panel NLR-B

From the UWPI data, two relevant time ranges were selected by the PE-UPI system operator and further processed to produce VTWAM amplitude images, see figure C2. These figures have also been included in figure 4.9 together with the NLR-B specimen drawing from figure A1. The figure shows that almost all defects in the panel (impact damages, artificial delaminations and disbonds) are reliably detectable. Only one small defect with size of 6 mm (skin-to-stiffener disbond SD1) is qualified as detectable with limitation. This is, in fact, the same conclusion as was drawn for the baseline UT C-scan inspection, see Chapter 4.1. Also the sizing of the defects is of the same accuracy (in the range of 1 to 2 mm diameter).

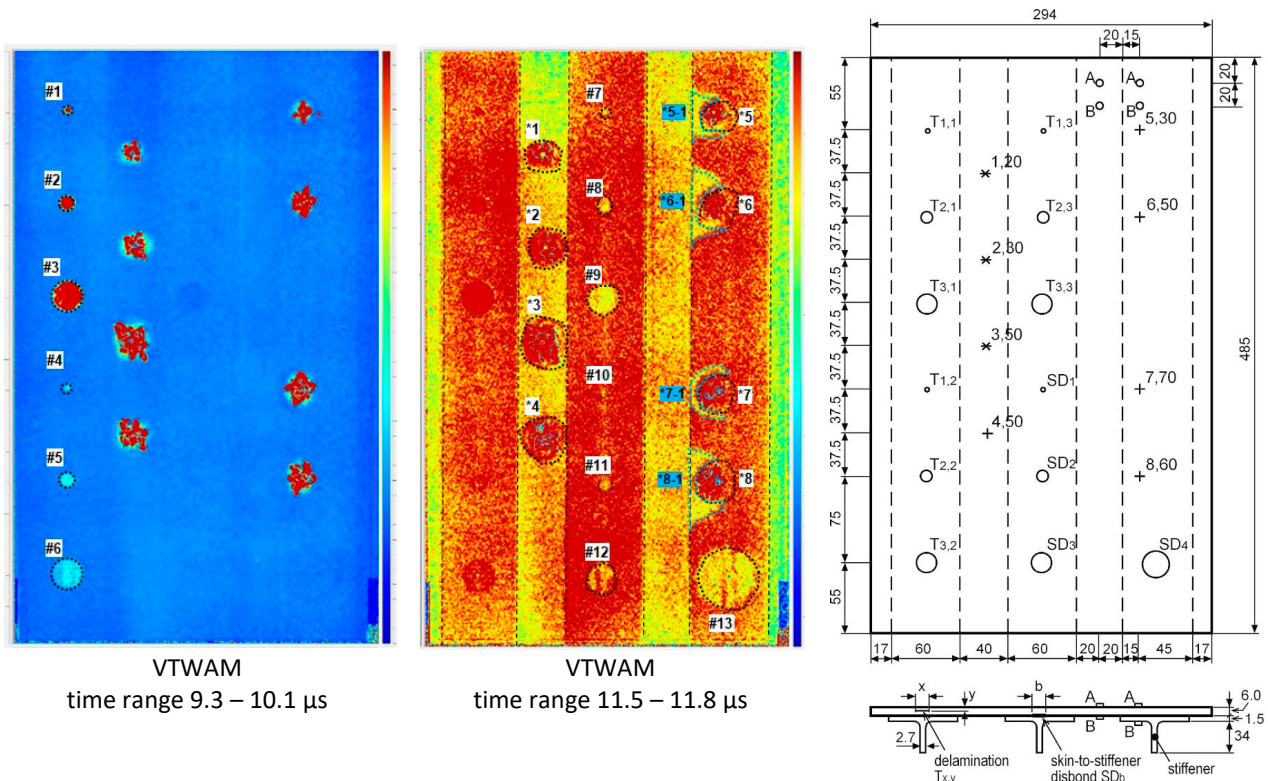


Figure 4.9: PE-UPI VTWAM results of two time ranges from the UWPI wave propagation movie of panel NLR-B

Figure 4.10 gives a comparison of the PE-UPI VTWAM results with baseline UT C-scan results (PEFR and PEBR images). The figure shows that the baseline UT-scan images give a slightly better definition of the defects and their size and the presence of substructure (stiffeners) is also more clearly defined. However, this can also be expected because the baseline C-scan inspection was performed with a coupling medium (immersion mode) and used a focused UT transducer. All-in-all, it can be concluded that the PE-UPI system is capable of detecting relevant defects and that it is, hence, a viable option for in-service UT inspection of structures similar to the panel NLR-B configuration.

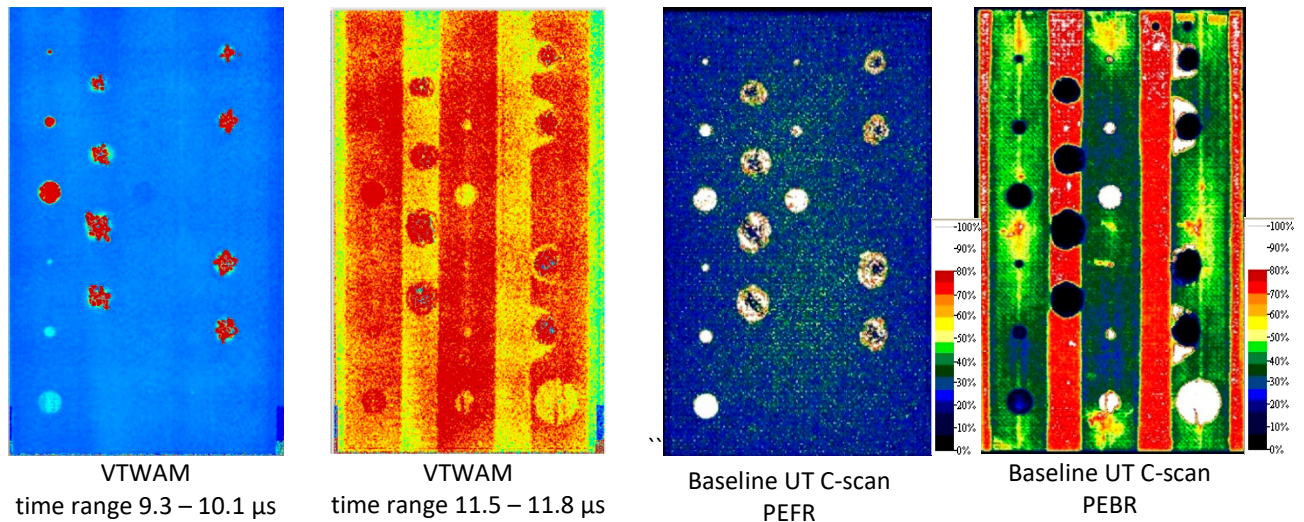


Figure 4.10: Comparison of PE-UPI VTWAM results with baseline UT C-scan results of panel NLR-B

4.2.2.2 CFRP specimen NLR-D

The PE-UPI inspection results for specimen NLR-D are given in Appendix C, figures C3 – C5. Because of the large size of the specimen and the limitation in scan range of the PE-UPI system the specimen was scanned in two parts with scan area of 420 x 900 mm² each. The two UWPI movies in figures C3 and C4 contain again the sequential display of all individual C-scan images of the reflected UT wave amplitudes in time over a total time period of 51.1 μ s. Figure C3 shows two examples (freeze frames) of the UWPI results of the left side of panel NLR-D and figure C5 two examples of the UWPI results of the right side of the panel. These times have again been selected by the PE-UPI system operator as being relevant and providing information about the presence of defects in this panel. Figure 4.11 includes the two UWPI freeze frames of the panel right side and an additional freeze frame at the specific time of 10.5 μ s. The different images in this figure clearly show the different views of present defects and structural details such as the presence of the ribs and honeycomb (filled or not filled with potting).

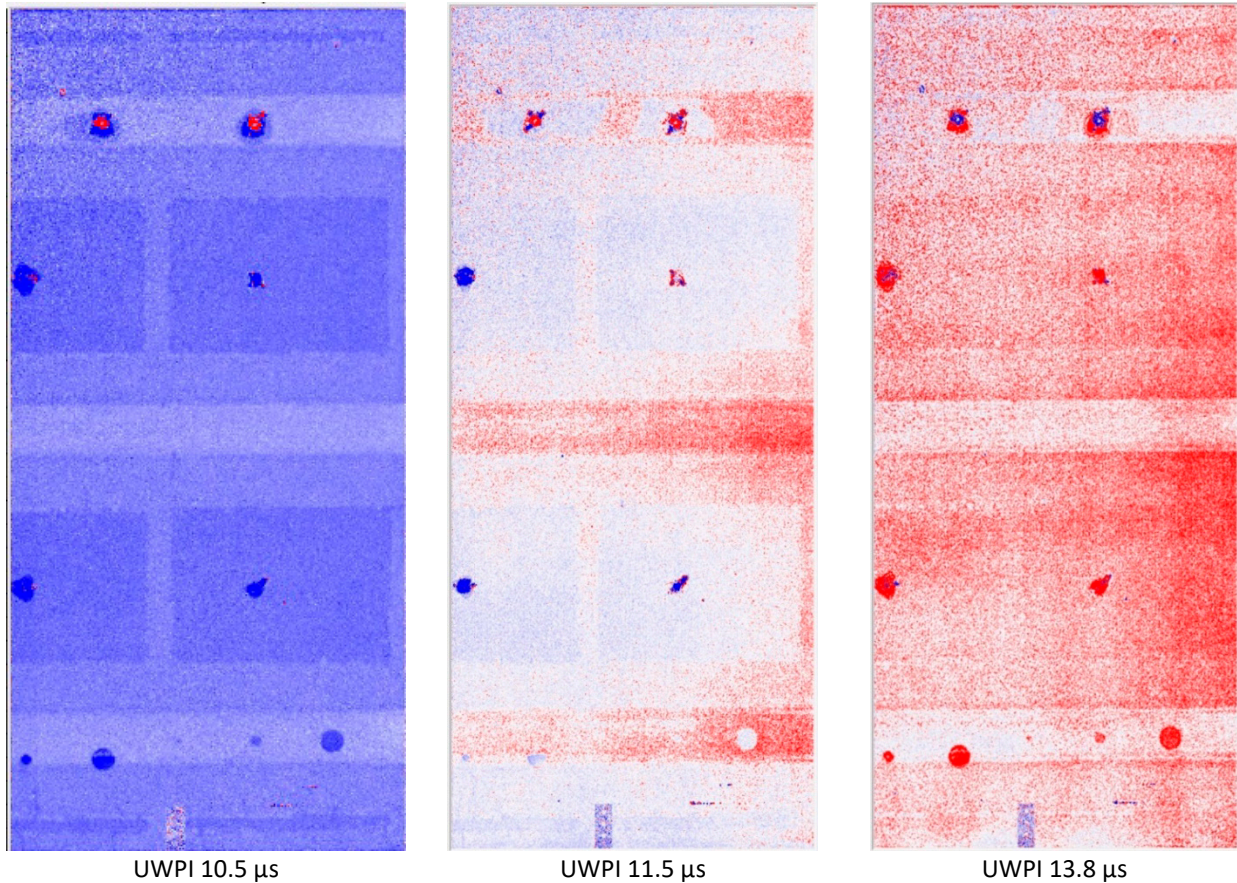
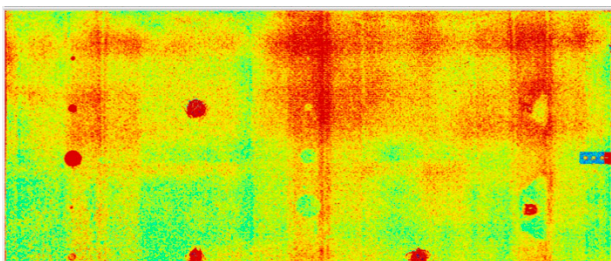


Figure 4.11: Three PE-UPI freeze frames at different times from the UWPI wave propagation movie of the right side of panel NLR-D (lower half of Fig. A2)

From the UWPI data relevant time ranges were selected by the PE-UPI system operator and further processed to produce VTWAM amplitude images, see figures C4 and C5. These figures have also been included in Figure 4.12 together with the NLR-D specimen drawing from figure A2. The VTWAM images have herewith been rotated 90° clockwise to resemble the panel view in figure A2. Figure 4.12 shows almost all defects in the panel (impact damages, artificial delaminations and disbonds) are reliably detectable. Only the small skin-to-rib disbond SD1 is qualified as detectable with limitation. This is, in fact, the same conclusion as was drawn for the baseline UT C-scan inspection, see Chapter 4.1.

VTWAM 'left' side, time range 10.5 μ s – 13.5 μ s



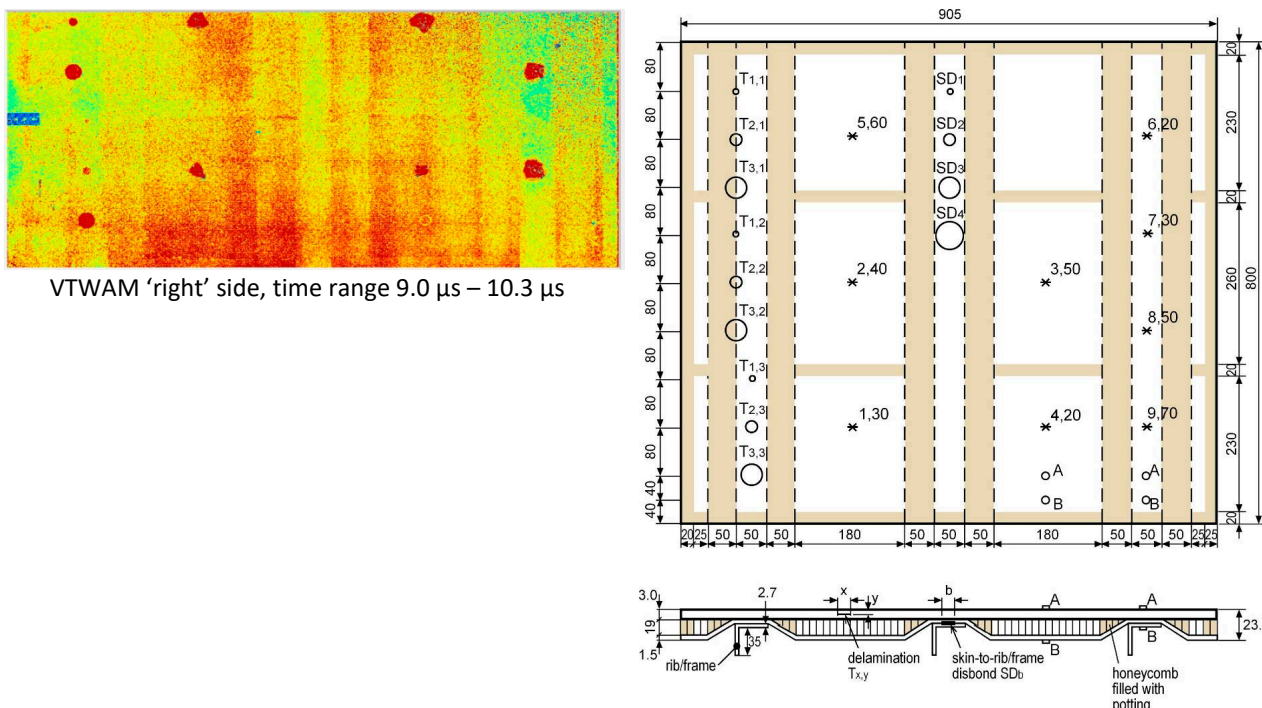


Figure 4.12: PE-UPI VTWAM results from the UWPI wave propagation movies of the left and right sides of panel NLR-D

Figure 4.13 gives a comparison of the PE-UPI VTWAM results with baseline UT C-scan results (PEFR and PEBR images, not the TT image because TT is not an in-service option with one-sided accessibility). The figure shows that the baseline UT-scan images have a slightly better defect detectability and a better definition of the presence of substructure. However, this can again be expected because the baseline C-scan inspection was performed with a coupling medium (immersion mode) and used a focused UT transducer. All-in-all, it can be concluded (as with panel NLR-B) that the PE-UPI system is capable of detecting relevant defects and that it is, hence, a viable option for in-service UT inspection of structures similar to the panel NLR-D configuration.

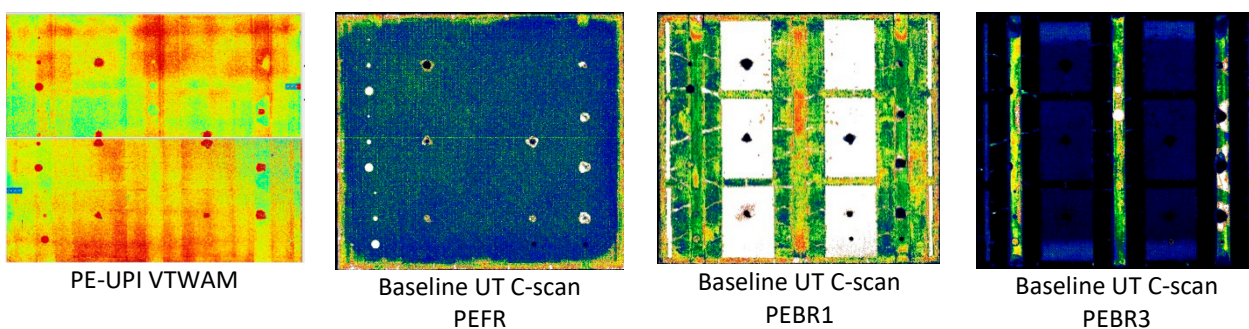


Figure 4.13: Comparison of PE-UPI VTWAM result with baseline UT C-scan results of panel NLR-D

4.2.2.3 RTM specimen #2118

The PE-UPI inspection results for RTM specimen #2118 are given in Appendix C, figure C6. A scan area of 100 x 200 mm² was used for this specimen. The UWPI movie in figure C6 contains again all individual C-scan images of the reflected UT wave amplitudes in time over a total time period of 51.1 μs. Figure C6 shows one example (freeze frame) of the UWPI at the specific time of 17.5 μs. Figure 4.14 includes this UWPI freeze frame and two additional freeze frames at the specific times of 6.8 and 10.4 μs. The figure shows that most defects in this panel are not detectable. Only the near-surface FBH C6 (depth 1 mm) is considered reliably detectable, and some FBH's at a depth of 4.4 mm (A5 and B5) and at a depth of 8.9 mm (A4 and B4) show some defect indication but with a poor signal-to-noise ratio.

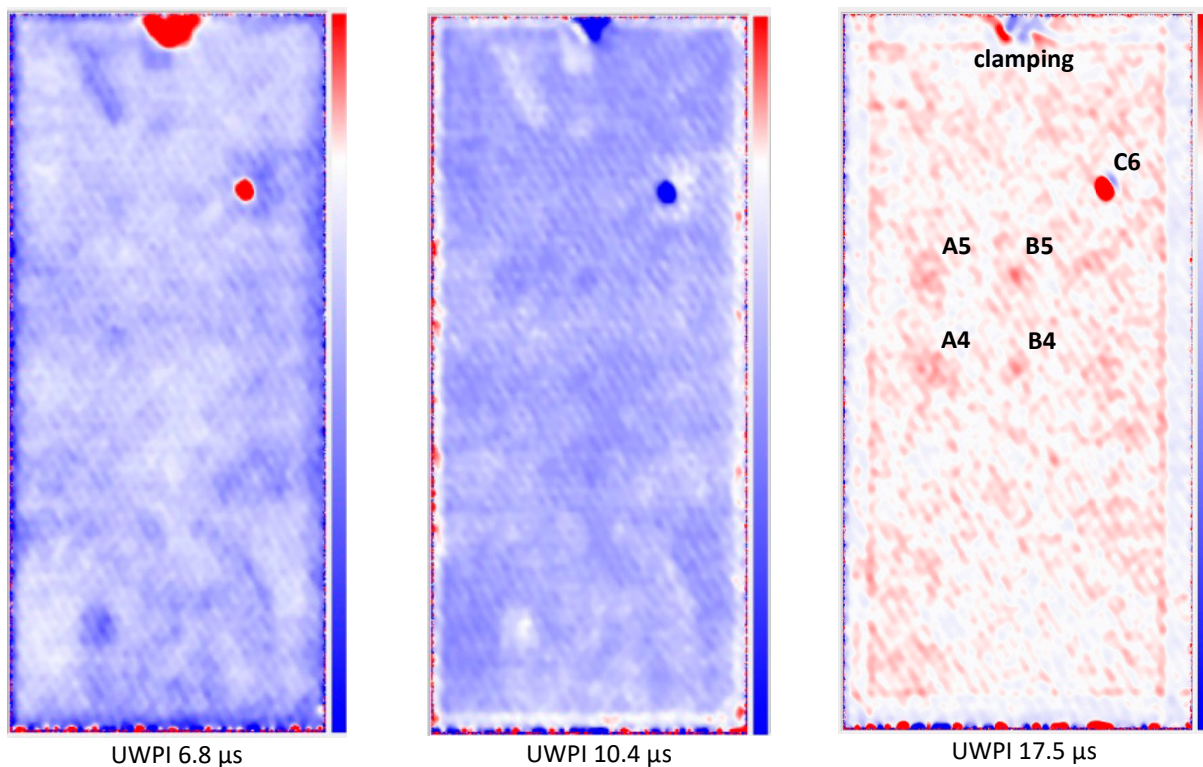


Figure 4.14: Three PE-UPI freeze frames at different times from the UWPI wave propagation movie of specimen #2118

From the UWPI data, one relevant time range was selected by the PE-UPI system operator and further processed to produce a VTWAM amplitude images, see figure C6. This figure has also been included in figure 4.15 together with a baseline UT C-scan result (PEFR image) and the specimen drawing from figure 3.3. As with the UWPI image, only the near-surface FBH C6 is considered reliably detectable in the VTWAM image. FBH's A5 ($\varnothing 12\text{mm}$ at 4,4 mm depth) and B5 ($\varnothing 8\text{mm}$ at 4,4 mm depth) are considered detectable but the other FBH's at a depth of 4.4 and 8.9 mm have a too low signal-to-noise ratio. The other FBH's at larger depth and the manufacturing defect (foil) are clearly undetectable. This poor defect detectability is in great contrast with the result for the baseline UT inspection. A possible explanation for the poor defect detectability might be the specimen thickness (27 mm) and/or the fibre waviness present in this specimen. However, these explanations are not definite and more investigation is needed to conclude the cause of this poor performance. A contributing factor can also be the surface finish of specimen #2118 (shiny and unpainted, in contrast with the NLR-B and NLR-D specimens that are painted and have a mat finish) that can influence the effectiveness of the laser systems. All-in-all, it can be concluded that the PE-UPI system seems not a good option for in-service UT inspection of structures similar to the RTM specimen #2118 configuration.

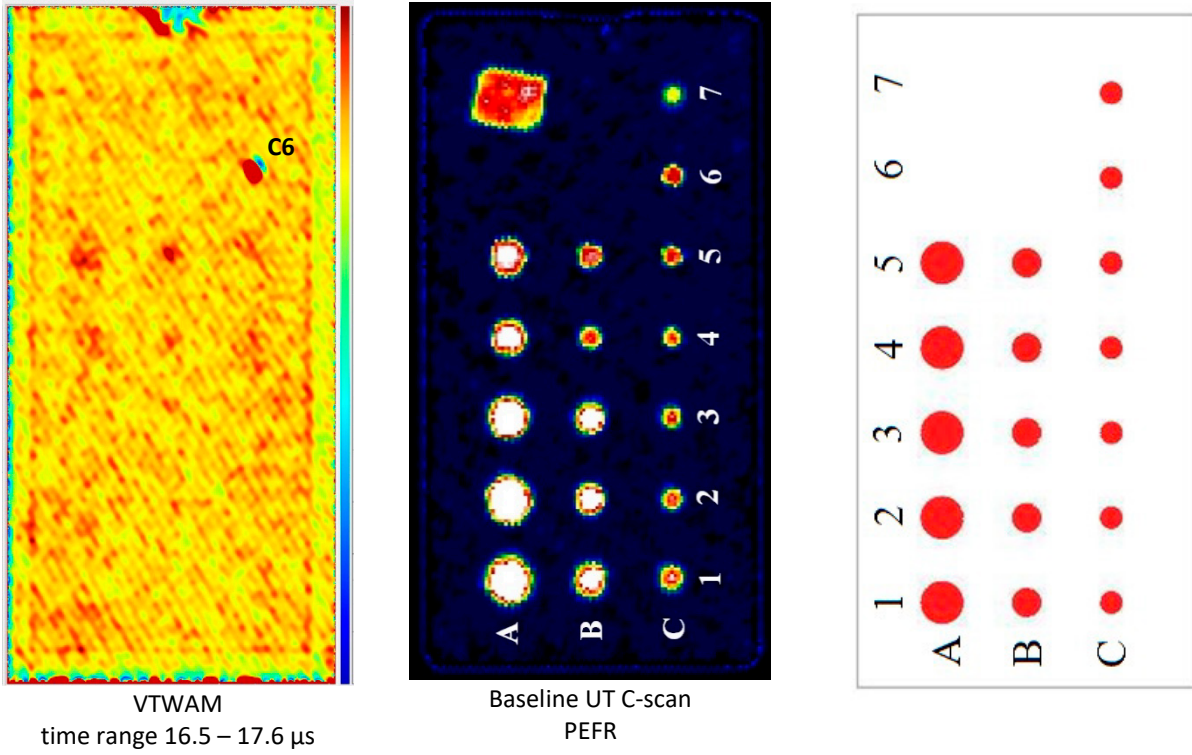


Figure 4.15: PE-UPI VTWAM result of RTM specimen #2118 together with a baseline UT C-scan result (PEFR image) and the specimen drawing

4.3 Tecnatom

4.3.1 TecnaLUS

The LUT-measurements with a TecnaLus system are carried out at the site of Airbus Military Centro Bahia de Caduz on the June 27th and 28th 2018. The TecnaLus system consists of two lasers:

1. A pulsed CO₂ generation laser with an energy of 180 mJ/puls at a wavelength of 10.6 μm . Main advantage of a CO₂ laser is the efficient generation of longitudinal waves in composite specimen, in contrast to the Nd:YAG laser with much smaller wavelength, where many wave types are generated (besides longitudinal, transverse, Lamb and Rayleigh waves). This laser also gives less chance on surface damage. Main disadvantage is that CO₂ have to use periscopic or mirror systems to guide the waves and cannot be integrated with fibre transmission.
2. Nd:YAG detection laser with a wavelength of 1.064 μm in combination with a Fabry-Perot interferometer.

Both laser systems are co-linear aligned (towards the common surface point). The TecnaLUS system has been optimized by the manufacturer with the consequence that relative minor settings can be altered by the user. Main setting parameter is the surface spot size of the generation laser (variation between 10 and 16 mm). A smaller spot size increases the energy share in the ultrasonic high frequency band. Stand detection frequency band in operation is between 0.5 and 20 MHz, for composites the band is somewhat lower between 0.5 and 8 MHz. The broadband spectrum leads to a good near-surface resolution. Ultrasonic generation with a CO₂ laser has a large tolerance with respect to laser incident angles: flat surfaces $\pm 25^\circ$ and rough surfaces $\pm 40^\circ$. The inspection philosophy of Tecnatom is that their system is less suitable for the inspection of large flat structure/components but more suitable to inspect smaller components with a complex geometry. The price of the used system is about 2.5 M€.



Figure 4.16: Tecnatom TecnaLUS system

TecnaLUS equipment can be placed on robotic arms (KUKA robotics). For the present tests, the static set-up with the TecnaLUS system is used (fixed LU measurement head, black system at the top of fig.4.16). De test panels were placed on a metal plate with dimensions of 1.50 x 1.50 m². The distance between the test panels and the laser was kept constant being about 1.8 m.

4.3.2 Experimental results

Tecnatom results are reported in references 27-30.

4.3.2.1 CFRP specimen NLR-B

The equipment and scan parameters are listed in tables 4.1 and 4.2.

Table 4.1: Equipment parameters

Equipment parameters	
Generation Pulse duration: 100 ns	Interferometer type: Confocal Fabry Perot
Generation wavelength: 10.6 μm	Generation Pulse Energy: 180 mJ/pulse
Detection wavelength: 1.064 μm	Generation spot size: 12 mm
Acquisition Parameters	
Acquisition rate: 600 Hz	A-Scan length: 2048 points
Digitizer rate: 50 MHz	DAC (on/off): off

Table 4.2: Scan parameters and panel

Inspection Time (s):	36
Inspection pose:	1
Step Size (mm):	2
X dimension (mm):	315
Y dimension (mm):	505
X center (mm):	0
Y center (mm):	0



Scan results of the TecnaLUS system (both delamination $T_{x,y}$ and Disbonds SD_b) are good, both for the Amplitude as Time of Flight depending at different gate settings (Fig. 4.17).

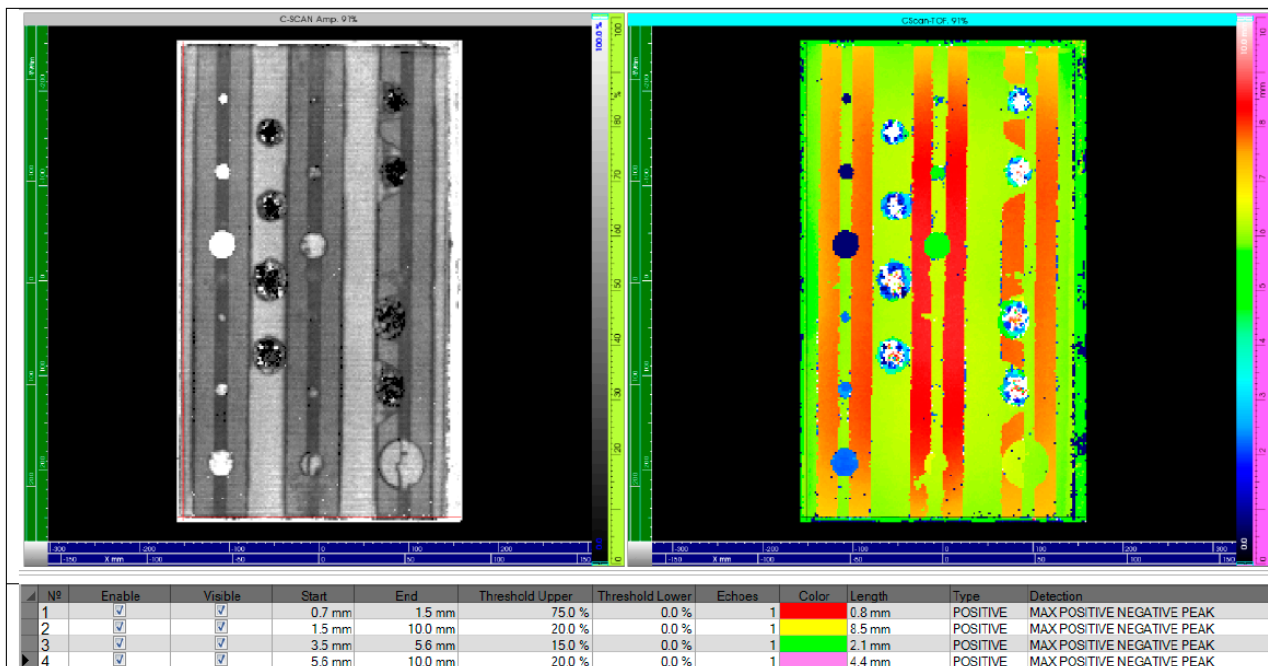


Figure 4.17: TecnaLUS C-Scan results on panel NLR-B (left amplitude, right time of flight)

Another convincing and illustrative example is the C-scan result (amplitude and time of flight) at gate setting 5.8 – 6.5 mm is shown in figure 4.18.

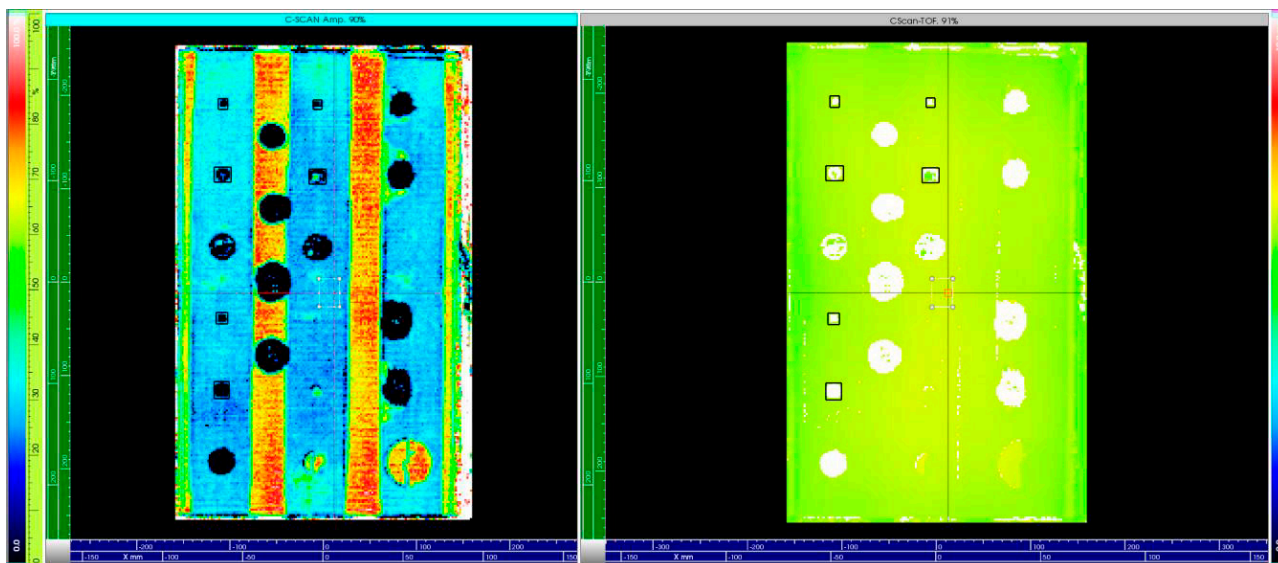


Figure 4.18: TecnaLUS C-Scan results on panel NLR-B (left amplitude, right time of flight) at gate setting 5.8-6.5 mm

The estimated depths in the indication report (table 4.3) perfectly match with the actual values between parentheses.

Table 4.3: Indication report

Indication Name	Measure Name	X Length (mm)	Y Length (mm)	Depth (mm)
Indication1	T1,1	10	12	0.7 (0.75)
Indication1	T2,1	18	16	0.8 (0.75)
Indication1	T1,2	12	12	2.2 (2.25)

Indication Name	Measure Name	X Length (mm)	Y Length (mm)	Depth (mm)
Indication1	T2,2	16	18	2.3 (2.25)
Indication2	T2,3	10	10	5.3 (5.25)
Indication2	T1,4	18	16	5.6 (5.25)
Indication3	SD2	12	12	6.4 (6.0)

4.3.2.2 CFRP specimen NLR-D

The equipment and acquisition parameters are the same as those of the NLR-B panel. Scan parameters are somewhat different (see table 4.4).

Table 4.4: Scan parameters and panel

Inspection Time (s):	4
Inspection pose:	1
Step Size (mm):	2
X dimension (mm):	940
Y dimension (mm):	840
X center (mm):	0
Y center (mm):	0



The results with the TecnaLUS system on NLR-D panel are good (Fig. 4.19).

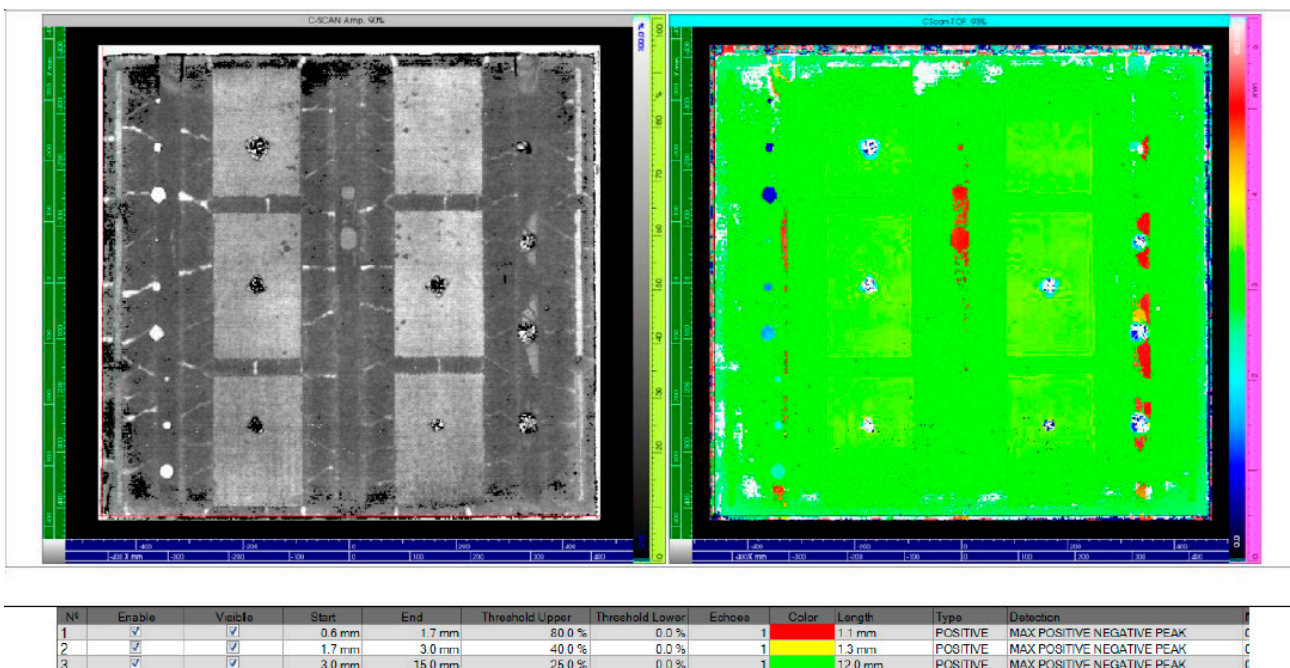


Figure 4.19: C-scan results (amplitude and TOF) of NLR-D panel, gate settings: 0.6 – 15 mm

Good results are also reproduced at different gate settings (3 – 3.5 mm, fig. 4.20).

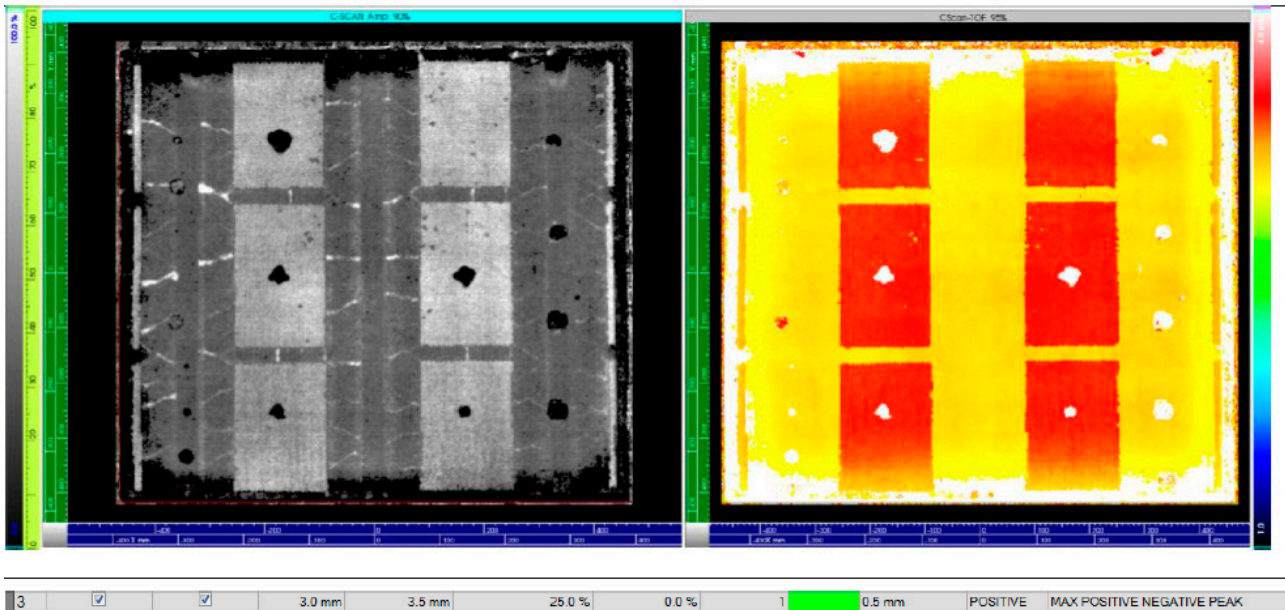


Figure 4.20: C-scan results (amplitude and TOF) of NLR-D panel, gate settings: 3 – 3.5 mm

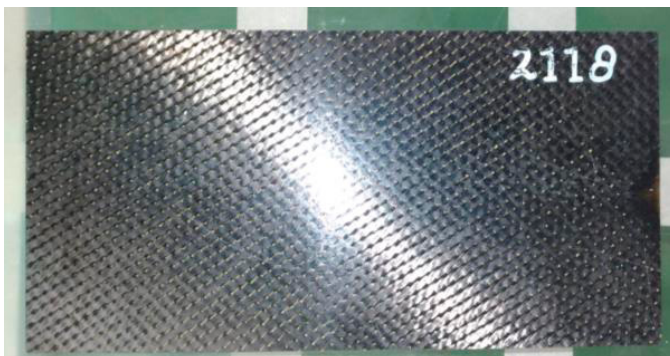
The estimated depths in the indication report (table 4.5) match well with the actual values between parentheses.

Table 4.5: Indication report

Indication Name	Measure Name	X Length (mm)	Y Length (mm)	Depth (mm)
Indication1	T2,1	16	16	1 (0.75)
Indication2	T2,2	16	16	1.5 (1.5)
Indication3	T2,3	16	16	2.3 (2.25)
Indication4	SD3	28	26	4.9 (4.5)
Indication5	SD4	34	46	4.9.5)

4.3.2.3 RTM specimen #2118

The equipment and acquisition parameters are the same as those of the NLR-B panel.



The result on the thick RTM panel (27.4 mm) with flat bottom holes are compared to the other results somewhat disappointing (Fig 4.21). A possible reason can be the shining surface which may be responsible for lower ultrasonic excitation energy level in combination with undulation effects and broad band excitation.

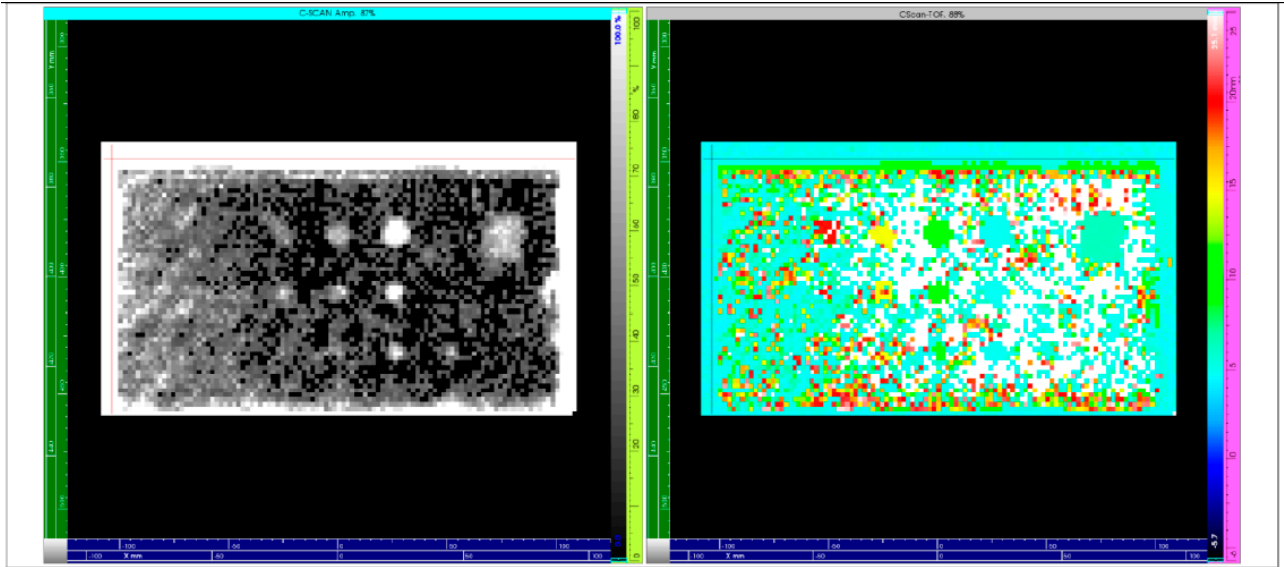


Figure 4.21: C-Scan overview (amplitude and TOF), gate setting 4.5-25.1 mm

The results at other gate settings (7 -15 mm) don't significantly improve the detection of FBH's (Fig. 4.22).

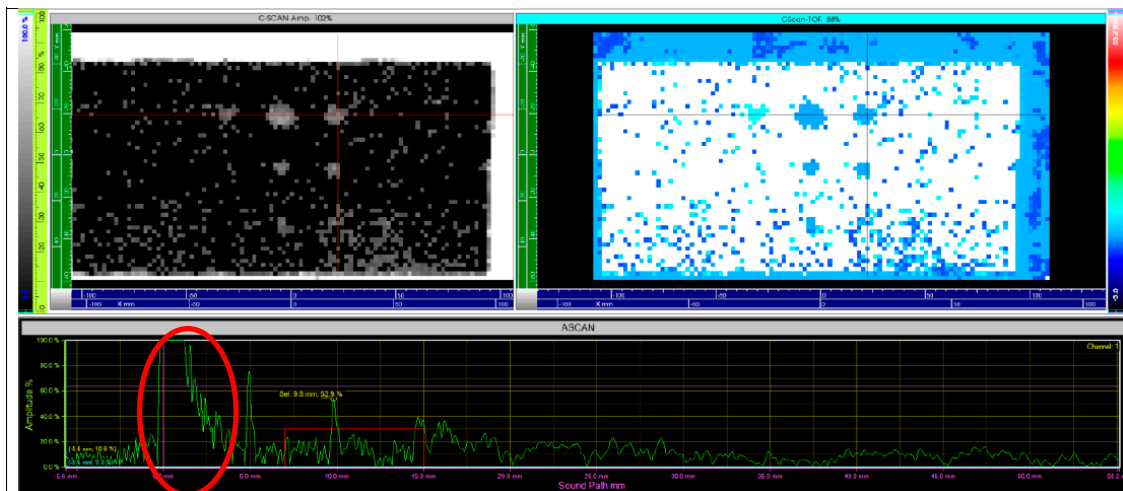


Figure 4.22: C-Scan overview (amplitude and TOF), gate setting 7-15 mm (without TCG)

4.4 Xarion

4.4.1 Xarion optical microphone

The Xarion technique is a combination of laser ultrasonic excitation and measurement with an optical microphone Eta450 (an ACUT technique, Air Coupled Ultrasonic Testing). Three types of measurements were foreseen:

1. In transmission mode (excitation at one side of the structure and measurement at the opposite side),
2. Pulse-Echo (single side excitation and measurements) and;
3. Pitch-catch mode (no co-linear single side excitation and measurement (with not collapsing excitation and measurement locations)).

The preferred measurement method was the Pulse-Echo mode with co-linear excitation. Xarion tried to realize this mode with the excitation laser through the microphone. Unfortunately the powerful response of the Xarion microphone on the front-echo response from the object masked the response due to the ultrasonic wave propagation within the material. Therefore, the alternative technique, the pitch and catch mode avoiding the strong front echo response, has been explored on two test panels (NLR-B and #2118, Fig. 4.23).

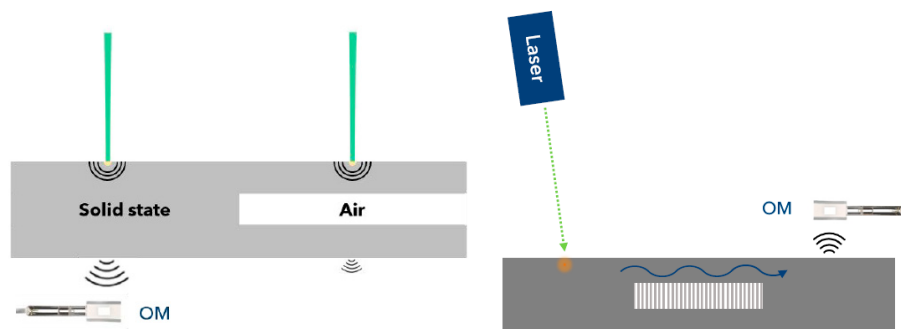


Figure 4.23: Transmission and pitch & catch mode using the Xarion optical microphone

It is noted that the transmission mode is hampered by the alignment of the excitation and detection probes, which also may limit the accessibility.

The detection probe consists of a small-sized optical microphone based on laser interferometry principles (Fig. 4.24, Ref 31). Features are:

1. Broad frequency range due to the absence of moving membranes (10 Hz to 2 MHz).
2. Immunity to electromagnetic fields.
3. Operational in air and liquids.
4. Long optical fibre cabling possible (attenuation 0.3 dB/km).



Figure 4.24: Xarion optical microphone (Ref. 31)

The frequency range for acoustic applications is rather broad, though for Ultrasonic applications still limited (but may be sufficient dependent on the application). Typical ultrasonic frequency bandwidth is 400 kHz, maximum bandwidth is 2 MHz. The transmission test set-up is shown in fig. 4.25.



Figure 4.25: The Xarion transmission set-up with aligned excitation laser (under) and optical microphone

4.4.2 Experimental results

The Xarion results are reported in References 32-36.

4.4.2.1 CFRP specimen NLR-B

Transmission measurements

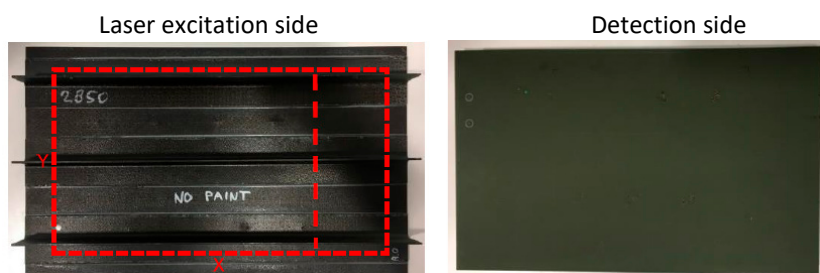


Figure 4.26: Excitation and detection sides of panel NLR-B

The excitation and detection side are depicted in figure 4.26. Due to the presence of the stiffeners, the ultrasonic microphone, which requires to be close to the test specimen in order of 10 mm, had to be placed on the flat surface side. Note that this is one of important limitations of this method. Results of the transmission mode measurements show clearly the locations of the defects (Fig. 4.27). Contrary to PE measurements, transmission mode measurements don't contain depth information. Remark: the transmission mode is not suitable for MRO applications because two sided access is needed.

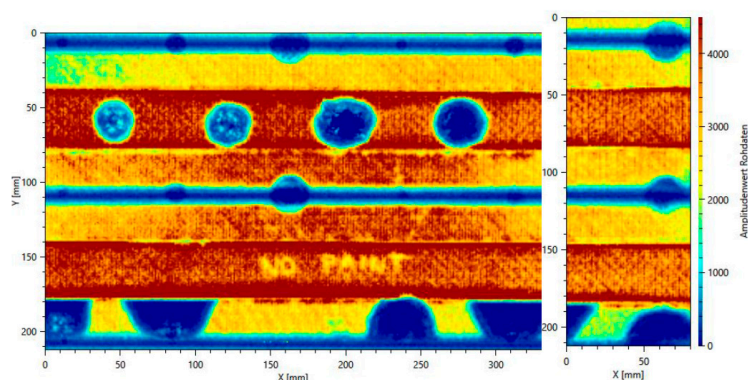


Figure 4.27: Xarion transmission mode amplitude results on panel NLR-B

Pitch & Catch measurements

The provisional results on the NLR-B panel in pitch & catch mode show results on the locations of the defects (Fig. 4.28). The displayed C-scans refer to the same measurements but represent different time frames.

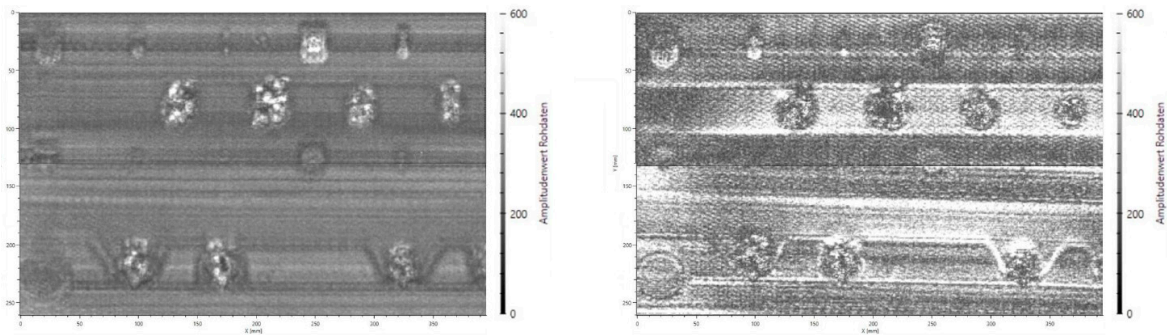


Figure 4.28: Xarion pitch & catch results on the NLR-B panel

4.4.2.2 CFRP specimen NLR-D

It is noted that for panel NLR-D only transmission measurements have been carried out.

Transmission measurements

Laser excitation on panel D is done at the flat surface and the Xarion optical microphone is located at the side with the stiffeners (Fig. 4.29).

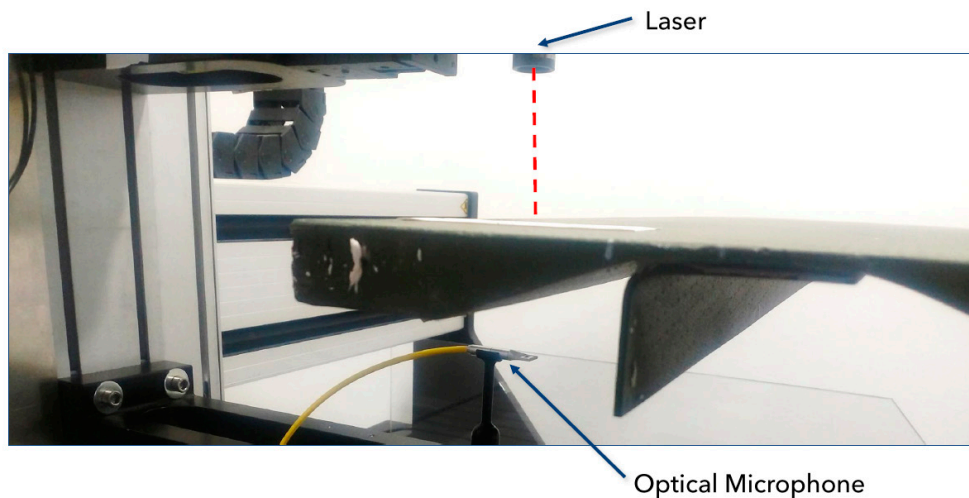


Figure 4.29: Xarion set-up for the NLR-D transmission measurements

Five excitation and measurement areas are indicated in figure 4.30. It is noted that these locations are near the panels edges due to the U-shaped transmission head, which at present prevents full area coverage.

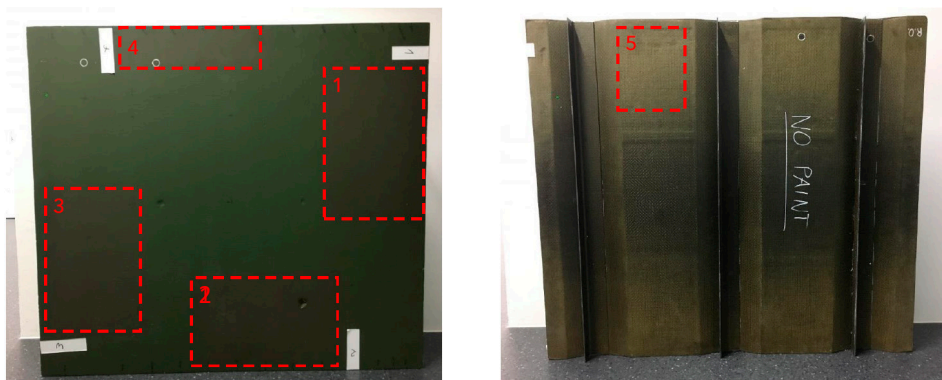


Figure 4.30: Numbering of measurement areas of panel NLR-D

The location of defects in area 1 are shown figure 4.31. The different C-scans refer to the same measurement with a different chosen time frame. Interpretation of the results is facilitated by the knowledge of the artificial defects.

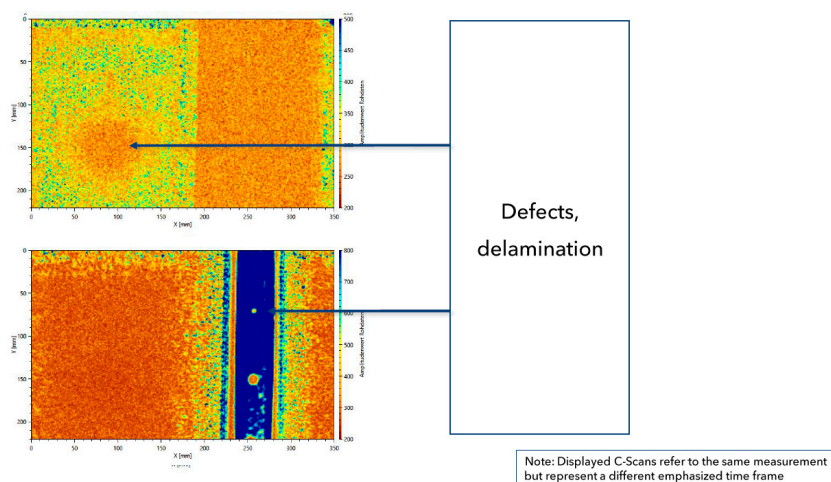


Figure 4.31: Xarion transmission result on area 2 of panel NLR-D

The results for areas 4 and 5 are given respectively in figures 4.32 and 4.33.

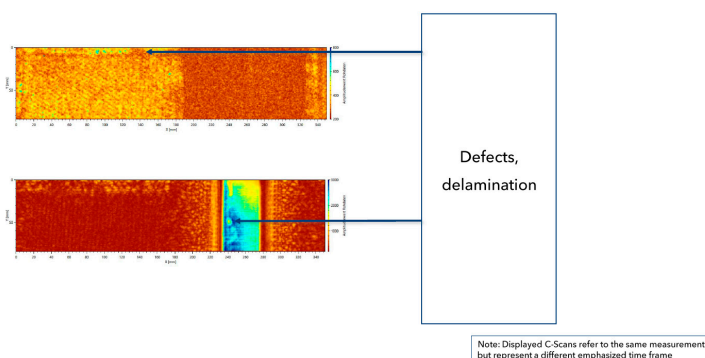


Figure 4.32: Xarion transmission result on area 4 of panel NLR-D

General impression is that the results on panel NLR-D are not as good as those on panel NLR-B. First of all, the full coverage of the panel inspection was not possible. Secondly, the single-sided inspection was also not feasible in this case due to the size of the panel.

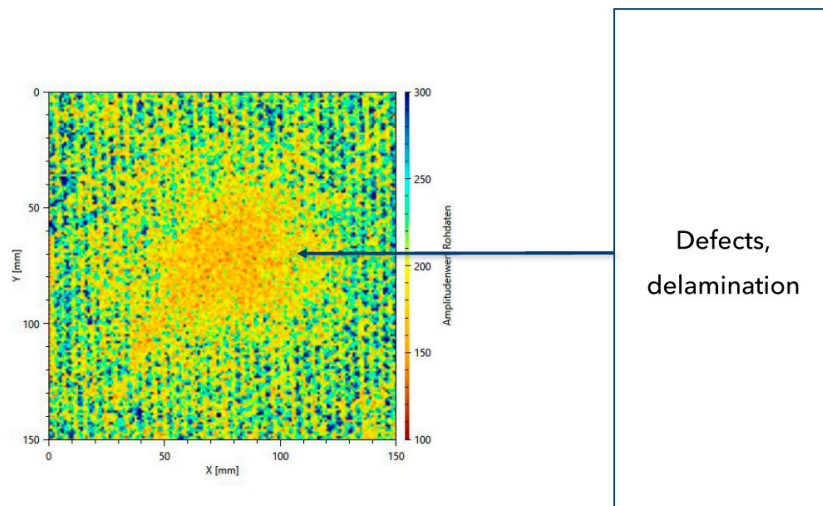


Figure 4.33: Xarion transmission result on area 5 of panel NLR-D

4.4.2.3 RTM specimen #2118

Transmission measurements

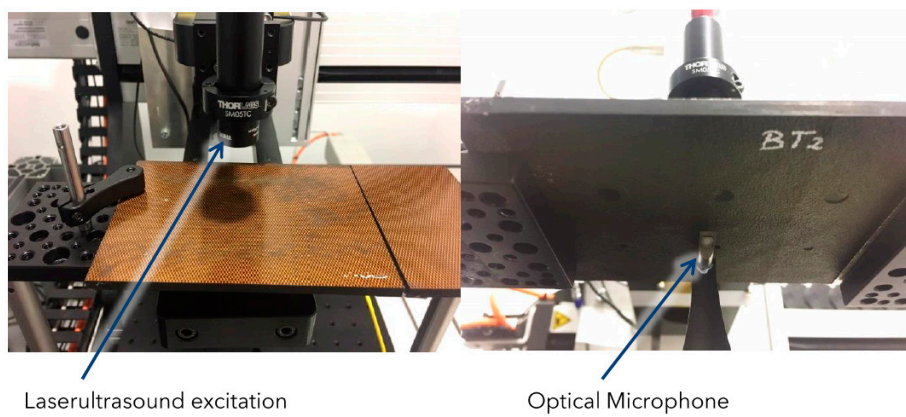


Figure 4.34: Xarion transmission set-up with excitation and detection sides of panel #2118

The excitation and detection side are depicted in figure 4.34. The transmission results based on attenuation and time of flight show clearly the locations of the FBH's (Fig. 4.35).

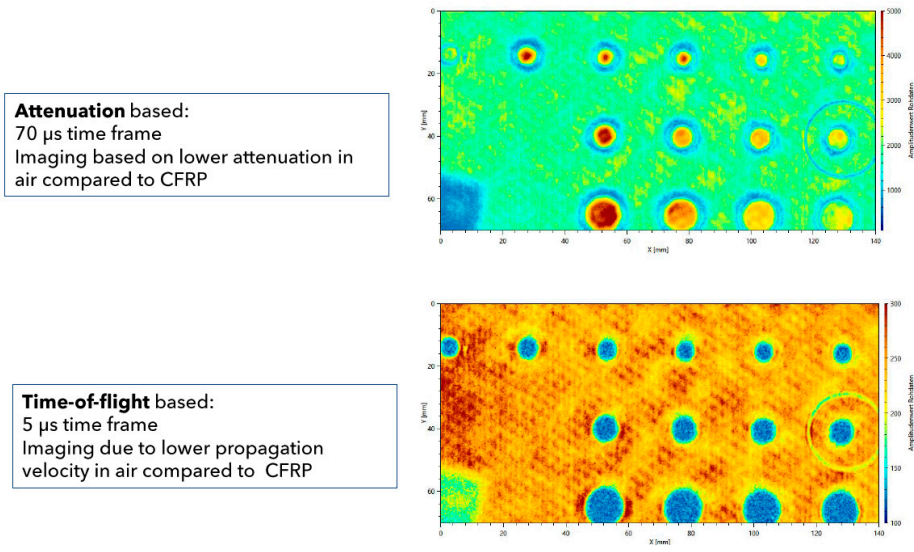


Figure 4.35: Results of Xarion transmission mode measurements on panel #2118

Some inventory work has been done to quantify the depth by looking at the signal attenuation (stronger in panel than in air) and increasing time delay (Fig. 4.36). This method, clear for FBH's, should be further explored for other defects.

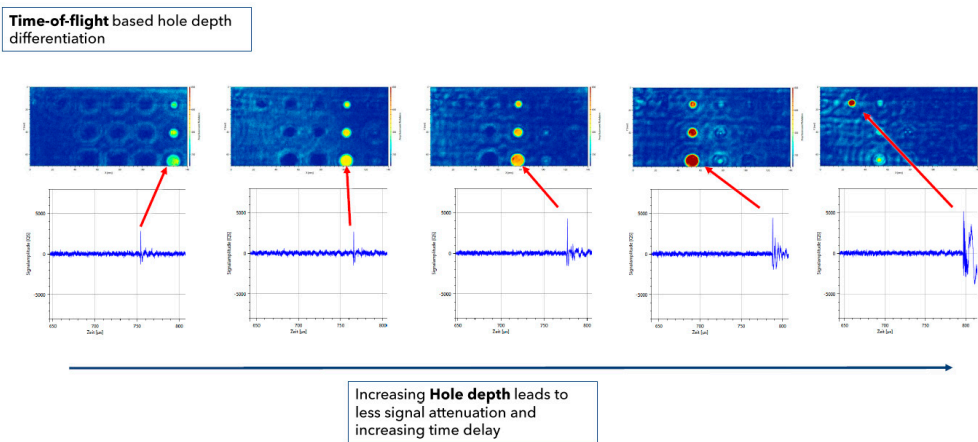
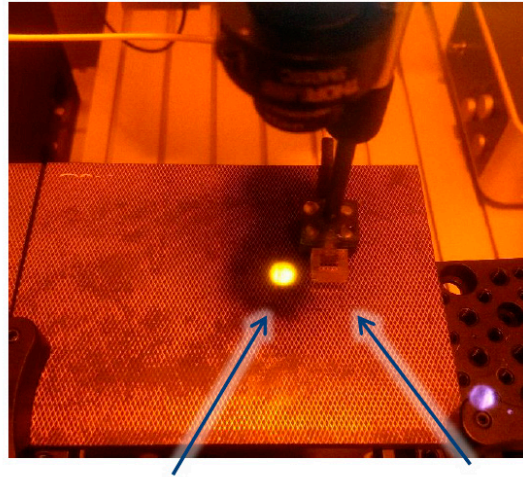


Figure 4.36: Provisional exploration of depth estimation by Xarion transmission measurements using attenuation and time-of-flight parameters

Pitch & catch measurements

The pitch and catch measurements on panel #2118 have been performed from the opposite side of the defects (flat surface, fig. 4.37).



Laser excitation

Optical Microphone (Eta450)

Figure 4.37: Xarion pitch & catch measurements on panel #2118

The flat holes are detectable in a single sided-set-up (Fig. 4.38). For the lowest hole depths, the scan needs further optimization. Note furthermore that also the depths are not quantified. The holes cause a change in the wave propagation velocity which is dependent on hole depth. Therefore the suitable time window is different for each hole depth, indicated by different time legs.

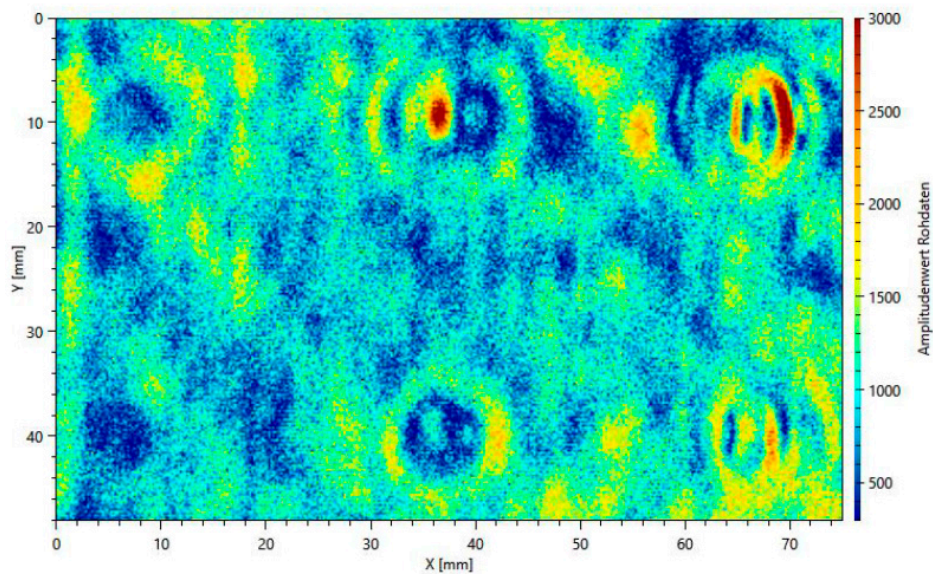


Figure 4.38: Final Xarion catch & pitch results on panel #2118

Pulse echo measurements have to be further explored, but needs more research on signal separation (excitation, principal and flaw reflections) and careful alignment, since the excitation laser shoots through the microphone resulting in a strong front echo response.

4.5 Tecnar equipment

For the round robin also Tecnar equipment is selected. The demo rig at Tecnar headquarter suffers from some scanning limitations (Fig. 4.39).

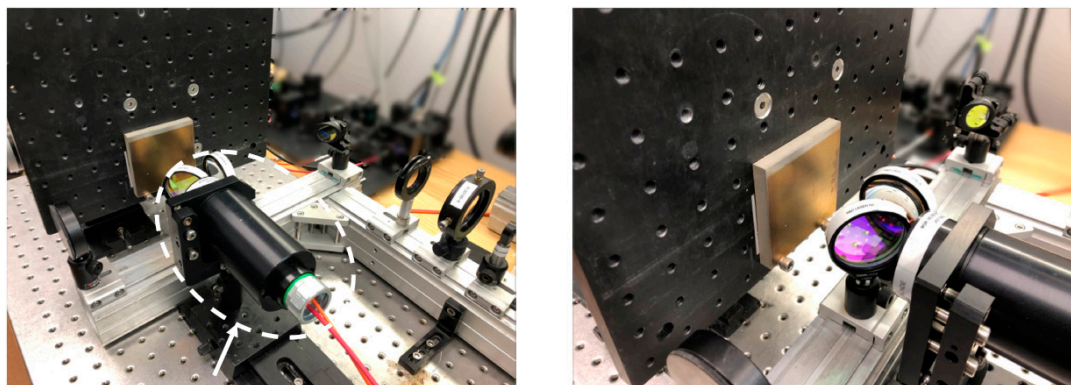


Figure 4.39: The demo equipment at Tecnar's head quarter with limited scan capacity ($100 \times 100 \text{ mm}^2$)

4.5.1 Tecnar equipment at CSL

As explained above and consultancy with Tecnar it is decided to test the panels at Centre Spatial de Liege (CSL), which operates Tecnar equipment (Figs 4.40 and 4.41). CSL has acquired a modular Tecnar system with an all-fibred lasers working at 532 nm generation and 1064 nm detection wavelengths. CSL decided not to buy a Tecnar turn-key system since they are also developing their own excitation laser (OPO with wavelength between 3 and 4 μm) and processing software.

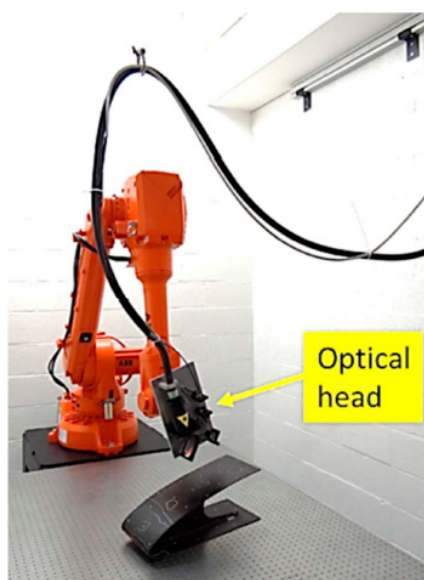


Figure 4.40: The CSL system based on Tecnar equipment placed on a 6-axis ABB robot

An all-fibred Tecnar ultrasonic system working at 532 nm generation and 1064 nm detections wavelengths operated by CSL mounted on a 6-axis ABB-robot for scanning.

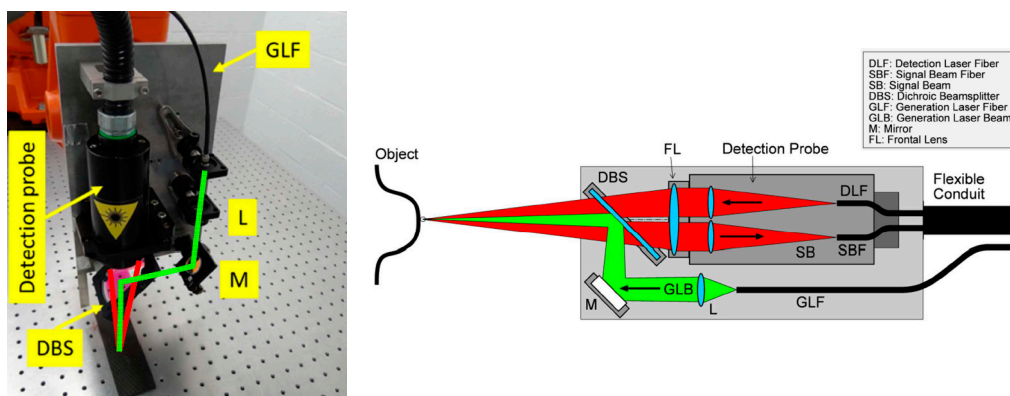


Figure 4.41: The fibre based CLS probe with Tecnar co-linear excitation and detection lasers

For clarity it is noted that the signal beam fibre transports the laser signal to the Two Wave Mixing interferometer, which stand a couple of meters from the CLS probe (where also the generation and signal lasers are located, fig 4.42).

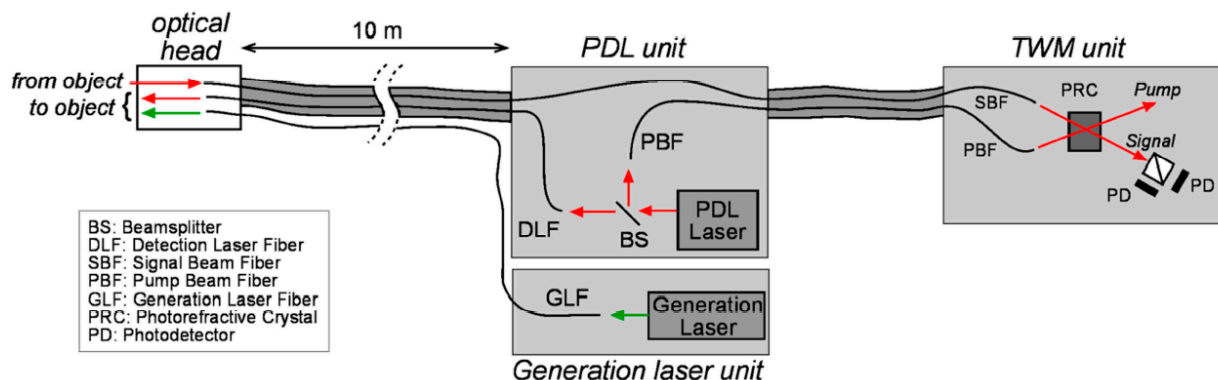


Figure 4.42: Overall scheme of CLS equipment

4.5.2 Experimental results

The laser tests with the Tecnar equipment on the three panels were postponed multiple times during the test campaign due to low signal to noise ratios of the detection lasers at panels #2118, NLR-B and NLR-D (due to either the high reflective surface of panel #2118 causing minor laser excitation and the discolouration of test panel NLR-D, see section 4.7). The limited results on these panels however are shortly described hereafter. To get meaningful results with the Tecnar equipment while preventing risk of ablation on the surface of reference specimen, NLR selected two alternative panels (see Appendix D and sections 4.5.2.4 and 4.5.2.5). It is noted that the raw data are processed with CSL software. See Reference 37 for the test report.

4.5.2.1 CFRP specimen NLR-B

The results of the time of flight measurements with the Tecnar equipment show very low signal to noise ratios causing no NDT-resolution to the artificial defects (Fig. 4.43).

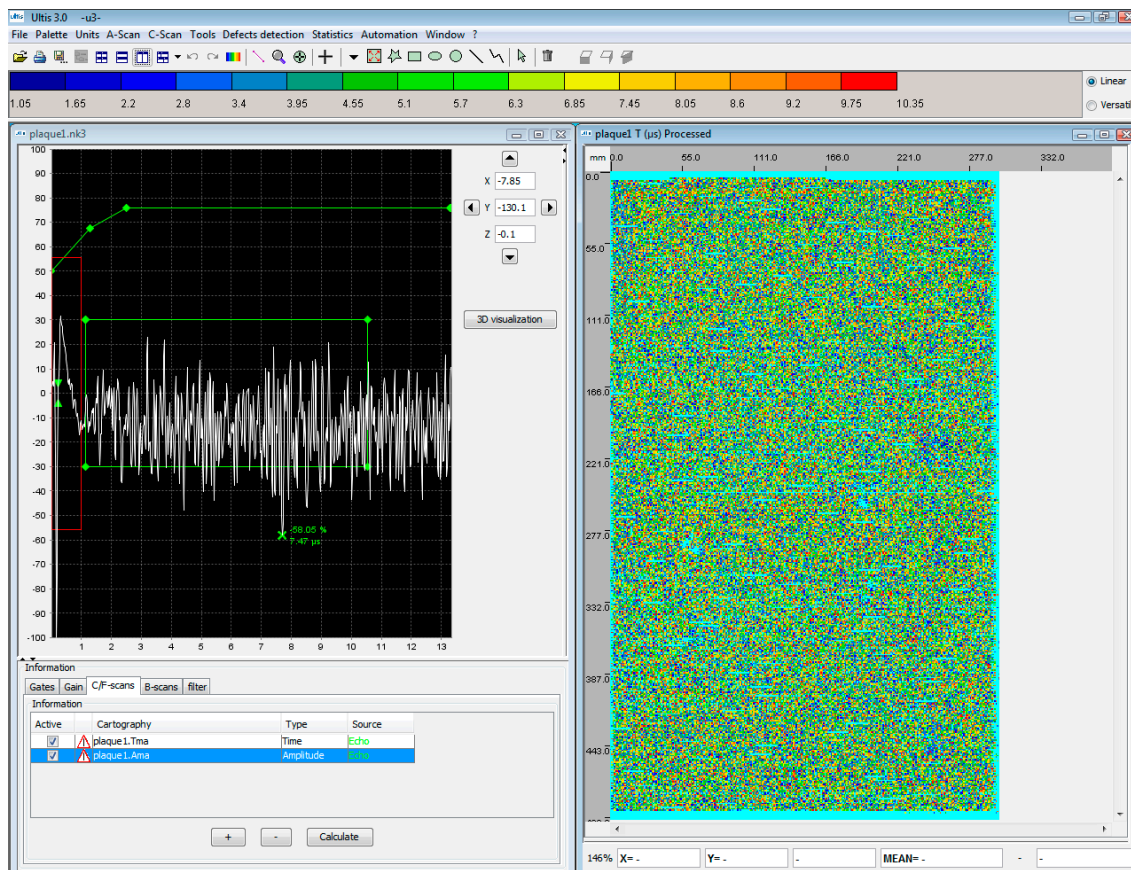


Fig. 4.43: C-scan time of flight response of the NLR-B panel (right window)

The results of the amplitude measurements with the Tecnar equipment show very low signal to noise ratios causing very limited NDT-resolution to the artificial defects (Fig. 4.44).

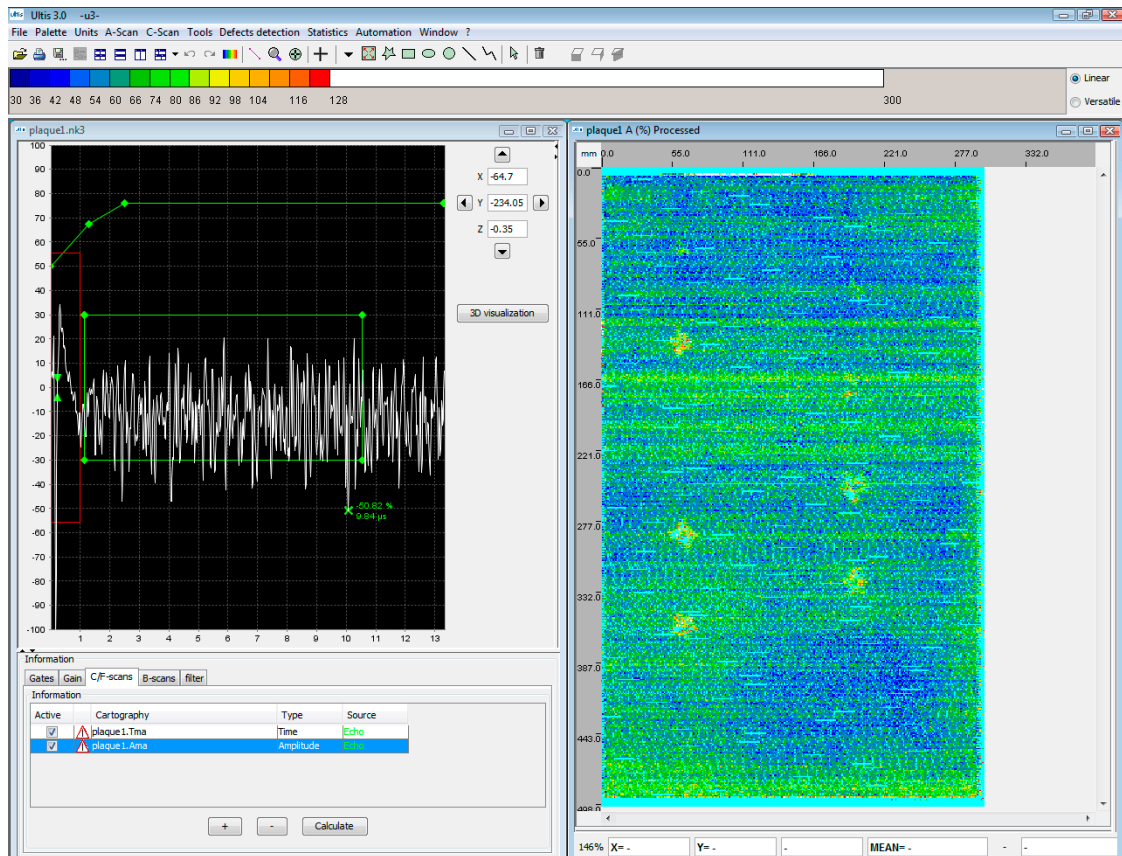


Fig. 4.44: C-scan amplitude response of the NLR-B panel (right window)

4.5.2.2 CFRP specimen NLR-D

The CSL tests with the Tecnar equipment were cancelled because of the discolouration of the front surface paint (see section 4.7).

4.5.2.3 RTM specimen #2118

CSL did only a colourisation test on the edge of the panel and concluded that no visible damage occurred (Fig. 4.45). The experiences gained in previous LU-tests on this sample with less successful results (also caused by the reflective front surface) made us decide to focus the tests with Tecnar equipment on samples NLR-B and D. It is finally remarked that investigations to assess laser generated damage effects are an essential step in the process of laser ultrasonic application.

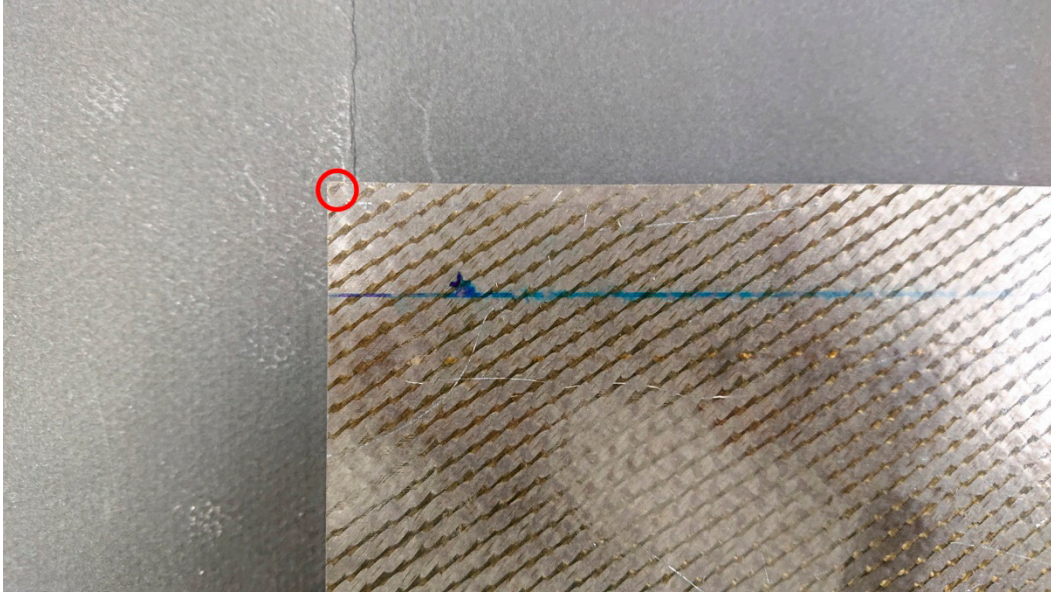


Fig. 4.45: Assessment of laser generated damage effects on panel #2118

4.6 Optech Ventures

4.6.1 Optech Ventures equipment

Remark: This chapter is derived from the company Opech Ventures.

The AIR-1550-TWM Laser Ultrasonic Receiver represents the state-of-the-art in non-contact laser ultrasonic testing. The AIR-1550-TWM is the first laser ultrasonic receiver operating at the telecom and eye-safe wavelength of 1550 nm (Fig. 4.46 to Fig. 4.48). Eye-safe lasers are important for the protection of researchers as well as for workers in production environments. The operating wavelength also enables the AIR-1550-TWM to work effectively with simple, low cost laser sources, such as DFB or fiber lasers, thereby reducing system cost and eliminating laser maintenance concerns. Although the 1550 nm wavelength is not visible to the eye, a visible guide beam (532 nm) is provided to visualize the detection beam on the target. The AIR-1550-TWM includes a compact fiber coupled measurement head. This sensor head enables remote measurement and is ideal for use with complex configurations or where measurement access is limited. The non-contact measurement capability of laser ultrasonics and its immunity to test-piece temperature and motion make it ideal for factory use. The AIR-1550-TWM is available configured for factory applications with a ruggedized measurement head and fiber optic cables.

Optech Ventures mainly focuses on the LU inspection on the metallic parts and additive-manufactured part inspection. They are less experienced in composite material. The Optech Venture hardware setup is presented in figure 4.46 to 4.48. The remote generation and measurement heads are fiber coupled. The generation laser is a Q-switched Nd:YAG laser with a wavelength of 1064 nm. The pulse width is 10 ns and the pulse energy can be varied (50, 200 or 400 mJ) The detection laser is a 2W continuous wave single frequency fiber laser at 1550 nm combined with a 1W continuous-wave, single-frequency DPSS laser at 532 nm for visualisation (probes displayed in Fig. 4.48).

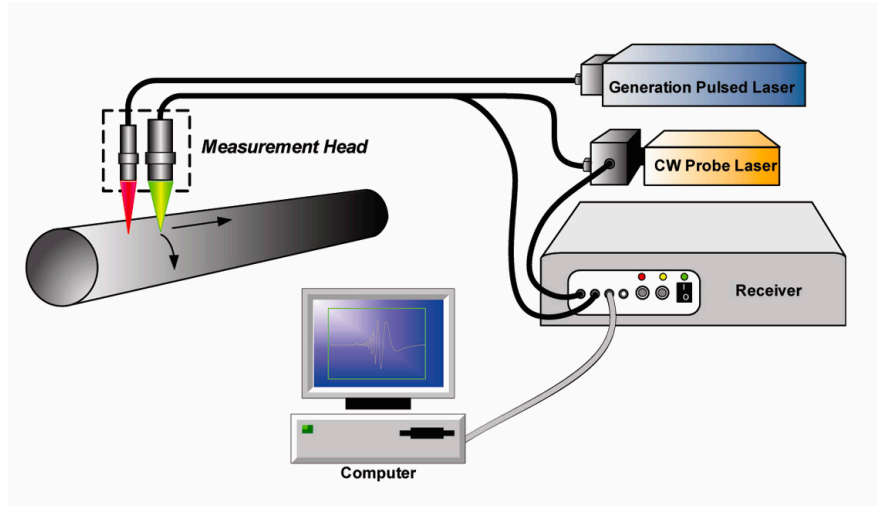


Figure 4.46: Overall scheme of Optech Ventures equipment

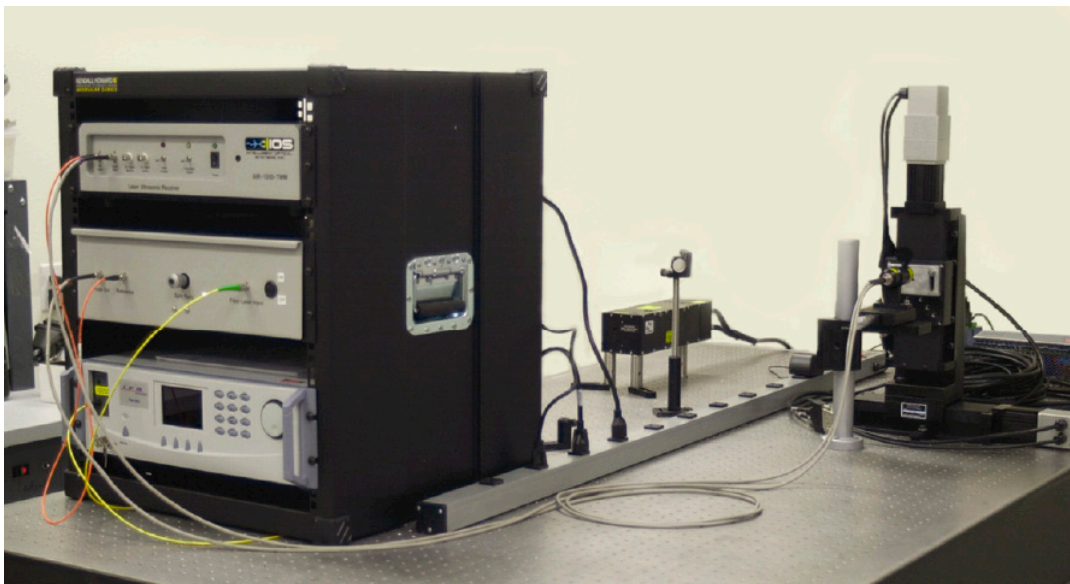


Figure 4.47: The Optech Ventures hardware in a 19" rack

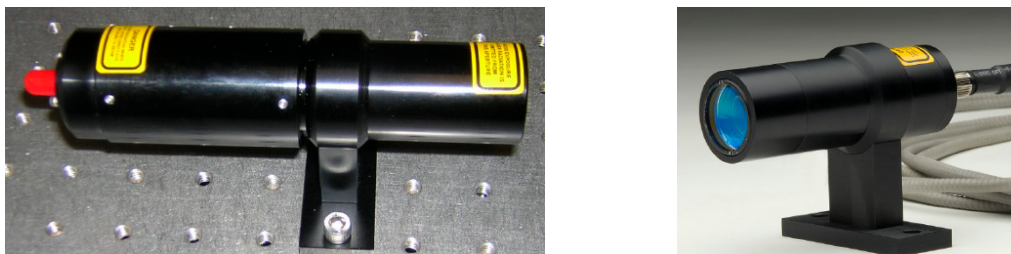


Fig. 4.48: Optech optical probes (left generation, right detection)

4.6.2 Experimental results

Before the experimental results will be discussed, some details are given of the witnessing of the tests at Torrance by the authors. This preface is related to the limited experiences of Optech Ventures with laser tests on composites and the discolouration of the test panels using laser generation and detection equipment. The latter was not confined to experiences with Optech Ventures. Discolouration problems with NLR test panels also occurred during the tests with Tecnar and Xarion equipment. These problems are separately discussed in section 4.7. Optech Ventures has reported the test results in reference 38.

Optech Ventures has much experience with welding inspections. The generation laser normally works in powerful ablative mode, contrary to the thermo-elastic mode for composite testing. Optech Ventures is also working on in-line inspection of metal additive manufacturing also in ablative mode. Just before our visit, Optech Ventures had done some preliminary tests on panel #2118 (the thick composite plate with flat bottom holes). From previous LU-tests, we have noticed that LUT-results are less pronounced than those of the conventional C-scan. At our visit, we asked Optech Ventures (Max Wiedmann) to start with the LU-test on panel NLR-B (6 mm composite plate with 3 stiffeners). It is noted that the flat front face of the panel is painted and the back wall (with the attached stiffeners) is untreated (bare composite material). It was noticed that at the first tests at the front side of panel B discolouration occurred. There is a trade-off between laser power (both for generation and detection) for preferred signal to noise ratio's and possible damage effects. These damage effects hold both for the generation as detections lasers with spot sizes of about 10 and 1 mm respectively. Laser ultrasonic testing is very sensitive to surface characteristics (reflective, absorptive, flatness, roughness and surface finishing (paint)). After 1½ day of (trial and error) testing, it was decided to excite NLR-B panel on the backside with the stiffeners with another detection laser using a tele lens of 200 mm (no paint system on the backside). Due to a limited test time confined results on a small part of panel NLR-B with dimensions of 5 x 10 cm² could be generated. To improve these results, the detection laser should be modified having a different modulation (shorter but more powerful pulses for the detection laser with intermittent and lower levels between the actual measurements). Another option would be to use different types of lasers for generation (CO₂ 10 µm or OPO 3 – 4 µm) and detection (modified wave lengths). No test results are available on panel NLR-D. The problems during the test campaign also impacted the scanning speed, which had a typical value of about 1 mm/s (which is two orders of magnitude lower than the reference speed of a conventional C-scan). Typical scanning time for the small selected region was about 1 hour. Optech Ventures test results are given in a confined power point presentation (Ref. 38).

4.6.2.1 CFRP specimen NLR-B

LU-tests were performed on a small selected region of the unpainted back wall with stiffeners of panel NLR-B. Some impact damages were present in the selected area (Fig. 4.49).

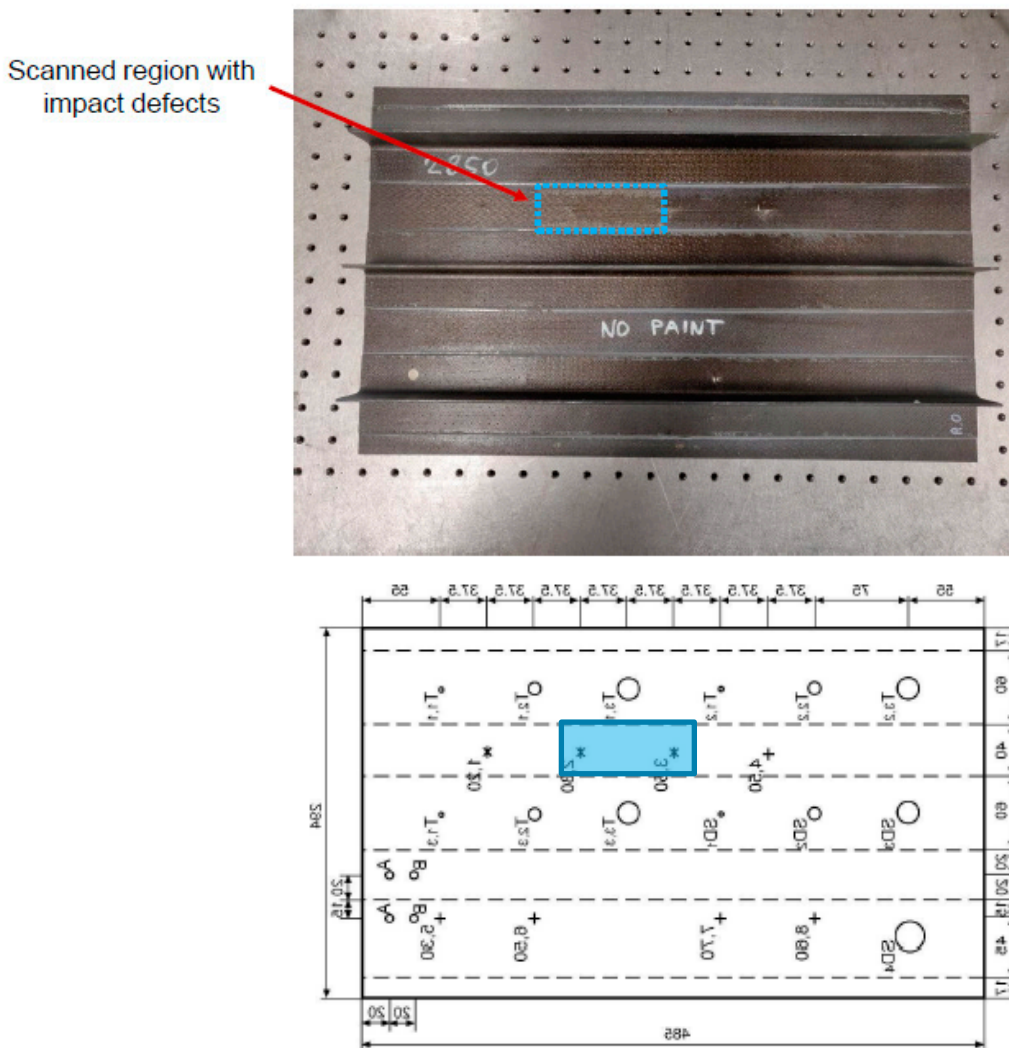


Fig. 4.49: Selected region on the unpainted back wall of panel NLR-B (to be checked)

B-scan results show longitudinal back wall signals over nominal regions and disruptive signals over the defects (Fig. 4.50). No further analysis (C-scan with detailed size and depth information) has been reported.

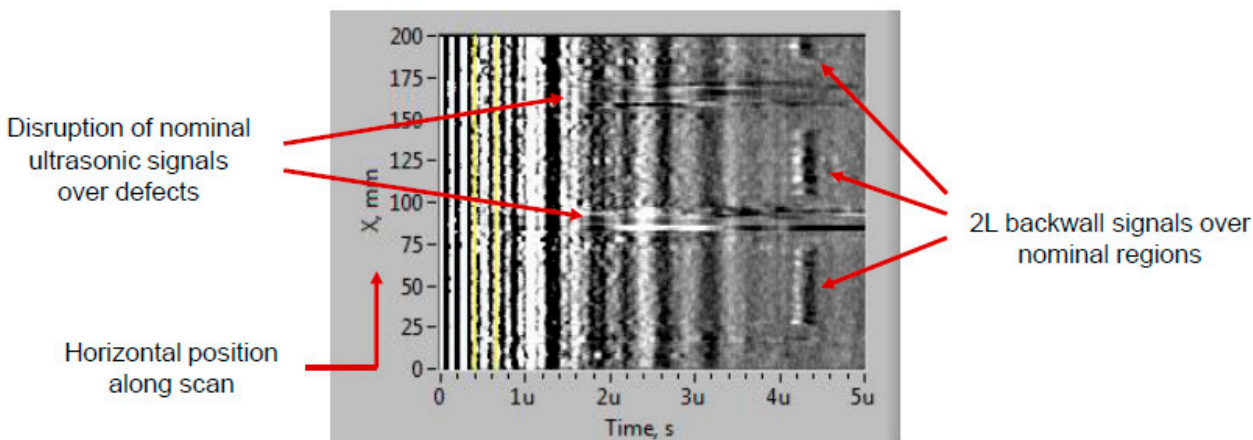
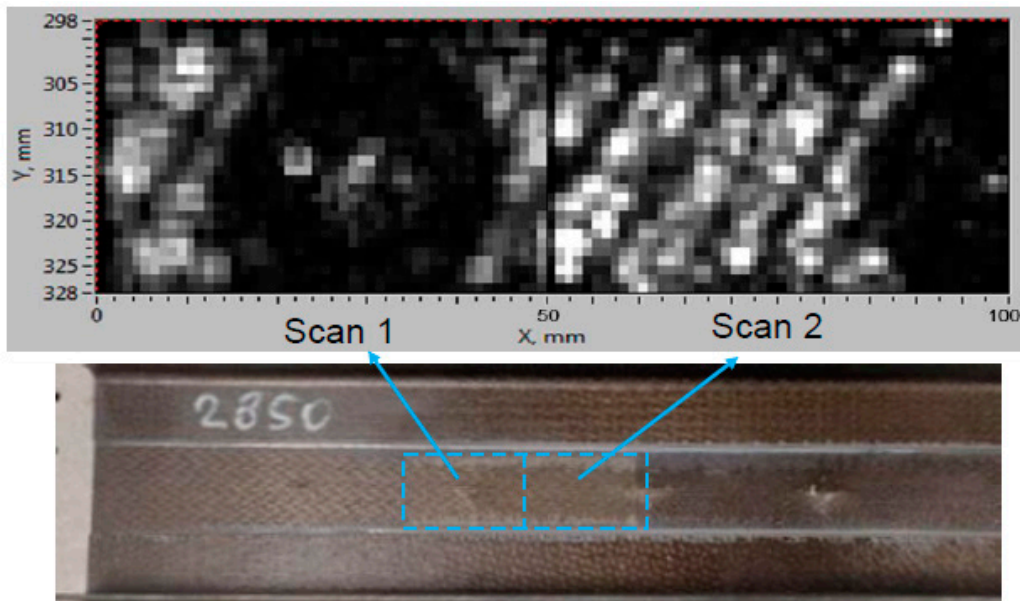


Fig. 4.50: B-scan results on selected region on panel NLR-B

Optech Ventures did a more thorough (high spatial resolution) analysis on the selected region. Two amplitude C-scans of the back wall signal of neighbouring areas are combined (Fig. 4.51) to deliver the combined C-scan (Fig. 4.52). Although this technique according to Optech Ventures would reduce noise, the authors still encounter difficulties to unambiguously interpret the defects in the plot. Remarkable is the presence of the oblique blue lines characterizing the fiber weave pattern.



Two C-scans were acquired in neighboring regions then combined. Each C-scan was generated by plotting the peak-to-peak amplitude of the 2L backwall signal at each position

Fig. 4.51: High resolution C-scan of two neighbouring areas

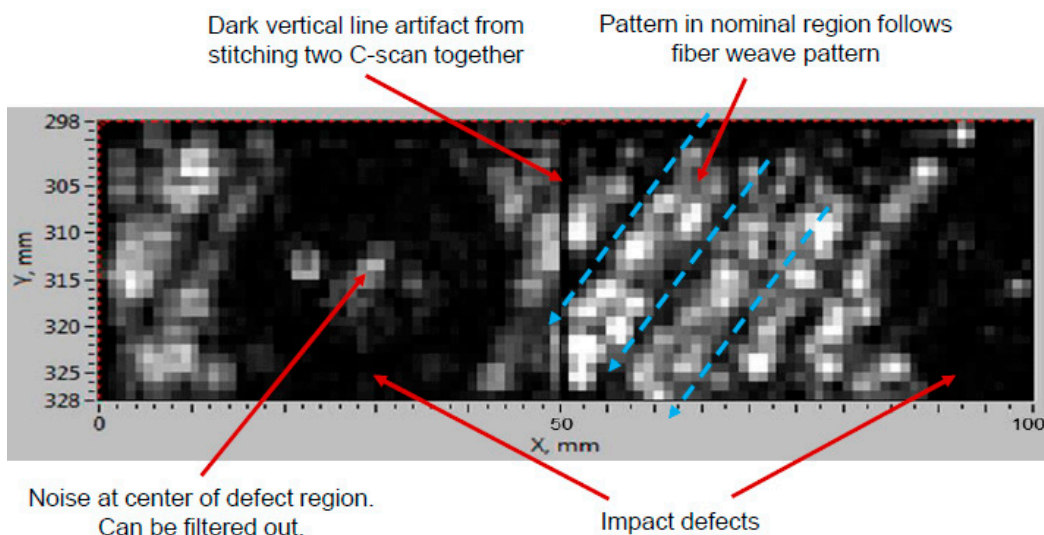


Fig. 4.52: Combined high resolution C-scan of the impact defects

4.6.2.2 CFRP specimen NLR-D

As discussed in section 4.6.2 no tests have been carried out on this panel.

4.6.2.3 RTM specimen #2118

Panel #2118 was scanned along the row A covering the 12 mm flat bottom holes of various depths (Fig. 4.53).

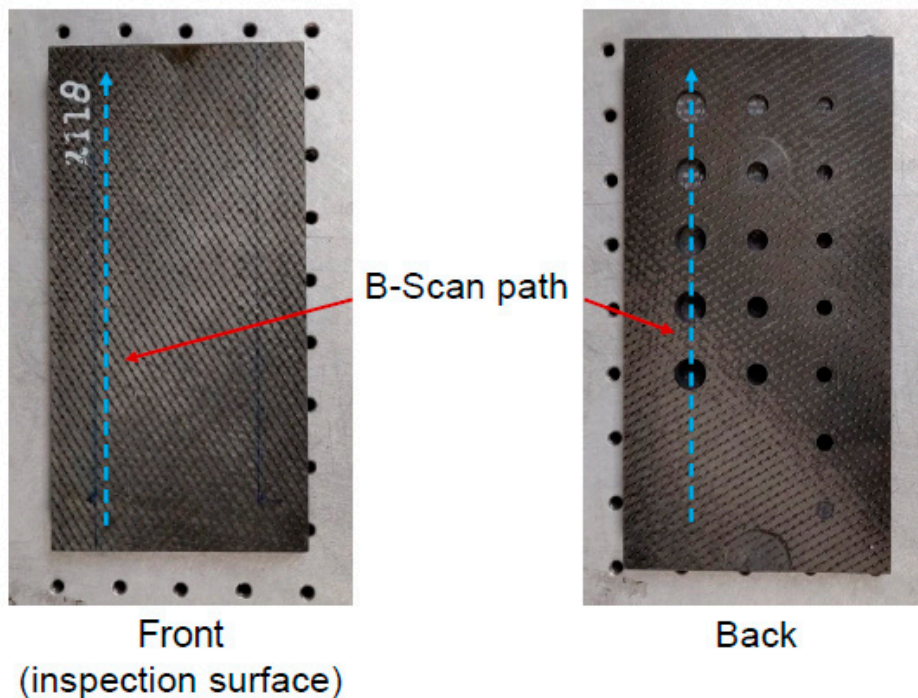


Fig. 4.53: Scanning line of panel #2118

B-scan results from the scanning line show strong 2L back wall signals of the deepest holes and weaker signals from the shallow holes (Fig. 4.54). No further processing has been done to obtain C-scan results.

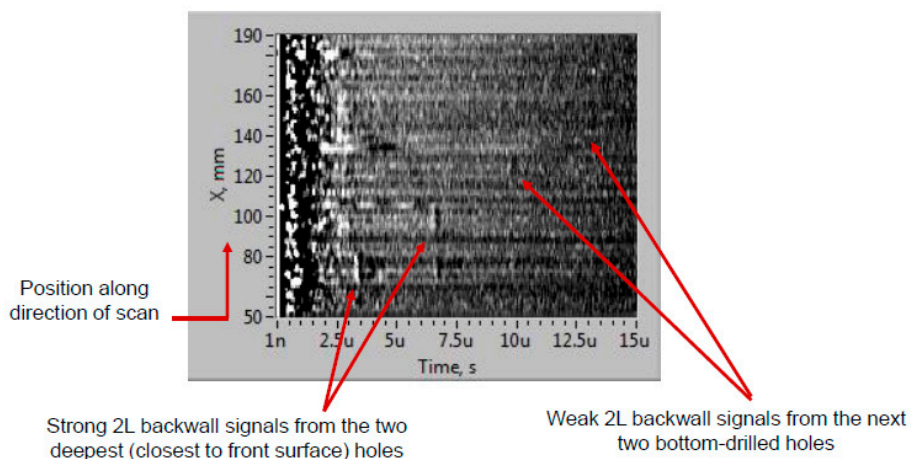


Fig. 4.54: B-scan results on panel #2118

4.7 Discolouration

Discolouration is damage effect to the test sample(s) obstructing the basic principle of NDT: non-destructive testing. The aim of LUT is to excite the composite structure in a thermo-elastic way without affecting the structure integrity. For completeness, it is noted that LUT applications on metal structures sometime are applied in ablative mode (vaporizing small surface particles). In the round robin program, we encountered several times problems with discolouration of the test panels. This effect could be both caused by the generation (larger spot size, typically 10 mm) and detection (point spot size, typically 1 mm) lasers. During the program we have faced these effects with the Xarion, Optech Ventures and Tecnar equipment. It is unknown of these (or minor related) problems also occurred with X-NDT UPI (the tests were not witnessed by NLR staff members) and Tecnatom (CO₂ laser (mirror controlled) with a wavelength of 10 µm and a Nd:YAG detection laser with a wavelength of 1.064 µm). These effects are dependent on material, surface finishing, reflectiveness, angle of incidence, wavelength and laser power. One clear example will be described hereafter identifying the issue: panel NLR-D tested at CSL with Tecnar equipment (Fig. 4.55).

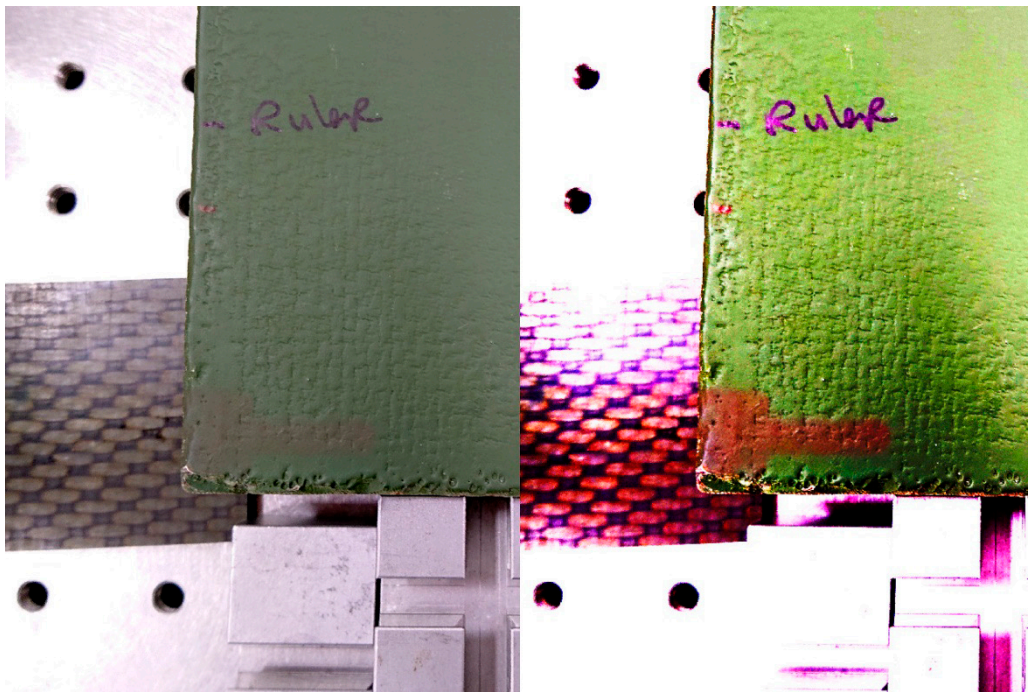


Fig. 4.55: Discolouration of NLR-D panel tested at CSL with Tecnar equipment

CSL before the test on test panel NLR-D would be carried out, did some preliminary testing with the Tecnar probe on the lower left corner. CSL noticed the discolouration of the surface from a green to a light brown colour. He processed the original picture somewhat to enhance the discolouration phenomenon (Fig. 4.55 left original photograph, right the result). In consultation with NLR, it was decided to cancel the test with the laser equipment and current experimental settings and parameters.

Based on the experiences in the DCMC round robin program, we have to come to the conclusion that the issue of discolouration of painted composite panels is a serious threat for the use of laser ultrasonic equipment in MRO applications. It is therefore not surprising that various operators (including CSL with their OPO generation laser) are looking for opportunities to modify their laser equipment and experimental settings and parameters (wavelength and power) to avoid this issue.

5 Discussion/recommendation

Generally, the measurements in Chapter 4 of this report have shown that laser ultrasonic equipment is well capable of detecting relevant defects such as impact damage and delaminations in composite structures with a configuration similar to the panels NLR-B and NLR-D. These panels however, consist of high quality CFRP material with a total thickness of less than 10 mm (base laminate plus stiffener/rib). For the thicker RTM specimen #2118 on the other hand, far less inspection performance is observed. This might be explained by the specimen thickness (27 mm) and/or the fibre waviness present in the specimen in combination with the relative broadband excitation using LUT. Another contributing factor could be the shiny surface, influencing the effectiveness of the laser systems/beams. Test experiences and results of some hardware suppliers indicate that the use of laser ultrasonics has not received the required maturity level for MRO applications and the test results compared to the base-line C-scan results are less detailed and clear. Robotizing the LUT probe head compared to the C-scan may affect the scan speed (typically C-scan speed is 100 mm/s). The issue of discolouration of painted composite panels is a serious threat for the use of laser ultrasonic equipment in MRO applications. When LUT equipment will be applied covering larger areas of inspection (typically 1 m²), complementary ultrasonic equipments (for example RapidScan™ & DolphiCam™) is recommended for detailed in-service inspection of relatively small areas (0.01 m²).

In the sequence, main results of all suppliers (X-NDT, Tecnatom, Xarion, Optech Ventures and Tecnar) are summarized and the quality of the equipment for DCMC MRO-applications is discussed. Furthermore, indications of scan speed and equipment prices are given.

X-NDT UPI-PE

C-scan results on panel NLR-B are good (Fig. 4.8 to 4.10). C-scan results on panel NLR-D are reasonable (Fig. 4.11 to 4.13). C-scan results on panel #2118 are poor and might be contributed to signal to noise problems (reflective front surface), broad band laser excitation (in comparison with small band excitation by conventional UT transducers) and thick sample with waviness plies. X-NDT delivers powerful processing software (i.e. VTWAM) and the scan velocity is assumed to be moderate (note that the tests were not witnessed by NLR staff members). Basic equipment amounts to a purchase price of 350 k€. Furthermore, the equipment can be used to explore the NDI-features of Lamb wave propagation.

Tecnatom Tecnalus

C-scan results on panel NLR-B are excellent (Fig. 4.17 and 4.18, approach NLR base line results). Also excellent C-scan results are found on panel NLR-D (Fig. 4.19 and 4.20). Temperate/reasonable results are found for panel #2118. The scan-speed is amazingly fast by the mirror system (about 15 s for a complete scan of the panel). The price of the equipment is very high and to be estimated above 2M€ if it would be commercially available (which is not the case yet). Tecnalus is the most advanced system and not based on fiber technology.

Xarion

Xarion developed the broad band optical (compared to a conventional) microphone as UT-sensor. During the tests, some discolouration problems with the excitation laser occurred. Xarion equipment could not be applied in pulse – echo mode. Tests have been done in transmission and pitch and catch modes, limiting this method for in-service inspection (single-sided inspection). Good C-scan transmission results are found on panel NLR-B (Fig. 4.27). Moderate C-scan transmission results on NLR-D are found (Fig. 4.31 to 4.33) and reasonable results on panel #2118 (Fig. 4.35 and 4.36). Moderate C-scan results on panel #2118 using the pitch and catch technique are found (Fig. 4.38). Scanning speed is dependent on the traversing system or robot. The price of the equipment amounts to about 100 k€.

Tecnar

The tests with the Tecnar equipment were carried out at CSL. There were serious problems with the discolouration of sample NLR-B. No tests were carried out on panel NLR-D. So far, no usable C-scan results could be obtained. Therefore it is proposed to send two other, less critical, test samples with artificial defects to CSL to obtain useful results to be included in this report. Scan speed is low. Tecnar equipment costs amounts to 350 k€. Co-operation with CSL gives the possibility to improve the hardware by the introduction of the in-house developed OPO laser, which might be less harmful to the composite panels. A basic Tecnar system amounts to a price of 350 k€.

Optech Ventures

Optech Ventures is more specialized on NDI work on metals (welding inspections and in-line monitoring of additive manufacturing process). Decolourisation problems were encountered during the tests. Panel NLR-D was not tested due to the limited test slot. Moderate C-scan results were found on panel NLR-B and #2118. Panel NLR-B was excited from the unpainted back wall with stiffeners. The scan speed on small selected areas was very low (about 1 mm/s). The price of basic equipment and software amounts to a price of 100 k€.

A brief summary of the results is shown in table 5.1

Table 5.1: Summary of the round robin test results on the composite panels NLR-B, NLR-D and #2118

Equipment	C-scan quality	Typical scan speed	Indicated market price	General remark (advantages, disadvantages)
X-NDT UPI PE	+	x mm/s	350 k€	Good results except on panel #2118
Tecnatom	++	1000 mm/s	> 2 M€	Superior results and scan speed, no fiber coupling, not commercially available
Xarion	+	10 mm/s	100 k€	No pulse echo (alternatively pitch and catch capability), good transmission results (requires two-sided access)
Tecnar	~	1 mm/s	350 k€	Problems with decolourization, co-operation on further developments with CSL
Optech Ventures	~	1 mm/s	100 k€	More experiences with metal inspection, problems with discolouration

Meaning symbols: ++ very good, + good to reasonably, ~just acceptable to short fall

Concluding, the primary technique for in-service inspection of composites remains visual inspection delivering a quick survey of large composite structures. This must indicate suspect areas where damage might be present. In case of suspect damage indicated by visual inspection then more advanced NDI is needed for damage verification. The recommended method is still ultrasonic inspection to detect and characterize (size and depth) the damage.

Instead of traditional ultrasonic laser ultrasonic equipment may be used for this purpose, for specific applications such as curved parts or parts where a non-contact method is required or preferred. However, at this moment it is anticipated that other UT techniques such as UT phased array or an UT array camera are better options, for example the RapidScan™ roller probe and the DolphiCam™ shown in figure 1.4. These array systems are more cost-effective and can work almost couplant-free (generally a fine water spray is used to provide a better inspection result). Their only drawback is the limited area of coverage; the RapidScan™ provides a scan area with the width of the roller probe (probes with a 50 to 100 mm active array width are available) and the DolphiCam™ presents a C-scan image over an area of only 31 x 31 mm. In-situ portable C-scan systems do exist (see Chapter 1) and they can provide a larger scan area but they always require a coupling liquid to be applied locally. So, the laser ultrasonic equipment might be an option for the in-service inspection of composite parts where operating non-contact is a requirement or preference

and where a larger C-scan image of roughly 500 x 500 mm is required. In case these boundary conditions do not exist and smaller area of coverage is allowed (e.g. for quick verification of suspect damage) then standard UT array equipment is more cost-effective.

Advantages of LU are clearly shown in this study: non-contact inspection, forgiving for the non-perpendicular incidence of the laser, and no need for (extensive) surface preparation and paint removal. Some LU inspections show comparable inspection quality and speed to the high-performance conventional ultrasonic inspection. Limitations of LU method is also clear: ablation danger, high acquisition costs and less effective on thick composite structures. Because laser ultrasonic equipment and its applications are still in development, while its advantageous properties are promising, it is advised to follow these developments in literature and OEM brochures.

Because laser ultrasonic equipment and its applications are still in development, it is advised to follow these developments in literature and OEM brochures. Regarding to the introduction of laser ultrasonics in the DCMC project, it is advised to start working with this inspection technique using relatively simple modular equipment (in contrast to an expensive turn-key system of main suppliers) and gain practical experience and know-how for the introduction of this technique in the in-service inspection for composite aerospace structures. In addition this gain in experiences with this technique can be very profitable in the selection process for turn-key DCMC laser ultrasonic equipment.

6 Conclusions

Test experiences and results of some hardware suppliers indicate that the use of laser ultrasonics has not received the required maturity level for MRO applications and the test results compared to the base-line C-scan results are less detailed and clear. Robotizing the LUT probe head compared to the C-scan may affect the scan speed (typically C-scan speed is 100 mm/s). The issue of discolouration of painted composite panels is a serious threat for the use of laser ultrasonic equipment in MRO applications. When LUT equipment will be applied covering larger areas of inspection (typically 1 m²), complementary equipment as RapidScan™ & DolphiCam™ is still recommended for detailed in-service inspection of relatively small areas (0.01 m²).

1. Laser ultrasonics (LU) is a relatively new NDI technique with great advantages for in-service inspection of composite aerospace structures. For example, it is essentially non-contact, requires only one-sided access and has a high tolerance relative to the incidence angle of the laser beam with the part ($\pm 20\text{-}35^\circ$) and to the distance between the scanning laser head and the part. It is therefore well suited for the fast and automated inspection of complex shaped composite parts.
2. The application of the current systems should be sought in the non-contact UT inspection of relatively small (area less than 1 m²) and thin composite parts (thickness up to about 10 to 15 mm) with a particular surface finish (e.g. standard paint system used on military weapon systems with mat surface poses no problem).
3. Investigations to assess laser generated damage effects are an essential step in the process of laser ultrasonic application.
4. For DCMC laser ultrasonics might be an option for the in-service inspection of composite parts where operating non-contact is a requirement or preference and where a C-scan image of say 500 x 500 mm is required. In case these boundary conditions do not exist and smaller area of coverage is allowed (e.g. for quick verification of suspect damage) then standard UT array equipment such as the RapidScan™ roller probe and the DolphiCam™ UT camera are more cost-effective.

Candidates for selected laser ultrasonic equipment for further exploration in DCMC (not directly to be used as turn-key equipment, but to maturise the technique further) are:

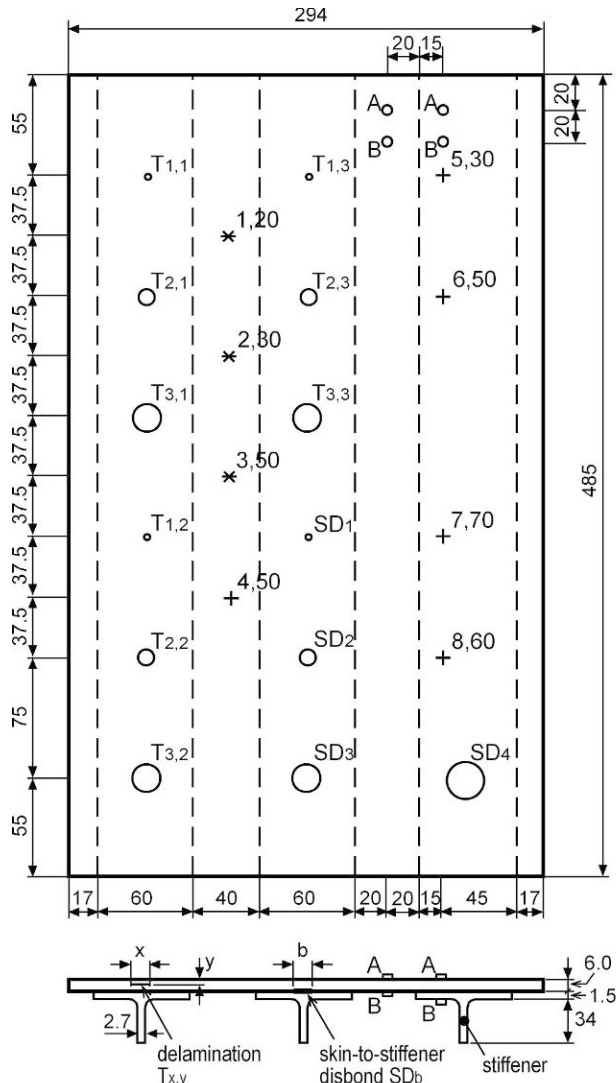
1. X-NDT UPI PE equipment; probably also the Lamb wave feature can then be further explored.
2. Tecnar equipment; either directly purchased from the OEM (standard equipment) or alternatively further developed in co-operation with CSL to avoid discolouration problems (OPO generation laser and Tecnar detection laser).

7 References

1. Heida, J.H. and Platenkamp, D.J.; Evaluation of non-destructive inspection methods, NLR report NLR-CR-2010-076, September 2010.
2. Chimenti, D.E.; *Review of air-coupled ultrasonic materials characterization*, Ultrasonics, Volume 54, pp. 1804-1816, 2014.
3. Huber, A.; *Non-destructive testing of future rocket boosters using air-coupled ultrasound*, 19th World Conference on Non-Destructive Testing, paper Tu.2.G.2., München, Germany, 13-17 June 2016.
4. Gaal, M., Daschewski, M., Bartusch, J., Schadow, F., Dohse, E., Kreutzbruck, M., Weise, M. and Beck, U.; *Novel air-coupled ultrasonic transducer combining the thermoacoustic with the piezoelectric effect*, 19th World Conference on Non-Destructive Testing, paper Mo.1.F.4., München, Germany, 13-17 June 2016.
5. Cuevas, E., Cabellos, E. en Hernandez, S.; Robot-based solutions for NDT inspections: Integration of laser ultrasonics for aeronautical components, 19th World Conference on Non-Destructive Testing, paper Th.3.F.4., München, Germany, 13-17 June 2016.
6. Freemantle, R.J., Hankinson, N. and Brotherhood, C.J.; *Rapid phased array ultrasonic imaging of large area composite aerospace structures*, Insight, Vol. 47, No. 3, March 2005, pp. 129-132
7. Heida, J.H., Platenkamp, D.J. and Bosch, A.F.; *In-service ultrasonic detection of impact damage in thick-walled composites*, NLR report NLR-CR-2016-202, July 2016.
8. Monchalain, J.-P., Néron, C., Padioleau, C., Lévesque, D. and Blouin, A.; *Laser ultrasonic, laser tapping and laser shockwave NDE technologies for polymer based composites*, NATO STO Workshop AVT-224 on Advanced Non-Destructive Evaluation Techniques for Polymer Based Composites in Military Vehicles, Riga, October 2013, paper #8.
9. Fahr, A.; *Aeronautical applications of non-destructive testing*, ISBN 978-1-60595-120-1, DEStech Publications, Inc., Lancaster (PA), USA, 2014.
10. Bossi, R.H., Technical Editor; *Aerospace NDT*, ASNT Industry Handbook, ISBN 978-1-57117-339-3, American Society for Nondestructive Testing, Inc., Columbus (OH), USA, 2014.
11. Dubois, M. and Drake, T. E.; *Signal processing techniques to improve laser-ultrasonic inspection of composites*, Materials Evaluation, Vol. 72, No. 7, July 2014, pp. 911-921.
12. Vandenrijt, J.-F., Walter, J., Brouillette, T. and Georges, M.P.; *Performances comparison of a laser ultrasonic system using 10.6 μm infrared or 532 nm visible generation beam for the investigation of CFRP*, 5th International Symposium on Laser-Ultrasonics and Advanced Sensing LU2016, Linz, Austria, 4-8 July 2016.
13. Vandenrijt, J.-F.; *Development of a fully fiber coupled laser ultrasonic system using mid-infrared OPO laser generation beam for CFRP inspection*, 6th International Symposium on Laser-Ultrasonics and Advanced Sensing LU2018, Nottingham, UK, 9-13 July 2018.
14. Tecnatom LUCIE
15. Optech Ventures LLC; *What is laser ultrasonic testing?*, LUT brochure, www.intopsys.com.
16. <https://www.tecnar.com/lus-laser/>

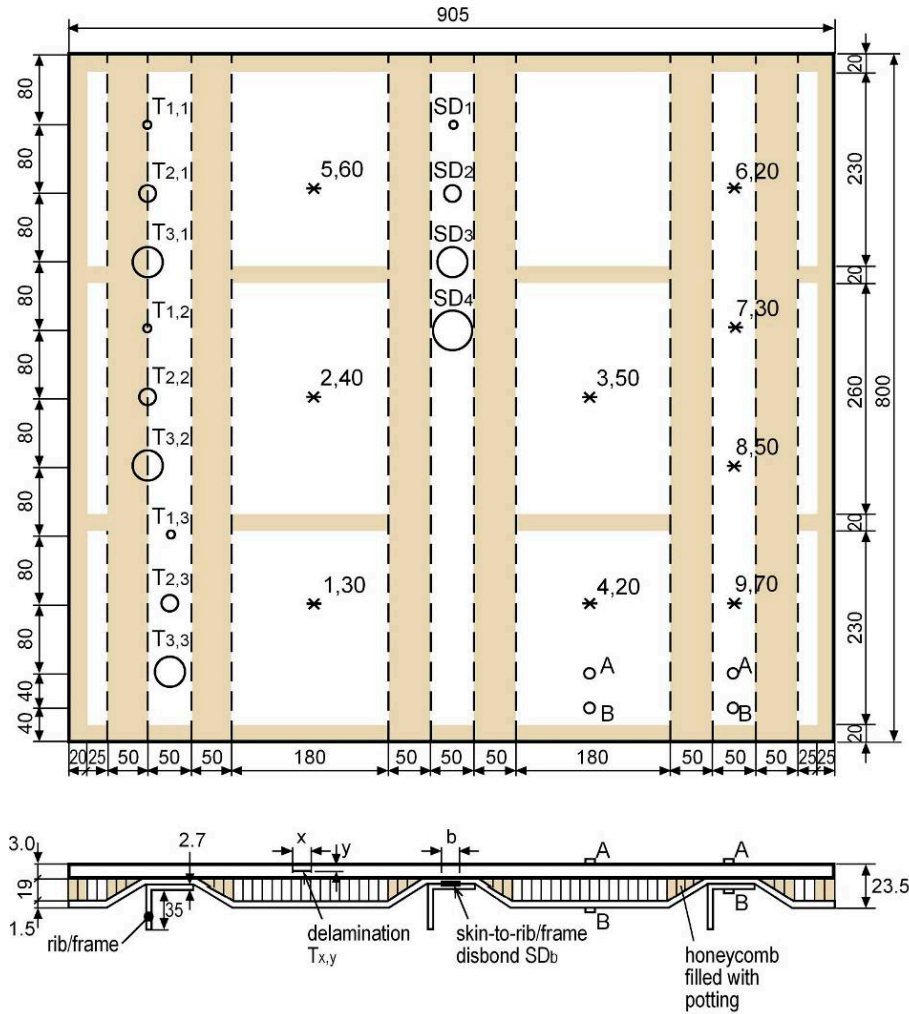
17. Space NDT X(-NDT) Inc.; *Ultrasonic propagation imaging*, <http://oesl.kaist.ac.kr/xndt>.
18. Lee, J.-R. and Sunuwar, N.; *Advances in damage visualization algorithm of ultrasonic propagation imaging system*, Journal of the Korean Society for Nondestructive Testing, Vol. 33, No. 2, pp. 232-240, 2013.
19. Hong, S.-C., Lee, J.-R. and Ihn, J.-B.; *In-situ NDE of composite repair patch and thick panel with substructures using mobile pulse-echo ultrasonic propagation imager*, Proceedings of the 11th International Workshop on Structural Health Monitoring, Stanford (CA), USA, 12-14 September 2017, pp. 2260-2267.
20. Shin, H.J., Hong, S.C., Lee, J.R. and Kim, J.H.; *Defect visualization of aircraft UHF antenna radome using full-field pulse-echo ultrasonic propagation imaging system*, Proceedings of the AEROTECH VI Conference on Innovation in Aerospace Engineering and Technology, Kuala Lumpur, Malaysia, 8-9 November 2016, paper 012027.
21. Opto-Electro-Structural Laboratory, *Research, Overall introduction*, South Korea, <http://oesl.kaist.ac.kr>
22. Testia ULTIS, <http://www.testia.com/products/ndt-products/ultis/>.
23. Shin, H.-J.; *PE-UPI Inspection report on NLR composite specimens*, XNDT-Report-04, X-NDT Inc., 18 June 2018.
24. Heida, J; *Laser ultrasonic testing of aircraft composite structures*, NLR-CR-2018-191.
25. Wikipedia, *Q-switching*, <https://en.wikipedia.org/wiki/Q-switching>.
26. Jean-François Vandenrijt , Dimitrios Kokkinos, Cédric Thizy, Fabian Languy, Juan Felipe Simar and Marc P. Georges, Development of a full fiber-coupled laser ultrasound robotic system using two-wave mixing 1064 nm detection and 532 nm YAG generation.
27. HTTU-EELUS-18-DEMO-04 ANNEX.pdf, Tecnatom test report 1
28. HTTU-EELUS-18-DEMO-04_FINAL.pdf, Tecnatom test report 2
29. HTTU-EELUS-18-DEMO-05 FINAL.pdf, Tecnatom test report 3
30. HTTU-EELUS-18-DEMO-06 FINAL.pdf, Tecnatom test report 4
31. Sensor magazin, *Optisches Mikrofon*, Magazin Verlag Hightech Publications KG, Ausgabe 3/September 2017.
32. Xarion test report 1, Report_NLR xarion measurements december 2018.pdf
33. Xarion test report 2, Scan NLR xarion panel with flat bottom holes transmission mode.pdf
34. Xarion test report 3, Scan NLR xarion result.pdf
35. Xarion test report 4, Scan NLR_pitch-catch update 011018.pdf
36. Xarion test report 5, Scan NLR_pitch-catch.pdf
37. CSL test report Tecnar results
38. Laser Ultrasonic Inspection of Composite Aerospace Components for NLR, Max Wiedmann and Marvin Klein, July 2, 2019, deliverable LU-tests at Optech Ventures

Appendix A Composite specimens



Defect type	
Delamination $T_{x,y}$	$x = 1, 2$ or 3 Diameter 0.25; 0.5 or 1.0 inch $y = 1, 2$ or 3 Depth 0.75, 2.25 or 5.25 mm
Skin-to-stiffener disbond SD_b	$b = 1, 2, 3$ or 4 Diameter 0.25; 0.5; 1.0 or 2.0 inch
Impact $+^{x,y}$ $*^{x,y}$	$+ / * $ Impactor tup diameter 0.5/1.0 inch $x = $ Impact number; $y = $ Impact energy [J]
Adhesive sticker	A $\varnothing 8$ mm on top side of skin B $\varnothing 8$ mm on bottom side of skin/stiffener

Fig. A1: Specimen **NLR-B**, solid laminate with three T-shaped stiffeners, and with artificial delaminations in the skin, skin-to-stiffener disbands, and low-velocity impact damages (Fig. A3 from Ref. 1)



Defect type	
Delamination $T_{x,y}$	$x = 1, 2$ or 3 Diameter 0.25; 0.5 or 1.0 inch $y = 1, 2$ or 3 Depth 0.75, 1.50 or 2.25 mm
Skin-to-rib/frame disbond SD_b	$b = 1, 2, 3$ or 4 Diameter 0.25; 0.5; 1.0 or 2.0 inch
Impact $+^{x,y}$ $*^{x,y}$	$+/*$ Impactor tup diameter 0.5/1.0 inch x = Impact number; y = Impact energy [J]
Adhesive sticker	A $\varnothing 12$ mm on top side of skin B $\varnothing 12$ mm on bottom side of skin/stiffener

Fig. A2: Specimen *NLR-D*, chamfered sandwich structure with three L-shaped stiffeners, and with artificial delaminations in the outer skin, skin-to-rib/frame disbonds, and low-velocity impact damages (Fig. A5 from Ref. 1)R

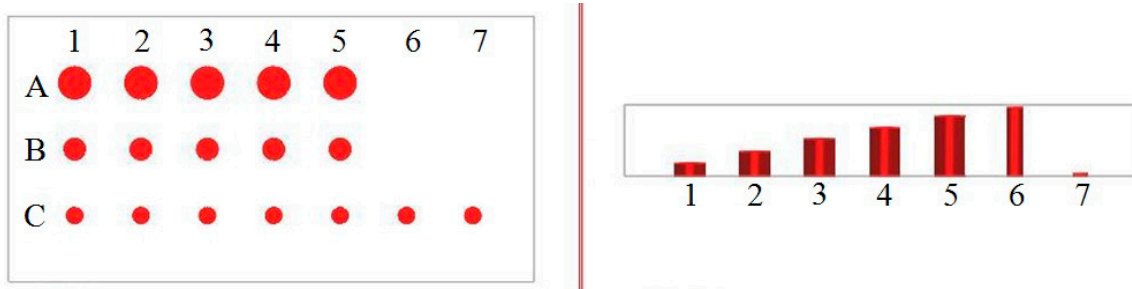


Fig. A3: Specimen #2118, RTM calibration specimen with flat-bottomed holes)

Table A.1: Diameter and distance to front surface for the FBH's in RTM specimen #2118

FBH No.	1	2	3	4	5	6	7
A \varnothing 12 mm	22.5	18.0	13.1	8.9	4.4	-	-
B \varnothing 8 mm	22.5	18.0	13.1	8.9	4.4	-	-
C \varnothing 6 mm	22.5	18.0	13.1	8.9	4.4	1	26.4

Appendix B Base-line UT inspection

Appendix B.1 Specimen NLR-B

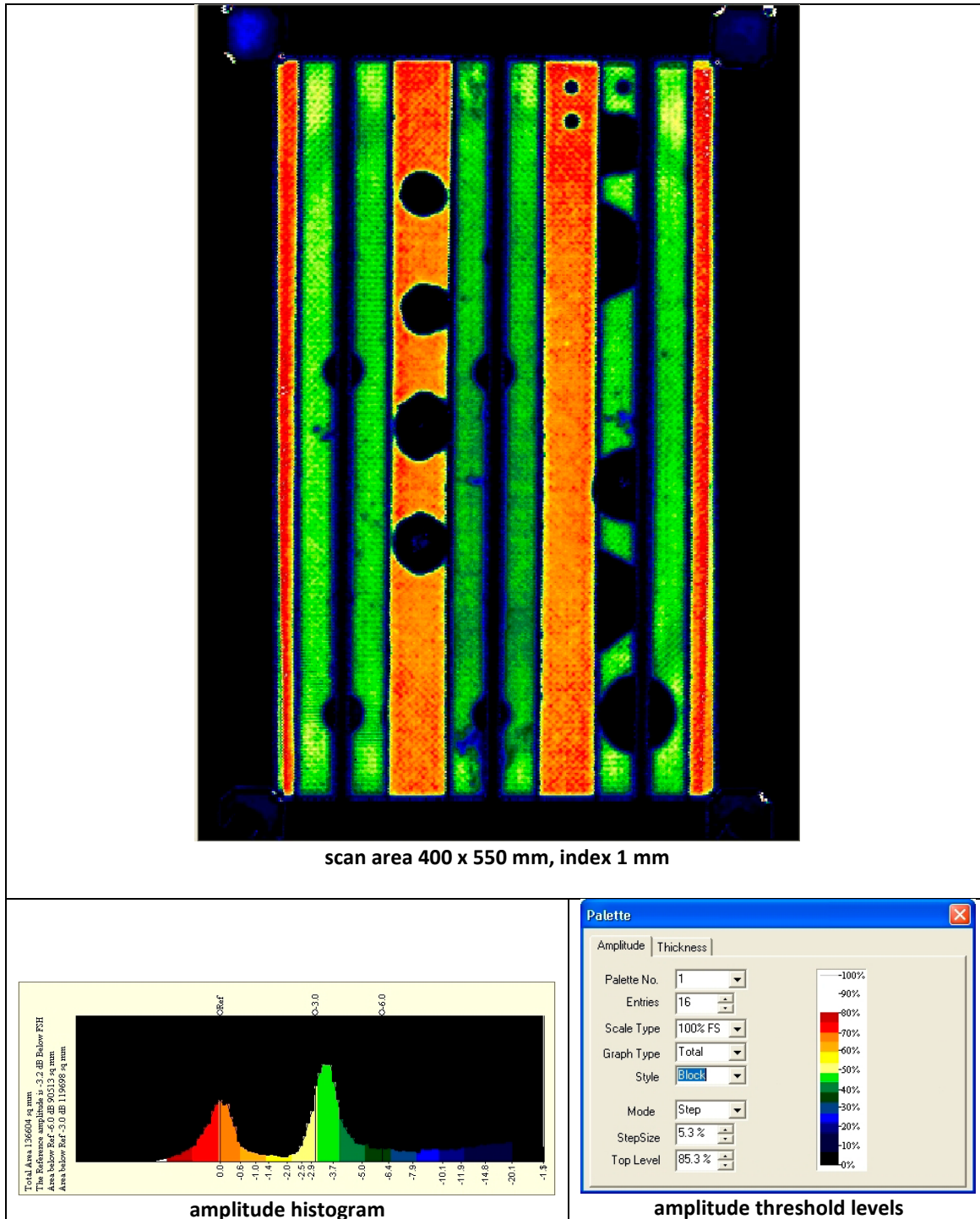


Fig. B1: Ultrasonic C-scan inspection of specimen NLR-B. Immersion mode. Double-through transmission (DTT) inspection with a 5 MHz focused transducer (Fig. B7 from Ref. 1

Appendix B.1 Specimen NLR-B (continued)

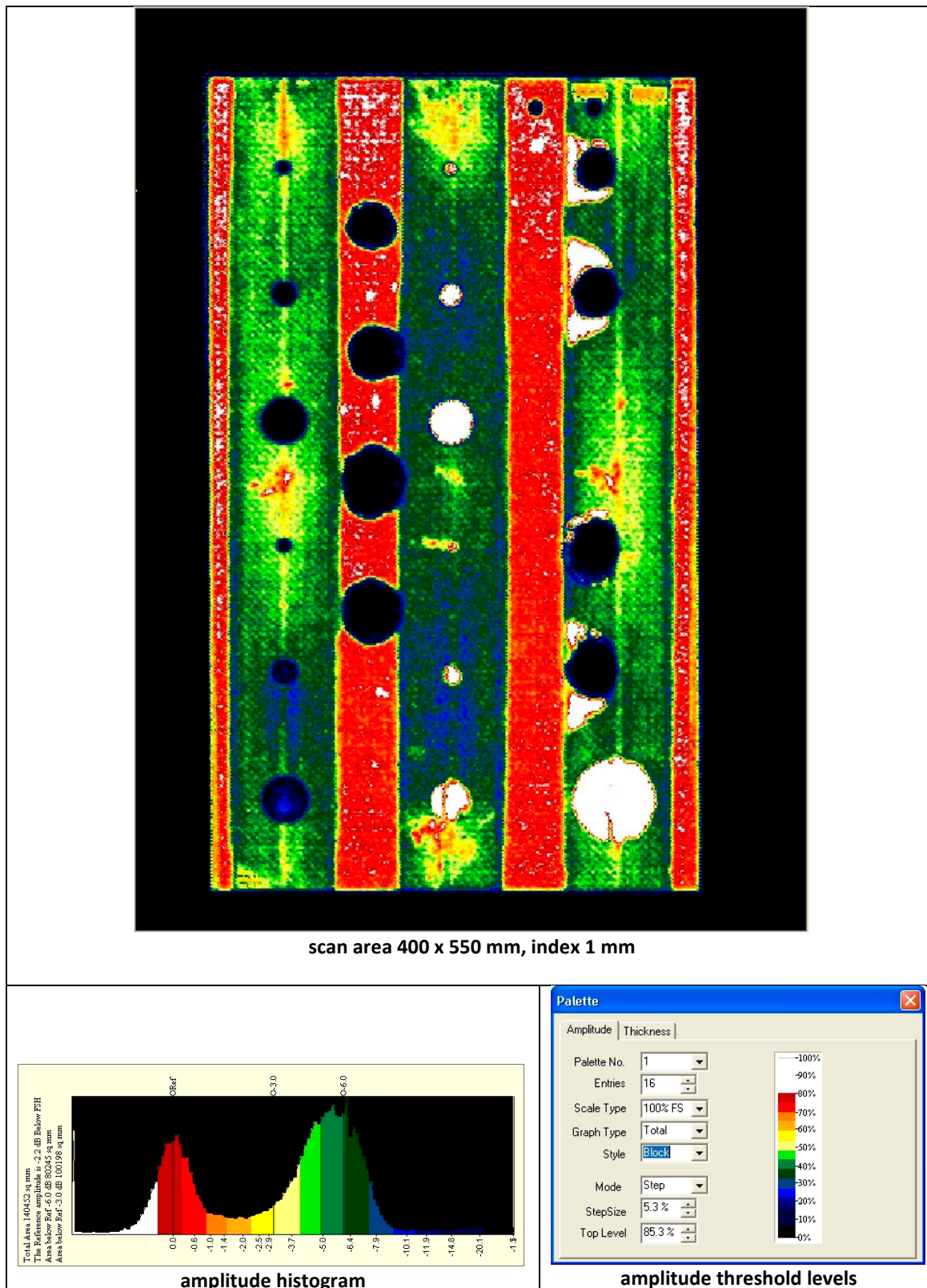


Fig. B2: Ultrasonic C-scan inspection of specimen NLR-B. Immersion mode. Pulse echo backwall-skin reflection (PEBR1) inspection with a 5 MHz focused transducer (Fig. B8 from Ref. 1)

Appendix B.1 Specimen NLR-B (continued)

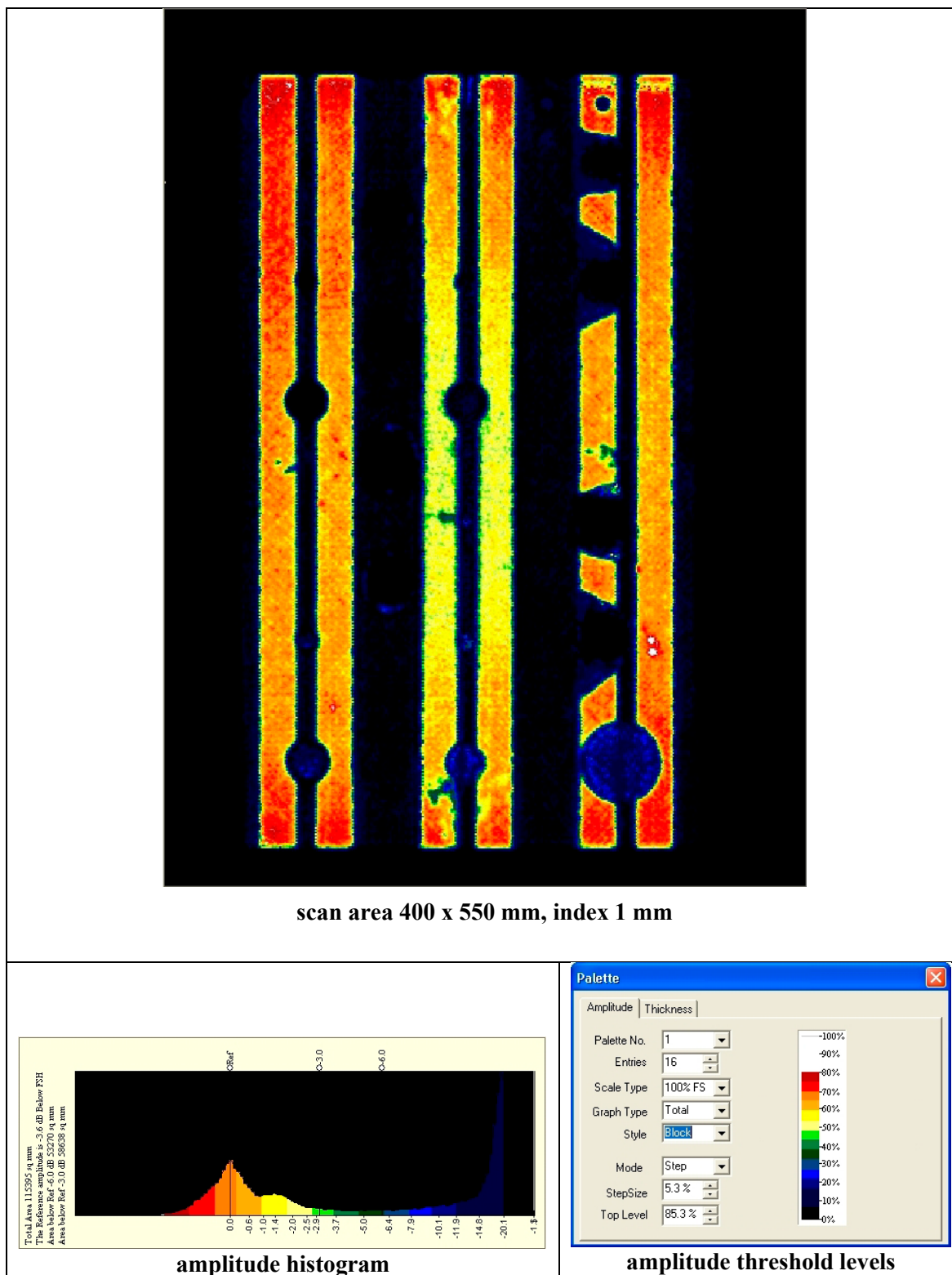


Fig. B3: Ultrasonic C-scan inspection of specimen NLR-B. Immersion mode. Pulse echo backwall-stiffener reflection (PEBR2) inspection with a 5 MHz focused transducer (Fig. B9 from Ref. 1)

Appendix B.1 Specimen NLR-B (continued)

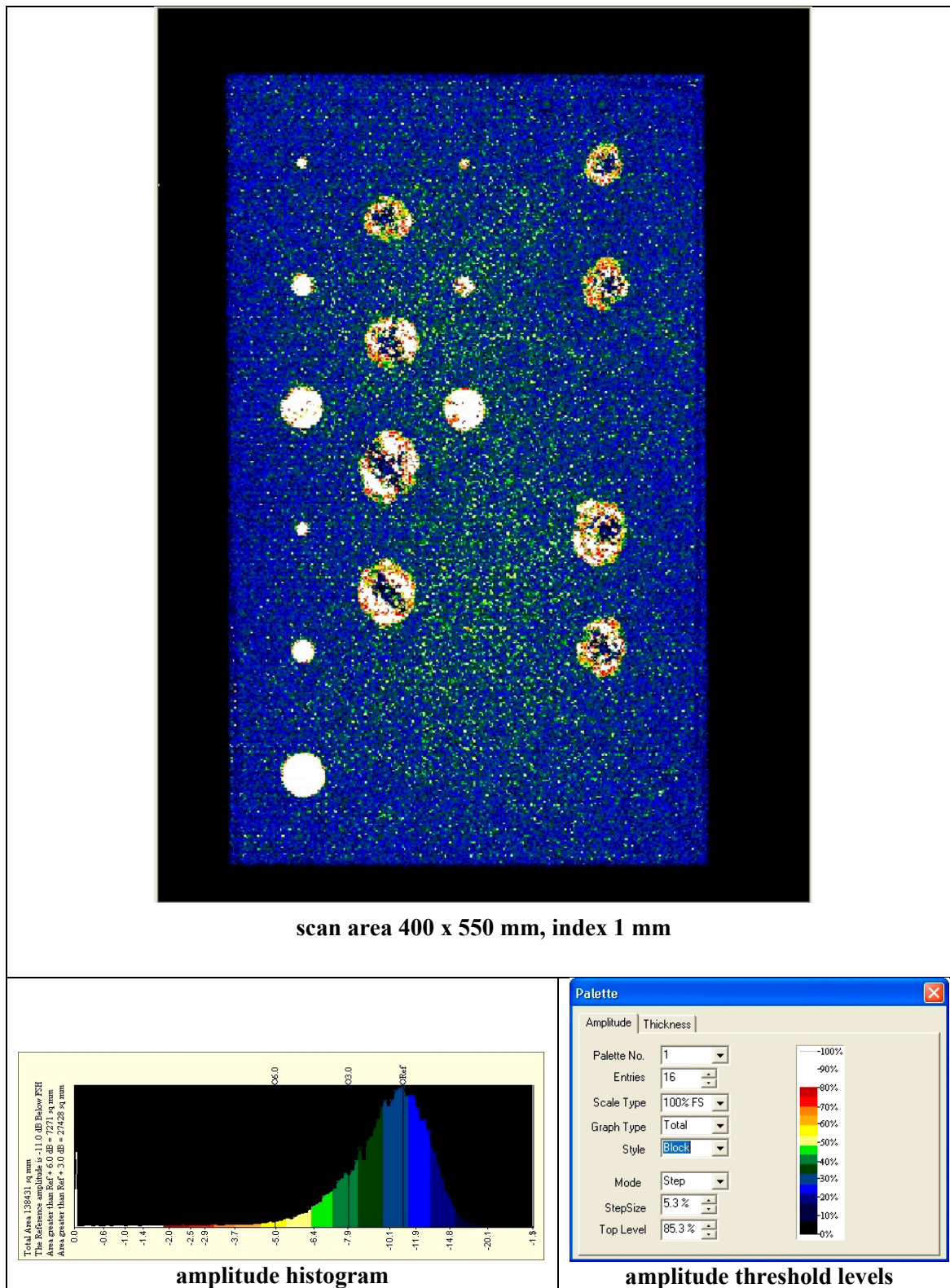


Fig. B4: Ultrasonic C-scan inspection of specimen **NLR-B**. Immersion mode. Pulse echo flaw reflection (PEFR) inspection with a 5 MHz focused transducer (Fig. B10 from Ref. 1)

Appendix B.2 Specimen NLR-D

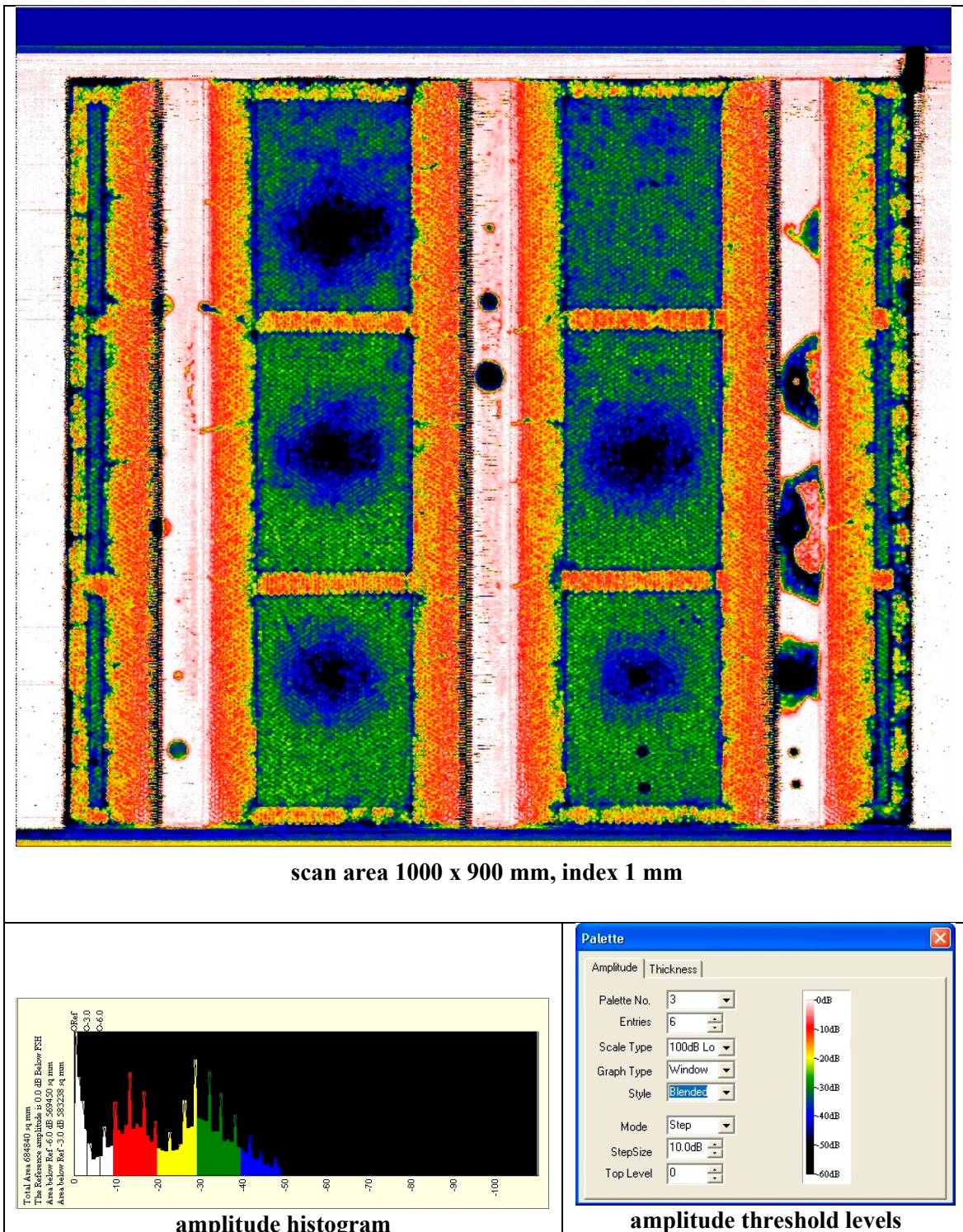


Fig. B5: Ultrasonic C-scan inspection of specimen **NLR-D**. Water-jet mode. Single through transmission (**TT**) inspection with a 2.25 MHz focused transmitter and a 2.25 straight-beam receiver (Fig. B14 from Ref. 1)

Appendix B.2 Specimen NLR-D (continued)

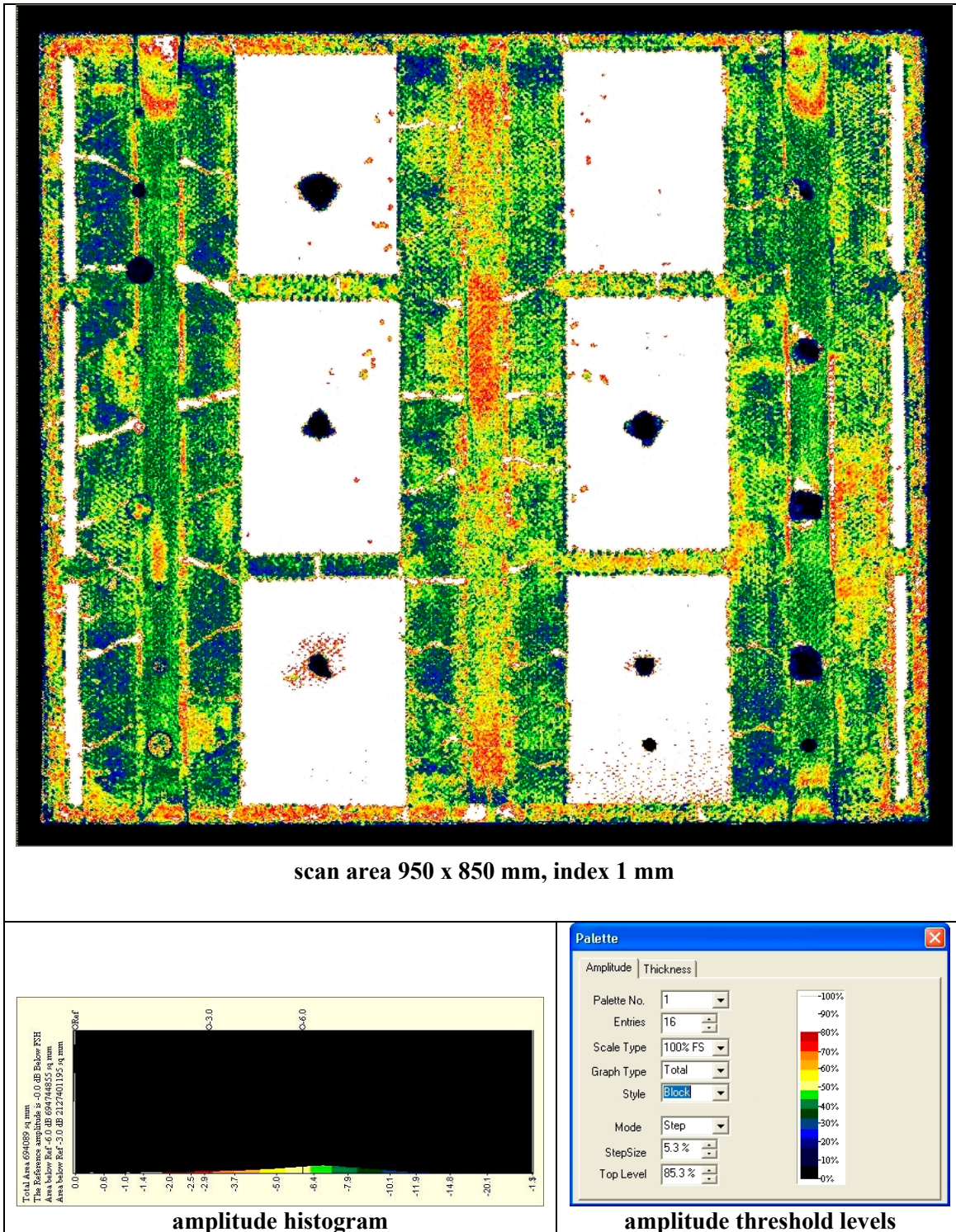


Fig. B6: Ultrasonic C-scan inspection of specimen *NLR-D*. Immersion mode. Pulse echo backwall-outer skin reflection (*PEBR1*) inspection with a 5 MHz focused transducer (Fig. B15 from Ref. 1)

Appendix B.2 Specimen NLR-D (continued)

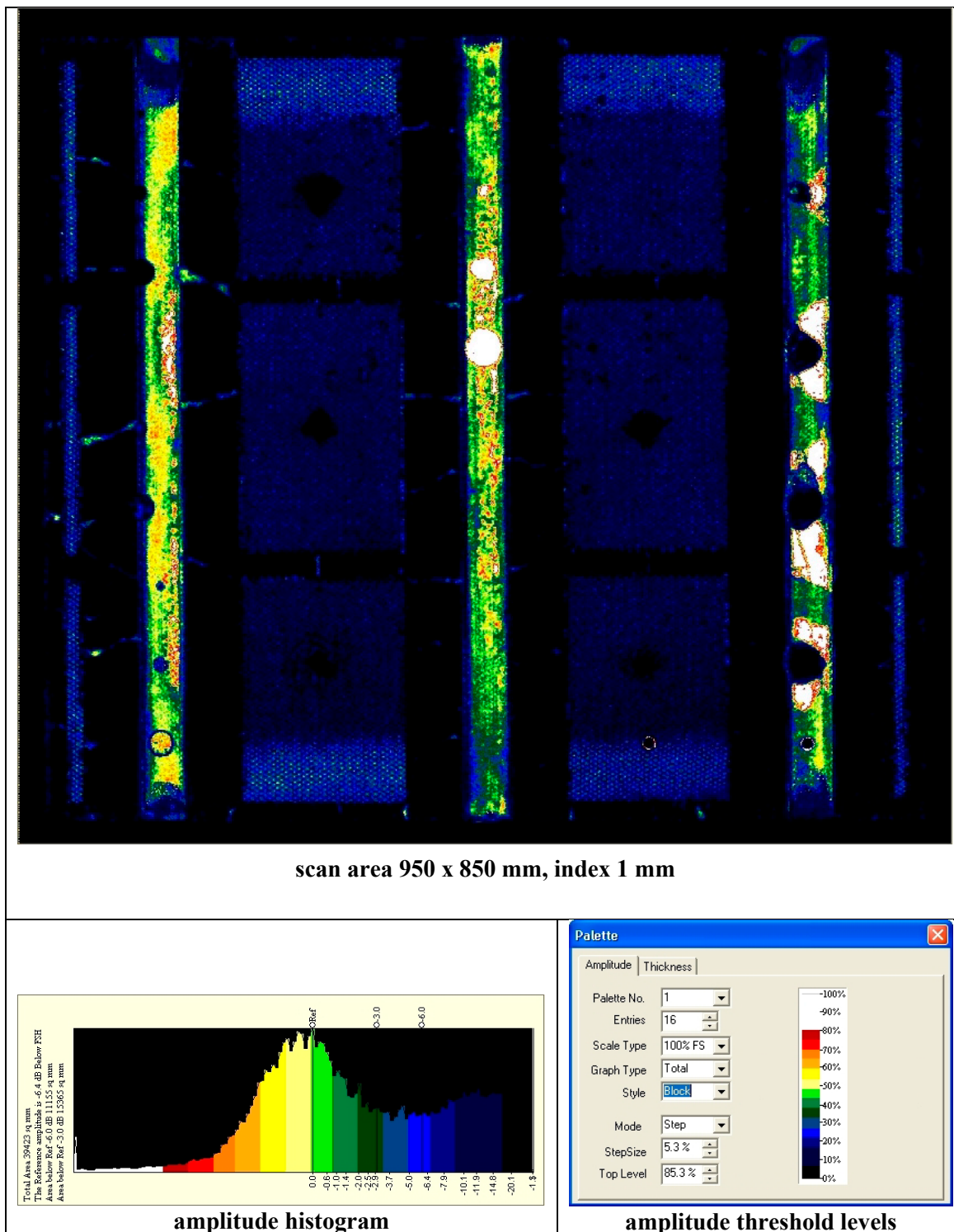
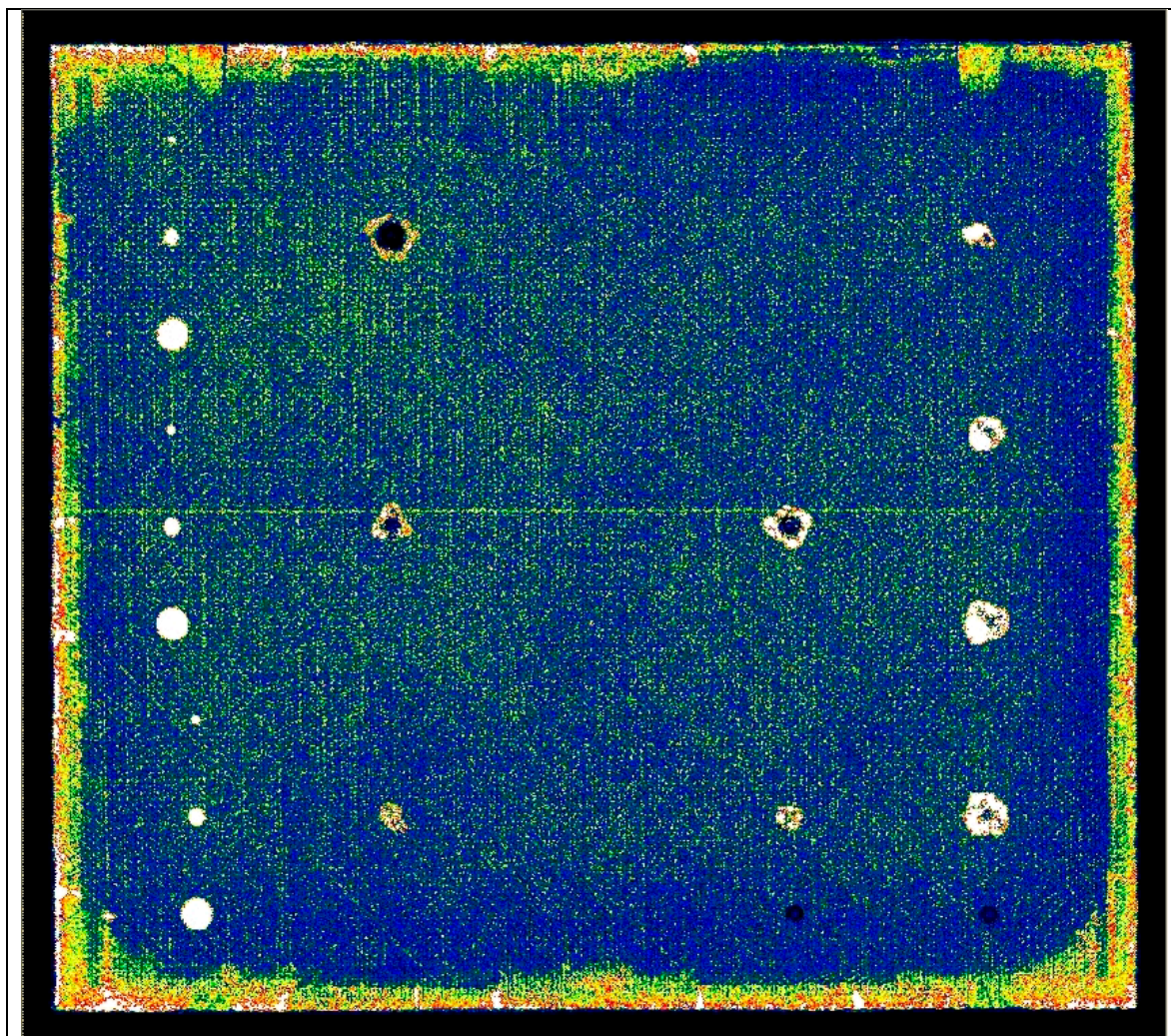
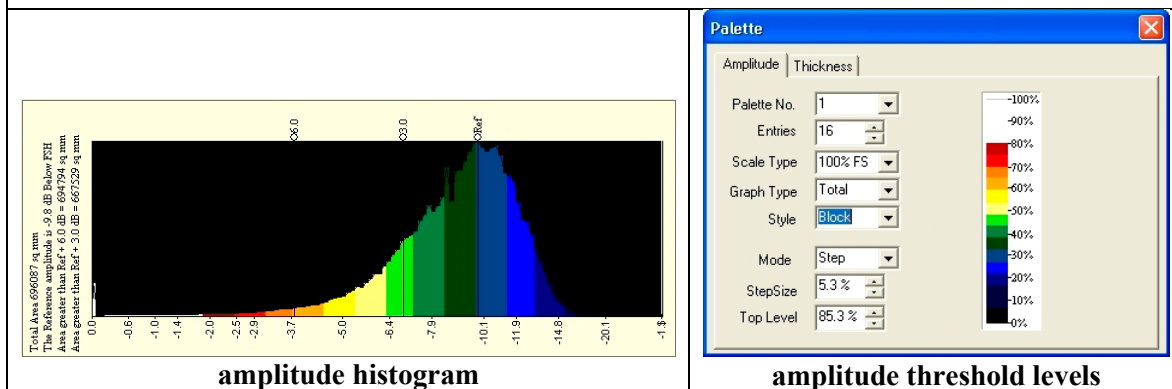


Fig. B7: Ultrasonic C-scan inspection of specimen **NLR-D**. Immersion mode. Pulse echo backwall-inner skin reflection (**PEBR3**) inspection with a 5 MHz focused transducer (Fig. B16 from Ref. 1)

Appendix B.2 Specimen NLR-D (continued)



scan area 950 x 850 mm, index 1 mm

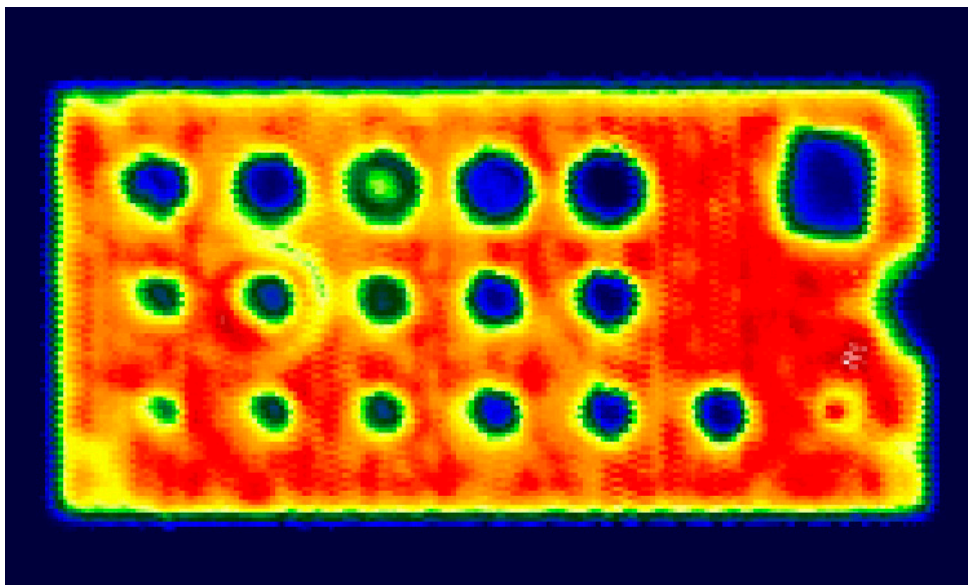


amplitude histogram

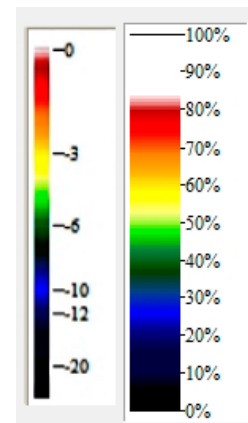
amplitude threshold levels

Fig. B8: Ultrasonic C-scan inspection of specimen **NLR-D**. Immersion mode. Pulse echo flaw reflection (PEFR) inspection with a 5 MHz focused transducer (Fig. B17 from Ref. 1)

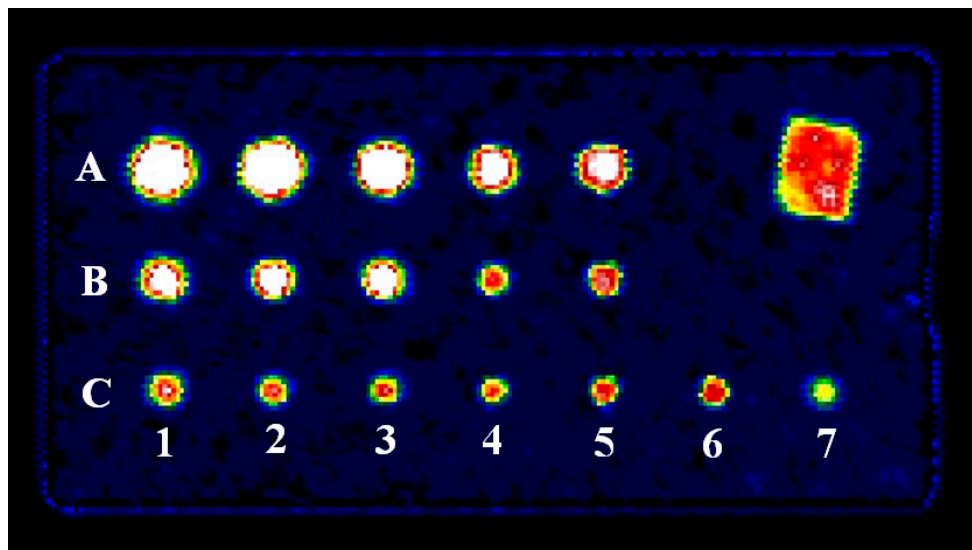
Appendix B.3 RTM specimen #2118



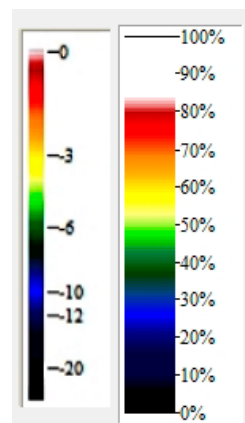
Pulse-echo backwall reflection (PEBR)



Colour palette with [dB] and [%] scale



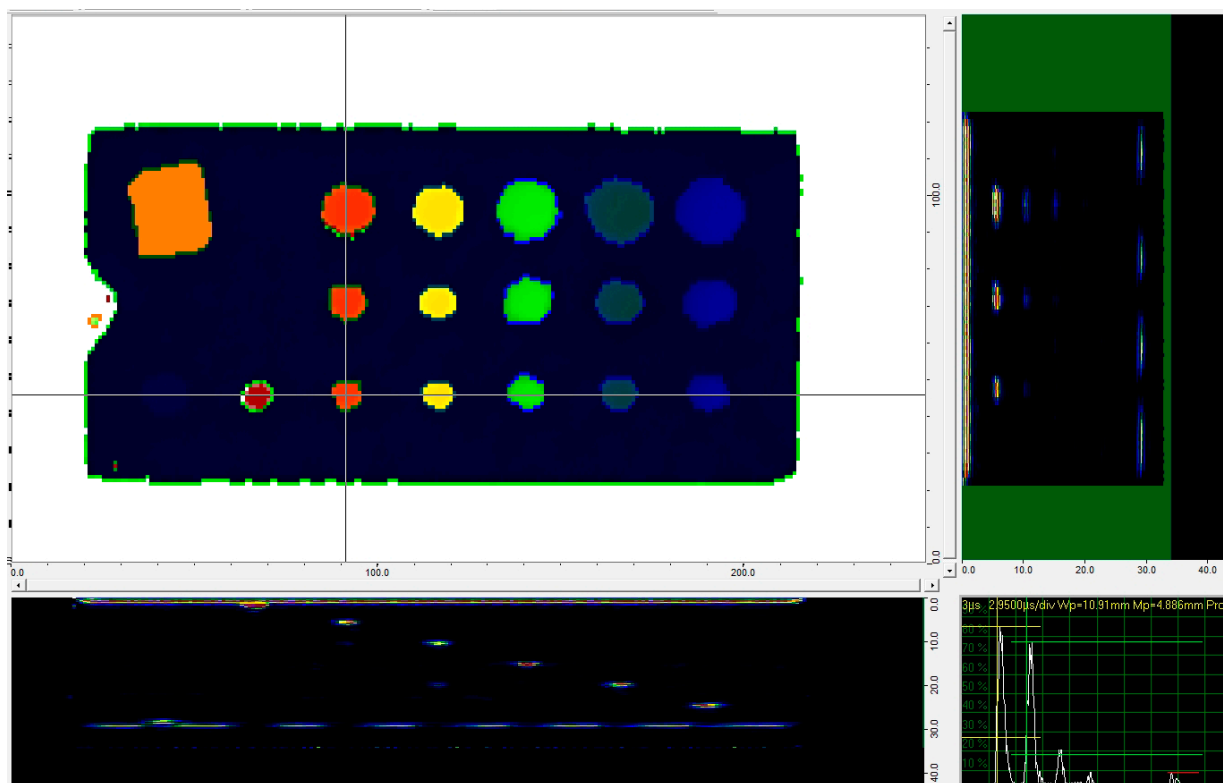
Pulse-echo flaw reflection (PEFR)



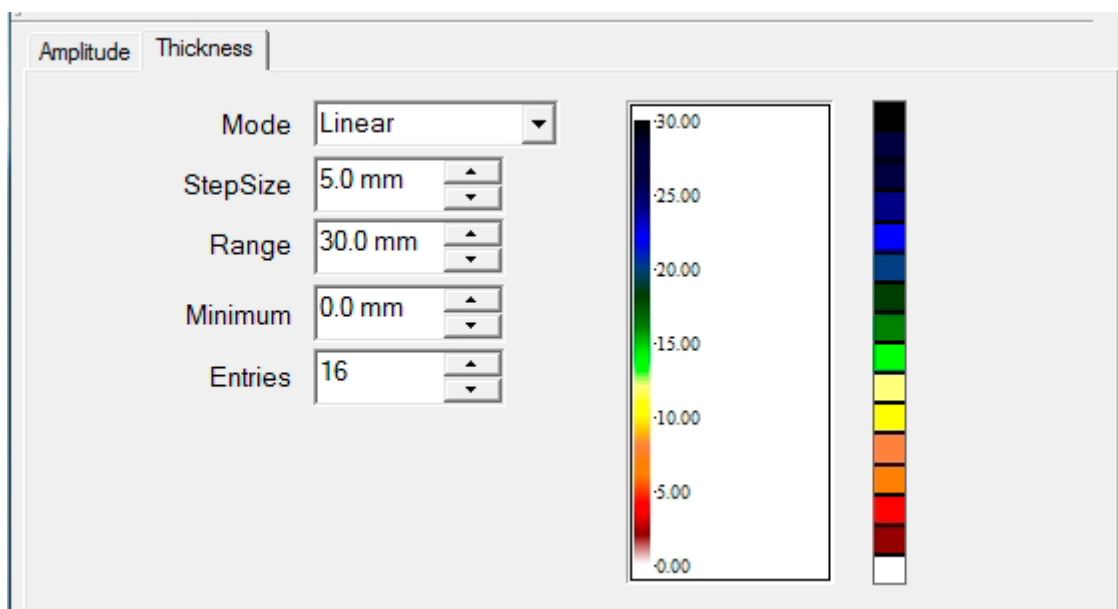
Colour palette with [dB] and [%] scale

Fig. B9: UT C-scan inspection of RTM calibration specimen #2118. PEBR and PEFR inspection with a 2.25 MHz focused transducer (Figs. 17 and 18 from Ref. 23)

Appendix B.3 RTM specimen #2118 (continued)



Time-of-flight inspection (TOF), with corresponding A-scan and B-scans at the cross-lines



TOF colour palette, linear scale (maximum thickness 30 mm)

Fig. B10: UT C-scan inspection of RTM calibration specimen #2118. TOF inspection with a 2.25 MHz focused transducer (Fig. 19 from Ref. 23)

Appendix C Laser ultrasonic PE-UPI inspection

Appendix C.1 Specimen NLR-B

Inspection report

X-NDT Inc. Address: (561-756) Room# 304, The Engineering Institute-Korea, 567 Baekje-daero, Duckjin-gu, Jeonju-si, Jeonbuk	Report No.	XNDT-Report-04
	Implemented By	Hye-Jin Shin 
Buyer: dhr, A.J. Otter BSc. • e-mail : Jaap.Heida@nlr.nl • Date of Issue : Apr. 26, 2018	Approved By	Jung-Ryul Lee 

1. Inspection Name : PE-UPI inspection on composite specimens

2. Inspection Items : Composite Specimens

Specimen	Specification	Quantity	Remarks
NTP-B	481 mm×294 mm×32 mm	1	
NTP-D	905 mm×800 mm×41 mm	1	
#2118	200 mm×100 mm×27.4 mm	1	Composite Specimen with 17 flat-bottomed holes (FBH).

3. Inspection Date : May 18, 2018 – May 31, 2018

4. Inspection Results : Please see attached "Inspection Results".

※ This inspection report is a report prepared by the test conditions required by the customer for equipment that does not maintain traceability, or items that are outside the scope of KOLAS accreditation. This report is forbidden to use for any other purpose.

June 18, 2018

X-NDT Inc. CEO *Jung-Ryul Lee* 

Composite specimen(NTP-B) UWPI result

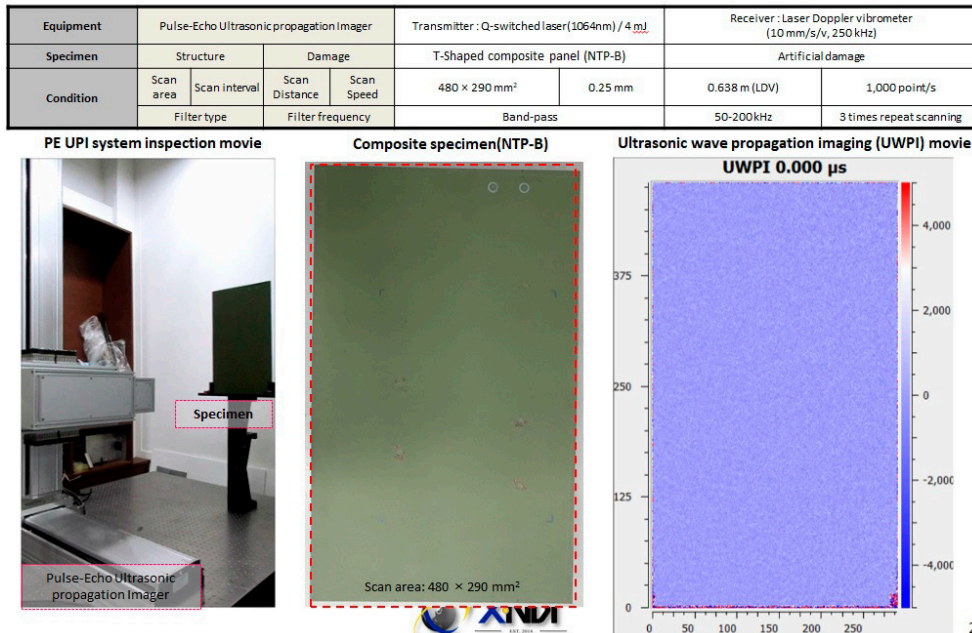
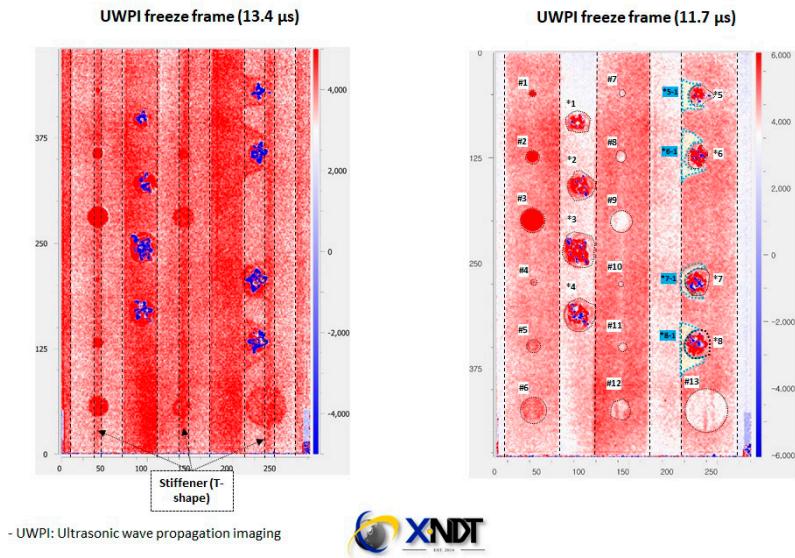


Fig. C1: PE-UPI inspection of specimen NLR-B. Inspection report and test set-up

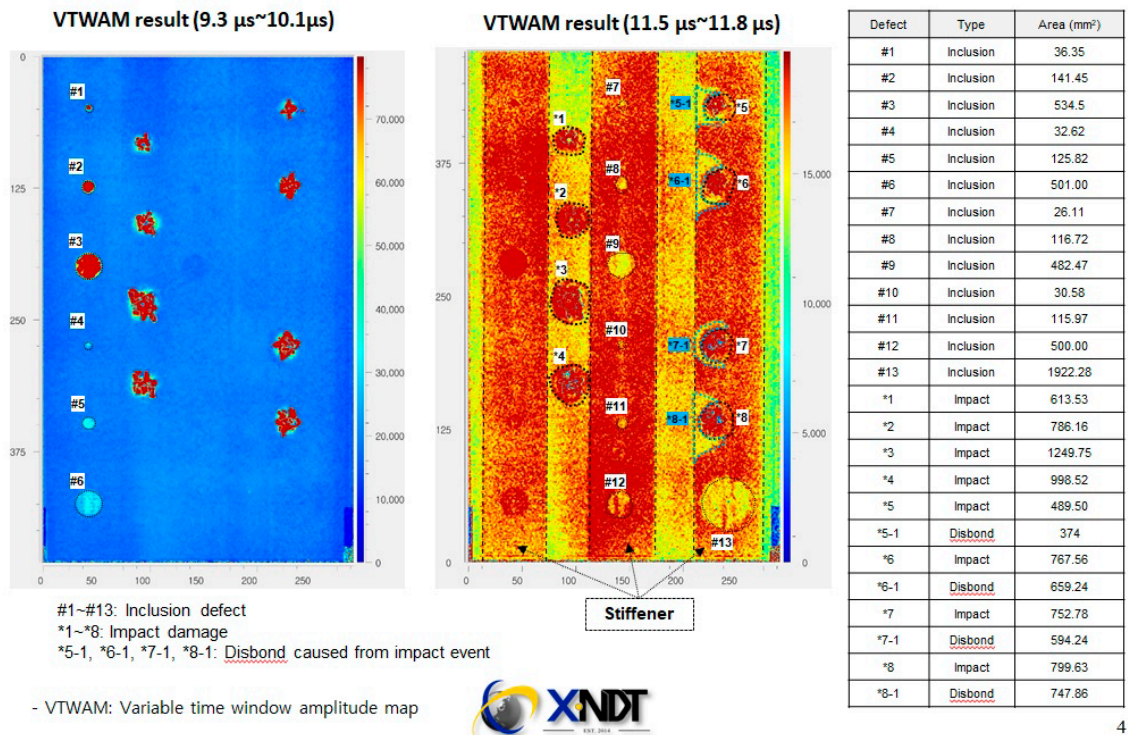
Appendix C.1 Specimen NLR-B (continued)

Composite specimen(NTP-B) UWPI result



3

Composite specimen(NTP-B) VTWAM result



4

Fig. C2: PE-UPI inspection of specimen NLR-B. UWPI and VTWAM results

Appendix C.2 Specimen NLR-D

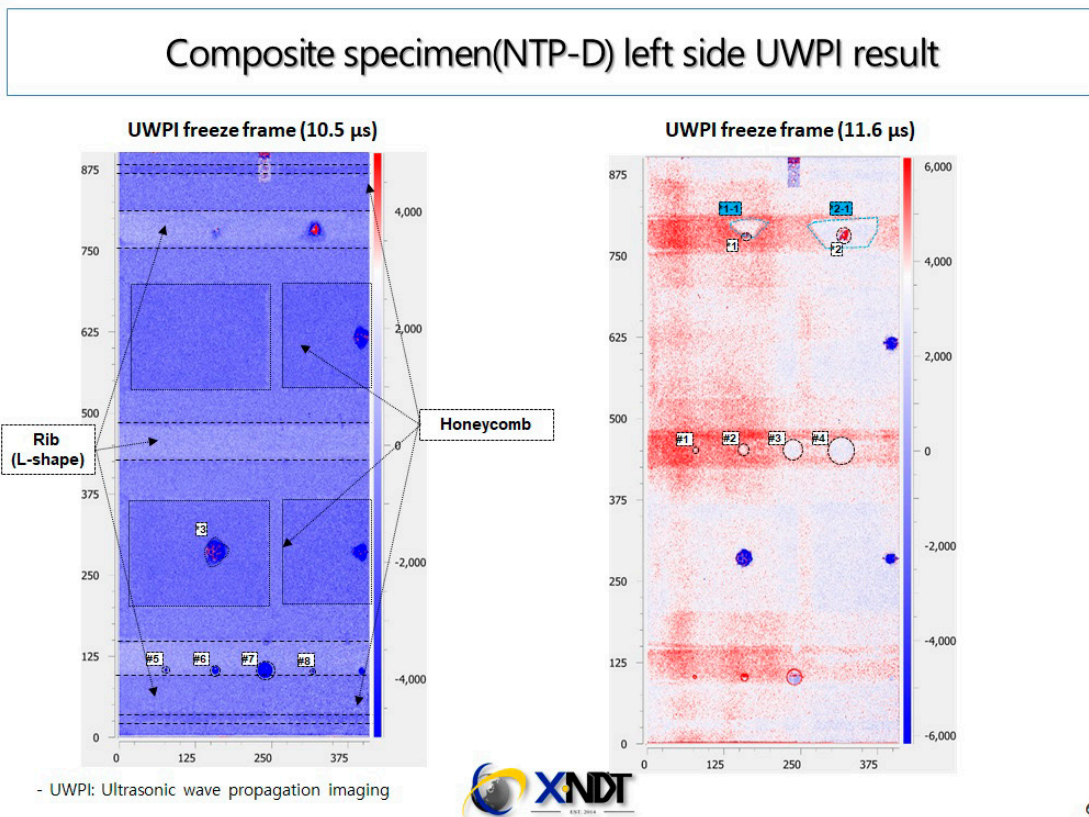
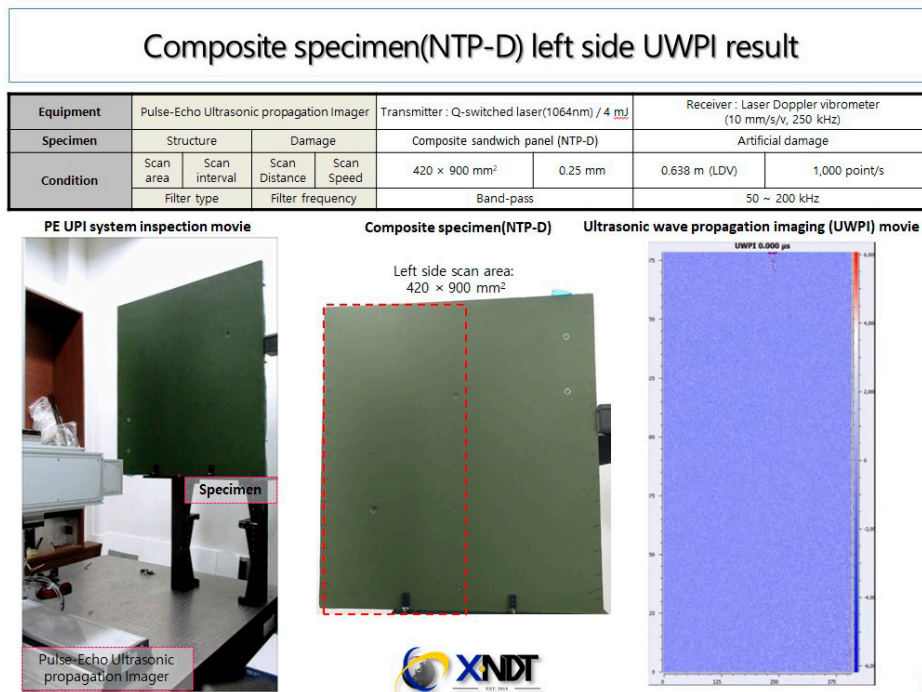
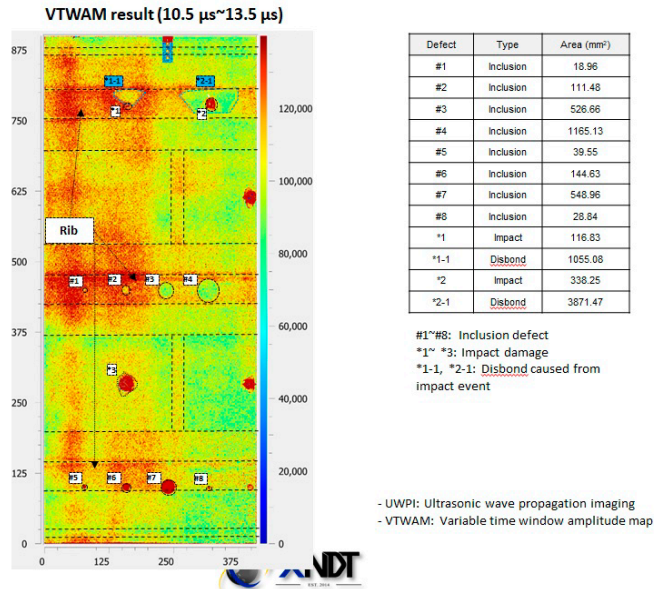


Fig. C3: PE-UPI inspection of specimen NLR-D (left side, lower half of Fig. A2). Test set-up and UWPI result

Appendix C.2 Specimen NLR-D (continued)

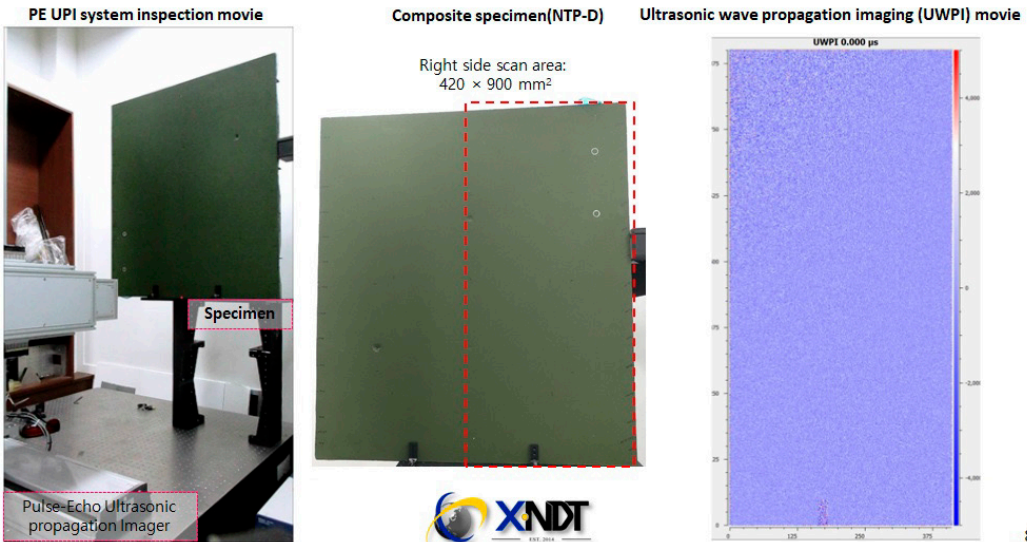
Composite specimen(NTP-D) left side VTWAM result



7

Composite specimen(NTP-D) right side UWPI result

Equipment	Pulse-Echo Ultrasonic propagation Imager		Transmitter : Q-switched laser(1064nm) / 4 mJ		Receiver : Laser Doppler vibrometer (10 mm/s/v, 250 kHz)	
Specimen	Structure		Damage		Composite sandwich panel (NTP-D)	
Condition	Scan area	Scan interval	Scan Distance	Scan Speed	420 × 900 mm ²	0.25 mm
	Filter type	Filter frequency	Band-pass		0.638 m (LDV)	1,000 point/s
						50 ~ 200 kHz

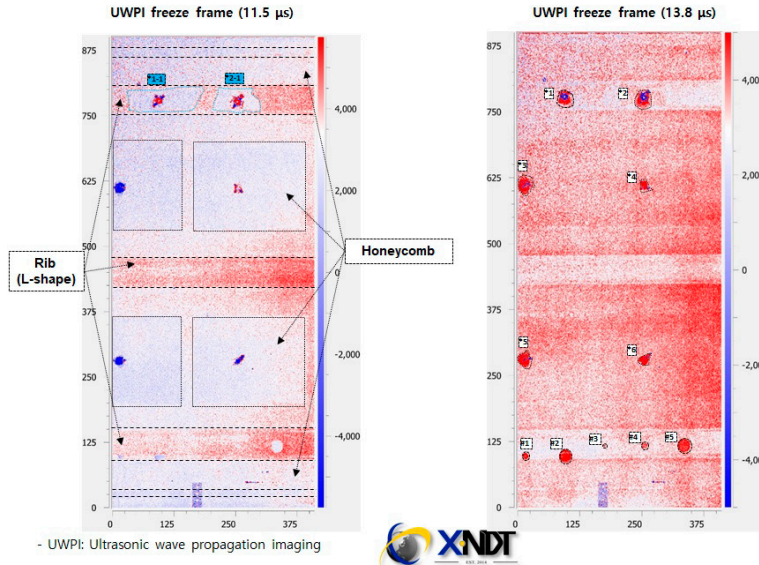


8

Fig. C4: PE-UPI inspection of specimen NLR-D. VTWAM result (left side, lower half of Fig. A2) and test set-up (right side, upper half of Fig. A2)

Appendix C.2 Specimen NLR-D (continued)

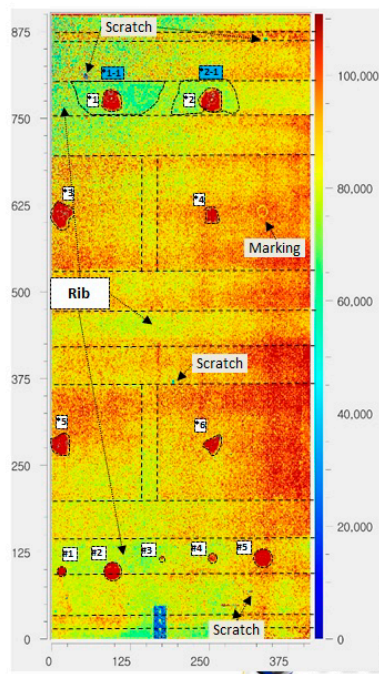
Composite specimen(NTP-D) right side UWPI result



9

Composite specimen(NTP-D) right side VTWAM result

VTWAM result (9 μ s~10.3 μ s)



Defect	Type	Area (mm ²)
#1	Inclusion	127.92
#2	Inclusion	501.36
#3	Inclusion	20.51
#4	Inclusion	116.50
#5	Inclusion	522.87
*1	Impact	634.80
*1-1	Disbond	4669.43
*2	Impact	784.16
*2-1	Disbond	2760.06
*3	Impact	819.22
*4	Impact	382.98
*5	Impact	669.95
*6	Impact	384.67

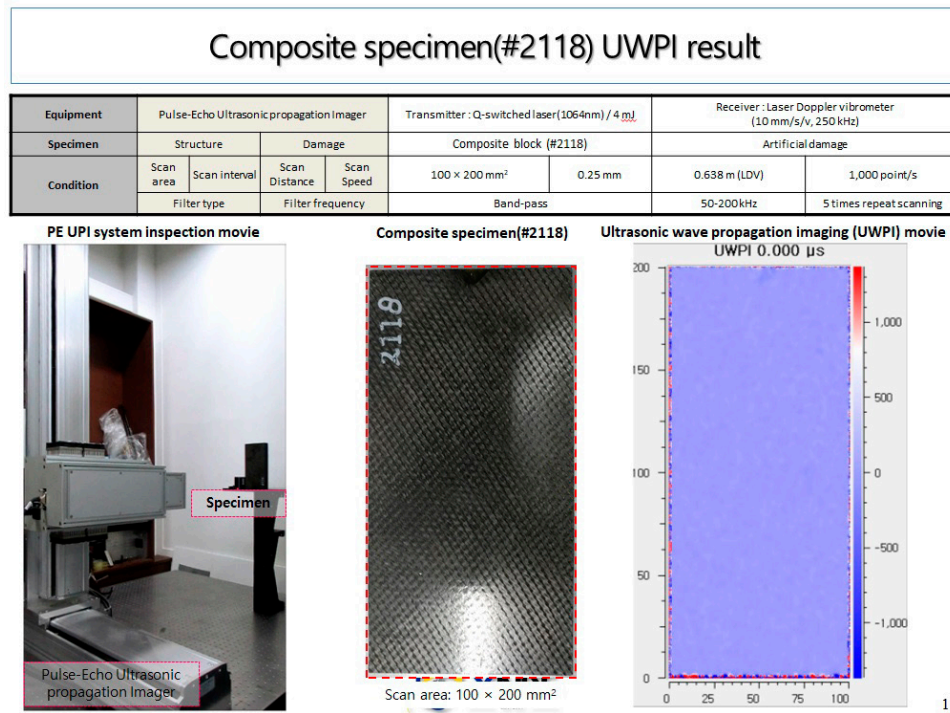
#1~#5: Inclusion defect
 *1~*6: Impact damage
 *1-1, *2-1: Disbond caused from impact event

- UWPI: Ultrasonic wave propagation imaging
 - VTWAM: Variable time window amplitude map

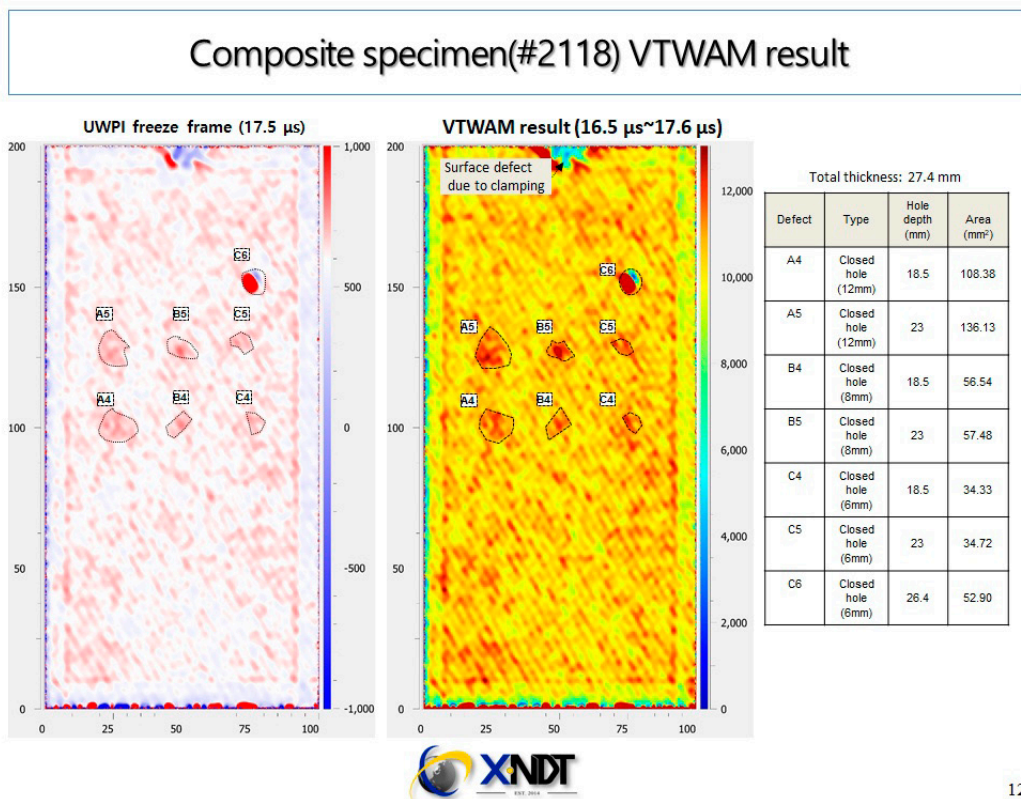
10

Fig. C5: PE-UPI inspection of specimen NLR-D (right side, upper half of Fig. A2). UWPI and VTWAM results

Appendix C.3 RTM specimen #2118



11



12

Fig. C6: PE-UPI inspection of RTM specimen #2118. Test set-up and VTWAM result



Dedicated to innovation in aerospace

Royal NLR - Netherlands Aerospace Centre

NLR operates as an objective and independent research centre, working with its partners towards a better world tomorrow. As part of that, NLR offers innovative solutions and technical expertise, creating a strong competitive position for the commercial sector.

NLR has been a centre of expertise for over a century now, with a deep-seated desire to keep innovating. It is an organisation that works to achieve sustainable, safe, efficient and effective aerospace operations.

The combination of in-depth insights into customers' needs, multidisciplinary expertise and state-of-the-art research facilities makes rapid innovation possible. Both domestically and abroad, NLR plays a pivotal role between science, the commercial sector and governmental authorities, bridging the gap between fundamental research and practical applications. Additionally, NLR is one of the large technological institutes (GTIs) that have been collaborating over a decade in the Netherlands on applied research united in the TO2 federation.

From its main offices in Amsterdam and Marknesse plus two satellite offices, NLR helps to create a safe and sustainable society. It works with partners on numerous programmes in both civil aviation and defence, including work on complex composite structures for commercial aircraft and on goal-oriented use of the F-35 fighter. Additionally, NLR helps to achieve both Dutch and European goals and climate objectives in line with the Luchtvaartnota (Aviation Policy Document), the European Green Deal and Flightpath 2050, and by participating in programs such as Clean Sky and SESAR.

For more information visit: www.nlr.org

Postal address

PO Box 90502
1006 BM Amsterdam, The Netherlands
e) info@nlr.nl i) www.nlr.org

Royal NLR

Anthony Fokkerweg 2
1059 CM Amsterdam, The Netherlands
p) +31 88 511 3113

Voorsterweg 31
8316 PR Marknesse, The Netherlands
p) +31 88 511 4444